# Uplift behavior of offshore shallow foundations during retrieval

## An experimental study on the pressure differences that occur during uplift of mud-mats of pre-piling templates

Bertie Rietema

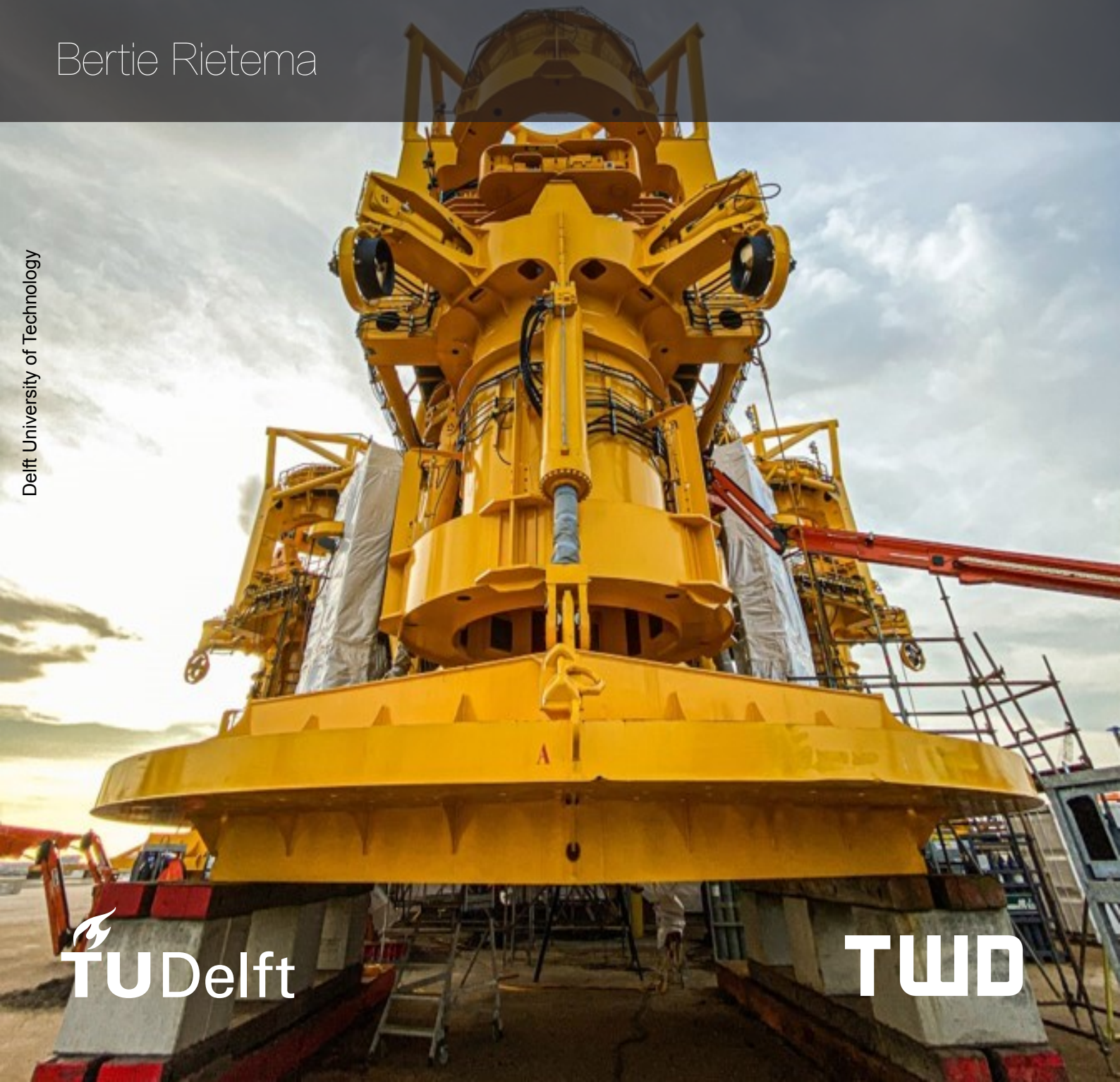

Delft University of Technology

TU Delft

TWD

Cover Image: TWD. (2019). Van Oord Wind Drilling Template St. Brieuc [Picture]. Internal
Back Image: TWD. (2019). Jan de Nul Wind Pre-Piling Template Taiwan [Picture]. Internal

# Uplift behavior of offshore shallow foundations during retrieval

## An experimental study on the pressure differences that occur during uplift of mud-mats of pre-piling templates

by

Bertie Rietema

MSc Student Geotechnical Engineering
Faculty of Civil Engineering and Geosciences
Delft University of Technology

| | | |
|---|---|---|
| Thesis committee | Chair: | Prof. Kenneth Gavin |
| | Second chair: | Prof. Pim van der Male |
| | Daily supervisor: | Dr. Vagelis Kementzetzidis |
| | Company supervisor: | Joost Remmers |
| | Second company supervisor: | Jelmar Termorshuizen |
| Company | | TWD |

TU Delft TWD

# Preface

*This thesis is written for readers with a basic understanding of soil mechanics and geotechnical engineering. Some of the terminologies are elaborated upon. This should allow for an overall understanding of the presented hypotheses and the experimental results.*

This thesis is written in fulfillment of my MSc degree in Civil Engineering. In this preface I will express my gratitude. I am truly thankful to everyone who helped me in finishing my studies and this thesis. Many thanks to the committee for allowing me to do an experimental study on such an interesting and relevant topic. Diving deep into a new understanding of soil behavior during foundation uplift allowed me to explore and compare many areas of foundation engineering. Ken, thank you for being the chair and for providing me with your excellent knowledge and genuine interest in the topic. Pim, thank you for joining the committee and shining your light on the topic from a non-geotechnical perspective. Your knowledge of the offshore industry and performing research helped me forward. Vagelis, I am grateful for our interesting biweekly sessions. You asked many critical questions which pushed me to further research the current literature and map the existing knowledge on the topic. Although your expertise is not in experimental studies, you truly were of great help and provided excellent feedback on the process, results, and interpretation.

Furthermore, I am so, so happy that TWD let me perform my research at their office and in their laboratory. Besides the fun and creative ambiance at the company, the joy I feel when looking back at the total process of graduation is indescribable. An interest in the topic from colleagues, fun at the office, amounts of clay that covered me during the summer months: it was all abundantly present. Although fixing the leaking container wasn't always successful, after multiple attempts the test set-up worked. I could conclude that graduation is a roller coaster. Joost, I want to thank you for the excellent supervision and help with the ups and downs of the roller coaster. Without you, all of this could never be possible. You really challenged me to get the most out of my time at TWD and to not be afraid of Arduino's or drilling equipment. I learned so much and your enthusiasm sticks. Jelmar, thank you for our sessions from which I learned so much about the offshore industry. Hopefully, I taught you something about geotechnical engineering. Next to that, I want to thank the lab team for our brainstorm sessions, the (practical) help in the lab, and the helpful tips regarding the research or experiments. Especially Bart, thank you for being my "*sparringspartner*".

Lastly, I want to thank my family and friends. Guido, thank you for listening to my adventures and struggles with the test bench. You always showed interest in my work and were an excellent support. Mom, dad, thank you for being there for me and trying to grasp the complexities of soil behavior. Your efforts are well appreciated. Simone, you are the most amazing sister I could wish for. My gratitude to my other friends who encouraged me during the process cannot be put into words. I will not stop sharing my geotechnical ups and downs with you!

$\pi\acute{\alpha}\nu\tau\alpha\ \dot{\varrho}\varepsilon\tilde{\imath}\ ?$

*Everything flows - Heraclitus*

*Bertie Rietema*
*Rotterdam, December 2022*

# Summary

The offshore industry desires efficient methods to mitigate resisting forces that occur during the uplift of shallow foundations. Offshore structures are often founded on mud-mat foundations which prevent the structure from settling. Pressure differences are generated under mud-mats during removal from the seabed. These differences lead to a force that resists the uplift and prevents the retrieval of the structure. Suction, which was previously generally accepted to be the negative excess pore pressure that develops within a soil body and the sole contributor to this resisting force, needs to be reconsidered. A better understanding of the resistance to uplift allows for more adequate mitigation, overcoming conservatism in the current design codes.

This research studies the generation of pressure differences by means of an experimental study. The literature study on breakout resulted in a hypothesized distinction of four mechanisms that occur during the uplift of offshore shallow foundations. The experimental program aims at confirming the hypothesis that these mechanisms exist and can be observed. Next to that, the sequence of mechanisms and the relative contribution to the total resisting force is investigated.

1. Negative pore pressures are generated as the upward load is initially carried by the pore water.
2. Adhesive bonding occurs between the soil and the foundation, depending on the soil cohesion.
3. The pore volume increases due to unloading by a combination of shear and tension, this induces additional negative pore pressures.
4. A void between the foundation and soil must be filled with water causing a viscous drag along the foundation invert, which leads to an underpressure in the water body.

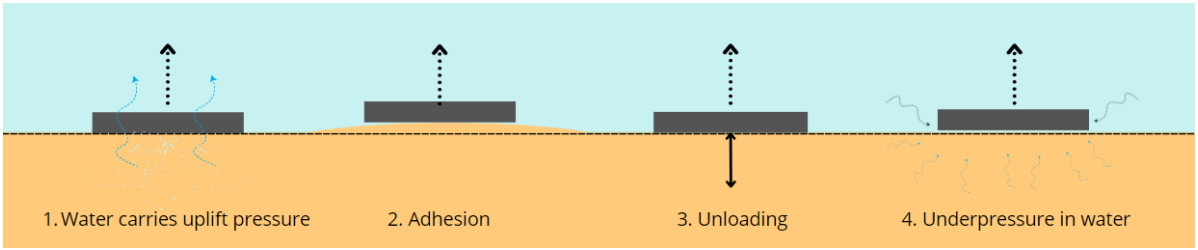


**Figure 1:** Four mechanisms that contribute to a resisting force during the uplift of offshore shallow foundations.

The analogy of the compression and uplift of shallow foundations is challenged as it is found that the ground behavior shows many differences. Applying equations for compression to model the uplift capacity of foundations is not suitable for non-skirted foundations. Next to studying suction *generation*, research on suction *relief* is presented as well. A mud-mat can be retrieved from the seafloor if the pressure differences are relieved and either the soil or the adhesion at the foundation invert fails. Research on mitigation is studied to map the existing mitigation measures and assess the suitability of the measures with an understanding of the mechanisms.

An experimental program was designed to study the four mechanisms. Tests on clay and sand were executed in the laboratory of TWD. A variety of mud-mats was connected to the test bench on which a container was placed that was specifically designed for this research. The clay or sand sample was prepared in the container, with a water column on top of the soil to represent offshore conditions. A load cell recorded the forces and a water pressure transducer was installed into the center of the mud-mat to measure the pore pressures.

The observations from the experiments led to the conclusion that uplift of shallow foundations results in multiple mechanisms that contribute to a resisting force in excess of the submerged weight. The

pore pressures become negative the instant that the uplift procedure has commenced, both in clay and sand. This indicates that the water carries the uplift pressure. In sands, an increase in peak force was observed for increasing load rates. This is likely caused by the pore water flow through the soil body to relieve the generated underpressures. Some experimental results suggest that adhesion increases over time and is present regardless of the application of any mitigation measures. Although trends in peak force are observed for changing preloads in clay and sand, no conclusions can yet be drawn on the effect of increasing preloads on changes in pore volume, pore pressures, and unloading behavior. An underpressure in a water-filled gap between a foundation and an underlying medium is observed to result in a resisting force. Water must fill the void that is left by the displaced foundation. The underlying medium can be porous or non-porous, a peak force was observed in both cases. The resisting force that is caused by this underpressure depends on the width of the gap. The underpressure in a gap leads to water getting sucked out of the sand body. This reduces the resisting force. The underpressure in water is studied by isolating the mechanism, while in practice the occurrence of mechanisms is continuous and possibly simultaneous.

The effectiveness of selected mitigation measures was studied, as was the effect of the mitigation measures on the mechanisms. It was found that the combination of perforating the mud-mat and applying geotextile at the foundation invert leads to large reductions in the peak force in the experiments: % in clay and % in sand. The application of perforations or geotextile separately also results in decreased peak forces. The effects of load rate, preload, and settling times with mitigation in place on the peak force were studied. No load rate dependencies were observed in clay and sand for the application of perforations and/or geotextile. This could indicate that adhesion becomes the predominant mechanism for a permeable foundation, as this does not depend on the load rate.

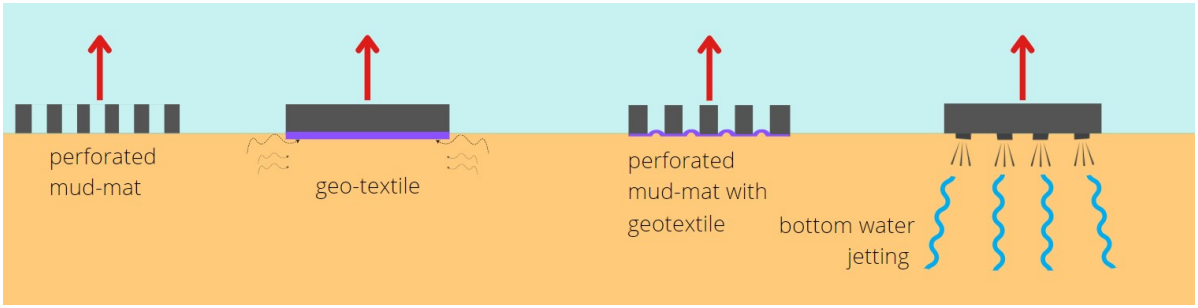


**Figure 2:** Mitigation measures that are most commonly equipped in practice to prevent the generation of pressure differences near the foundation invert or allow more rapid underpressure relief.

The existing calculation methods that model *suction* or quantify the breakout force are listed and evaluated in this research. It is assessed whether a distinction between the four different mechanisms was made, as well as the suitability of the parameters in the existing methods. It is believed that the results from the experimental program led to a comprehensive list of parameters that should be included in a design method. This method would model the total resisting force to uplift while taking the mechanisms into account. A trade-off should be made in a design method: The theoretically accurate quantification of pressure differences due to the different mechanisms is desired. However, the estimation of the resisting force with parameters that can be obtained with site investigation in offshore conditions is simple and fast. The trade-off will lead to the most accurate, upper-bound solution.

The distinction of several mechanisms that contribute to the resisting force to uplift is assumed to be proven, although further research on the underpressure generation should be conducted to study scale effects. Both the extrapolation in space to offshore practice, and in time to permanent foundations should be studied. This enables engineers to obtain improved predictions of pressure differences by deepening the understanding of soil behavior during offshore shallow foundation retrieval at the foundation interface.

# Samenvatting

Funderingen op staal die van de zeebodem verwijderd moeten worden, bijvoorbeeld aan het einde van hun levensduur of om naar een andere positie verplaatst te worden, ervaren zuiging tijdens het omhoog trekken. Die zuiging kan ervoor zorgen dat de fundering vast blijft zitten of dat er grote krachten nodig zijn om de fundering los te breken. De drukverschillen aan het raakvlak tussen de fundering en de grond die het lostrekken van de fundering moeilijk maken werden voorheen vaak zuiging genoemd. Dit onderzoek laat zien dat er meer gebeurt dan puur het ontstaan van een onderdruk in je grondlichaam. Als de wetenschap de ontstane onderdrukken beter begrijpt, kan de industrie de opgedane kennis toepassen om zuiging adequaat tegen te gaan met mitigatiemaatregelen. Daarnaast kan regelgeving bijgewerkt worden om tot economische en geoptimaliseerde funderingsontwerpen te komen.

Deze studie bestudeert de mechanismen die bedragen aan de onderdruk die ontstaat wanneer een fundering verwijderd wordt van de zeebodem. Een experimenteel programma is opgesteld waarin de optredende mechanismen onderscheidden worden. De vier veronderstelde mechanismen zijn hieronder genoteerd. Het is onderzocht of de mechanismen waargenomen kunnen worden in een experimentele testopstelling. Daarnaast is de volgorde en relatieve bijdrage aan de totale kracht die het omhoog hijsen van de fundering tegengaat onderzocht.

1. Het poriewater draagt initieel de opwaartse kracht, waardoor negatieve poriedrukken ontstaan.
2. Een adhesieve binding is aanwezig tussen de grond en de fundering, in cohesieve gronden.
3. Het porievolume zal toenemen tijdens het ontlasten van de grond door een combinatie van een schuifkracht en trek, wat leidt tot bijkomende negatieve poriedrukken.
4. Een onderdruk in het water is gecreëerd door de leegte die gevuld moet worden wanneer plots het contact tussen de fundering en de ondergrond verdwijnt.

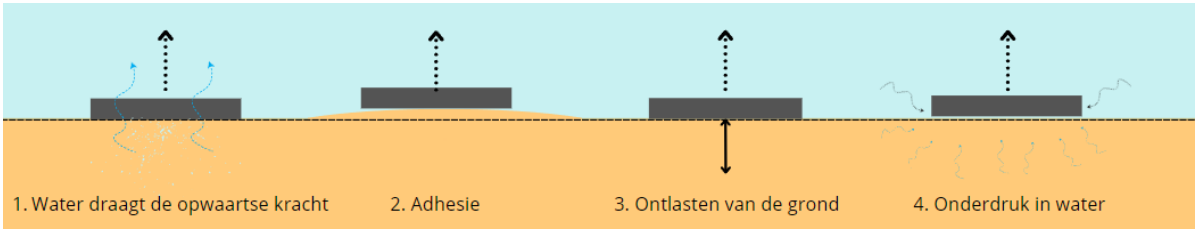


**Figure 3:** Vier mechanismen die bijdragen aan een kracht die optreed bij het verwijderen van een fundering van de zeebodem.

Voorheen werd de trekkracht die een plaatfundering kan weerstaan gelijk verondersteld aan de drukkracht. De mechanismen die optreden tijdens het drukken op en trekken aan een fundering tonen overeenkomsten maar zijn niet gelijk. De rekenmethodes die gebruikt worden in de praktijk voor een fundering onder trek vatten niet goed de complexiteit van het grondgedrag. Naast de onderzoeken over het *ontstaan* van onderdruk, wordt er literatuur gepresenteerd over hoe de onderdruk *verdwijnt*. De onderdruk in de grond moet afnemen of de adhesieve binding tussen de fundering en de grond moet falen om de fundering los te krijgen. Om deze onderdruk sneller te laten verdwijnen bestaan er mitigatiemaatregelen die bijvoorbeeld grondwaterstromingen op gang brengen.

Het experimentele programma maakt een onderscheid tussen testen in klei en zand, omdat zuiging naar verwachting sterk afhankelijk is van de cohesie en permeabiliteit. De testen zijn uitgevoerd in het laboratorium van TWD. Het grondmonster is volledig gesatureerd en een waterkolom boven het grondniveau wordt in stand gehouden om condities op zee na te bootsen. Verschillende funderingstypen worden gemonteerd aan de testbank, waarin het installatie- en ophaalproces wordt gesimuleerd. Een kracht meter registreert de krachten over tijd en een waterdruk meter is geïnstalleerd in het midden van de fundering om lokaal de (porie-)waterdruk te bepalen.

De experimenten hebben aangetoond dat er meerdere mechanismen zijn die bijdragen aan het ontstaan van een kracht die het omhoog hijsen van een fundering vanaf de zeebodem tegengaan. De poriedrukken veranderen instantaan wanneer de opwaartse kracht wordt opgelegd, in zand en klei. Dit suggereert dat het poriewater initieel de opwaartse kracht draagt. De piekkracht hangt af van de hijssnelheid in zand wat aantoont dat de zuiging gedissipeerd kan worden door een grondwaterstroming. In klei is deze afhankelijkheid niet waargenomen. De bevindingen suggereren dat adhesie toeneemt over tijd en niet verdwijnt door het toepassen van mitigatiemaatregelen. Daarnaast is het aangetoond dat er een onderdruk aanwezig is in het waterlichaam nadat het contact met de ondergrond is verloren. De onderdruk is aanwezig tussen een fundering en een medium, die niet poreus hoeft te zijn, wanneer de tussenliggende afstand klein genoeg is. De afstand tussen de fundering en ondergrond bepaalt de weerstand tegen het water en dus de piekkracht. In het geval van een zandlichaam, zal er water uit de grond gezogen worden om de leegte onder de fundering te vullen. Daarnaast zal ook water om de fundering stromen. Dit mechanisme is geïsoleerd in de testen, terwijl in de werkelijkheid de mechanismen elkaar opvolgen en potentieel tegelijk optreden.

Verschillende mitigatiemaatregelen zijn getest om te bestuderen wat de invloed is op de mechanismen en in hoeverre de onderdruk vermindert wordt. De piekkracht zal afnemen wanneer er een geperforeerde fundering geïnstalleerd wordt waar geotextiel is bevestigd aan de onderzijde. In het geval van klei zal deze reductie % zijn en in zand is een afname van % waargenomen. Als alleen perforaties of een geotextiel wordt toegepast zal de piekkracht ook afnemen, maar in mindere mate. Verder zijn de hijssnelheid, zettingstijd en voorbelasting gevarieerd en bestudeerd. Er is geen afhankelijkheidsrelatie ontdekt tussen de piekkracht en hijssnelheid. Dit kan erop duiden dat de adhesie dominant is bij deze mitigatiemaatregel, omdat een adhesieve binding niet verandert door de treksnelheid.

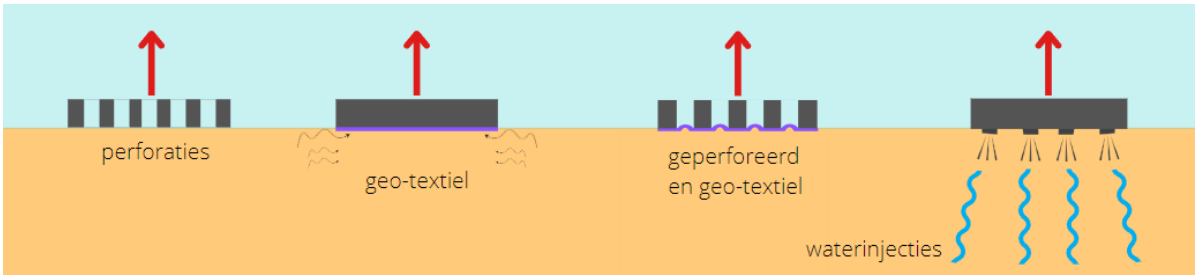


**Figure 4:** Mitigatiemaatregelen die worden toegepast in de praktijk om het ontstaan van onderdrukken nabij de fundering tegen te gaan of om waterstroming te vergemakkelijken.

Bestaande rekenmodellen voor zuiging of benodigde hijskracht zijn uiteengezet en beoordeeld. Voor elk model is nagegaan of er een onderscheid is gemaakt tussen verschillende mechanismen en de geschiktheid van de gebruikte parameters wordt geëvalueerd. De aanname wordt gedaan dat de experimentele resultaten leiden tot een lijst van parameters die geschikt zijn om de mechanismen die tot de onderdruk tijdens het hijsen leiden te modelleren. In de praktijk zal een afweging gemaakt moeten worden tussen het correct kwantificeren van de onderdrukken door de relatieve bijdrage van de verschillende mechanismen en het afschatten van de zuigingskracht die ontstaat door grove schattingen van grondparameters. Het optimum zal een accurate bovengrens geven van de weerstand biedende kracht.

De onderzoeksresultaten kunnen niet simpelweg geschaald worden in de ruimte en tijd. Verder onderzoek zal nodig zijn om aan te tonen dat de optredende mechanismen dimensieloos zijn. Dit onderzoek veronderstelt dat onder funderingen in de praktijk de mechanismen zullen optreden in eenzelfde volgorde als in de schaalexperimenten, maar met een andere magnitude. Daarnaast is het verwacht dat ook bij permanente funderingen de mechanismen zullen optreden. De staat van de grond aan het begin van het ontlasten zal echter verschillen, wat het optreden van de mechanismen kan veranderen. De totaliteit van het begrijpen van de onderdrukken zal ingenieurs in staat stellen verbeterde voorspellingen te maken van het grondgedrag tijdens het verwijderen van funderingen van de zeebodem.

# Contents

# Nomenclature

## Symbols

| Symbol | Definition | Unit |
|---|---|---|
| $A$ | Foundation area | $m^2$ |
| $A_{eff}$ | Effective foundation area | $m^2$ |
| $B$ | Foundation width | $m$ |
| $c$ | Cohesion | $kPa$ |
| $c_v$ | Coefficient of consolidation | $cm^2/s$ |
| $d_f$ | Depth factor | $-$ |
| $E$ | Young's modulus of soil | $kPa$ |
| $E'$ | Young's modulus of soil skeleton | $kPa$ |
| $e_{max}$ | Maximum void ratio | $-$ |
| $F$ | Force | $N$ |
| $F_{breakout}$ | Breakout force | $kN$ |
| $h$ | Embedded depth | $m$ |
| $i_f$ | Inclination factor | $-$ |
| $k$ | Hydraulic conductivity | $m/d$ |
| $k_p$ | Poincs' constant | $-$ |
| $K_D$ | Bulk modulus for pore fluid | $-$ |
| $K_S$ | Bulk modulus for solid material | $-$ |
| $m_v$ | Compressibility coefficient | $m^2/kN$ |
| $n_0$ | Initial porosity | $-$ |
| $N_c$ | Undrained bearing capacity factor | $-$ |
| $N_\gamma$ | Factor to account for unit weight | $-$ |
| $N_q$ | Factor to account for the surcharge | $-$ |
| $q$ | Bearing capacity | $kPa$ |
| $q_0$ | Initial applied stress | $kPa$ |
| $q_u$ | Uplift capacity | $kPa$ |
| $r$ | Radius | $m$ |
| $s_f$ | Shape factor | $-$ |
| $s_u$ | Undrained shear strength | $kPa$ |
| $t$ | Time | $s$ |
| $T_{in-situ}$ | In-situ time | $s$ |
| $u$ | Excess pore pressure | $kPa$ |
| $U$ | Degree of consolidation | $-$ |
| $v$ | Velocity | $m/s$ |
| $v_r$ | Longitudinal flow velocity | $m/s$ |
| $V$ | Voltage | $V$ |
| $W$ | Weight | $kN$ |
| $W'$ | Buoyant weight | $kN$ |
| $W'_s$ | Buoyant weight of soil displaced by object | $kN$ |
| $\alpha$ | Degree of development of reverse end bearing mechanism | $-$ |
| $\gamma$ | Unit weight soil | $kN/m^3$ |
| $\gamma'$ | Submerged unit weight soil | $kN/m^3$ |
| $\gamma_w$ | Unit weight water | $kN/m^3$ |
| $\zeta$ | $= \frac{\gamma_w(\kappa_S + n_0\kappa_D)}{n_0 k}$, Sawickis' constant 1 | $-$ |

| Symbol | Definition | Unit |
|---|---|---|
| $\theta$ | Addition of principal stresses | $kPa$ |
| $\kappa_D$ | Compressibility of pore fluid | $-$ |
| $\kappa_S$ | Compressibility of solid material | $-$ |
| $\sigma$ | Stress | $kPa$ |
| $\sigma'$ | Effective stress | $kPa$ |
| $\nu'$ | Poisson's ratio of soil skeleton | $-$ |
| $\xi$ | $= \frac{\gamma_w \kappa_S}{n_0 k}$, Sawickis' constant 2 | $-$ |
| $\rho$ | Density | $kg/m^3$ |

# List of Figures

# List of Tables

# 1 Introduction

## 1.1 Motivation

Offshore wind turbines grow in size and move to deeper waters to increase their energy production (Landbo et al., 2010). Industry desires efficient installation methods of foundations for offshore wind turbines. Among other structure types, jackets are installed as the sub-sea structure of the turbine. Pin-piles serve as the foundation of the jacket and can be installed with a pre-piling template. Pre-piling templates ensure the correct location and orientation of the piles, next to accelerating the installation operation, as displayed in Figure 1.1. Figure 1.2a shows a pre-piling template that can be utilized to install three pin-piles. Pin-piles are installed in increasingly challenging soil conditions with varying types of installation methods (Goncalves, 2021). Next to that, operational loads and installation time increase due to increasing pile diameter, length, and weight of the piles. Consequently, the complexity of designing mud-mats that prevent the pre-piling template from excessive settlement increases. Among other issues, the underpressure generation at the mud-mat/soil interface during removal from the seabed is a design driver of pre-piling template design (Bouwmeester et al., 2009).

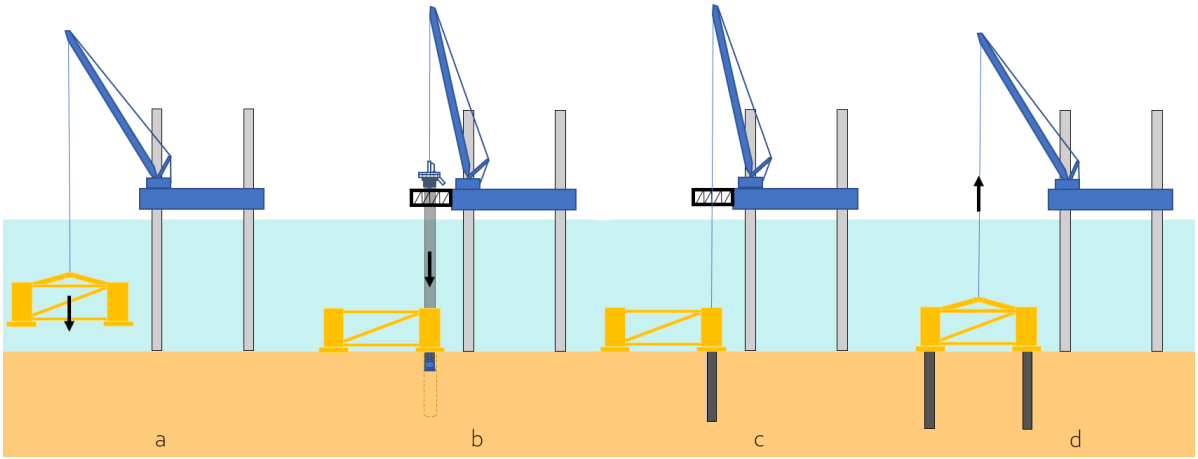


**Figure 1.1:** Timeline of one pre-piling template ”cycle”: (a) Pre-piling template placement, (b) Start pin-pile installation, (c) Install all pin-piles, (d) Retrieve pre-piling template.

### 1.1.1 Underpressure generation during uplift

Pressure differences occur at the mud-mat/soil interface during landing on the seabed, operation, and retrieval of the pre-piling template. Negative pore pressures develop within the soil upon removal. This is problematic as this generates a downward force that resists the detachment of the mud-mat from the seabed. It is hypothesized that after detachment a viscous drag within the water body contributes to resisting removal as well, for example by Zhou et al. (2008). Large forces are required to extract the pre-piling template, which can result in an uncontrolled breakout of the structure and damage to equipment. If lifting rates are lowered to reduce underpressure generation, additional time is required

for structure retrieval, with subsequent expenses and delays. Expensive mitigation measures such as jetting are implemented to prevent this suction from occurring. Although there are efforts in literature to estimate the force that is needed for the breakout of an object from the seabed, the exact mechanisms behind the negative pressure generation remain unidentified. Understanding and adequately mitigating the underpressure will lead to more efficient material use, the ability to equip cranes with reduced lifting capacity, and subsequently lowered operation costs.

**(a)** Template placement in St Brieuc.

**(b)** Ring-shaped mud-mats with perforations and short skirts.

**Figure 1.2:** Pre-piling template with mud-mats. (TWD, 2019b)

### 1.1.2 Design codes on mud-mats

The pre-piling template is lifted from seabed after all jacket pin-piles are installed. The procedure of installing all pin-piles for one jacket structure, including the pre-piling template placement and retrieval, is estimated to last at most $48\ hours$. Pre-piling template mud-mats are thus temporary foundations. Current design recommendations (e.g. DNV, 2019b) do not provide guidelines for calculations on temporary foundations and solely provide generic safety factors for permanent offshore structures. This could result in conservatism in mud-mat design. A range of geotechnical properties of the stratum can be encountered at the different jacket locations of the wind farm and stability needs to be guaranteed for every location, which could lead to further conservatism. Increasing mud-mat diameters is disadvantageous, as larger mud-mat diameters will likely result in increased underpressure generation during uplift. Furthermore, large diameters introduce operational difficulties. Steel reduction can be obtained when the resisting force is reduced or diminished if uplift is the prevailing load case for the pre-piling template. One of the DNV standards (2021c) states that for retrieval from seabed, formulae designed to model the bearing capacity of foundations under compression may be used to quantify uplift resistance. This comparability of soil behavior under compression and tension will be challenged in this research.

## 1.2 Goal

The primary goal of this research is to distinguish the mechanisms that contribute to underpressure generation during the uplift of temporary offshore shallow foundations and prove their respective physical presence experimentally. Currently, it is not sufficiently understood how the underpressure during uplift is generated. As the literature study performed for this research resulted in a hypothesized distinction of mechanisms, an experimental program is designed with the goal of determining whether these mechanisms can be observed in reality. The physical small-scale model tests explore the sequence or simultaneous occurrence of the mechanisms, as well as the corresponding relative contribution to the total force that resists uplift. The experimental results will aid in understanding which parameters influence the underpressure. Thereafter, measures to mitigate the underpressures are presented. The influence of each mitigation measure on the mechanisms is discussed. Test results of mud-mats with selected mitigation measures are utilized to further understand the mechanisms and the effectiveness of said measures. The investigation into the mechanisms allows for better mitigation of underpressures in the future.

## 1.3 Strategy

Literature research resulted in an understanding of what has been investigated in the past regarding the uplift of temporary and permanent foundations. Next, a deeper understanding of the parameters and mechanisms that influence and contribute to the underpressure is sought. This led to the definition of four mechanisms. Hypotheses for the mechanisms are drafted and form the basis of the experimental program. The results of the experiments in clay and sand are presented, compared to other research, and discussed. An overview of mitigation measures known from literature is presented. The effect of each mitigation measure on the mechanisms and total resisting force is discussed. A further testing campaign was drafted, utilizing the results of the experimental test campaign without any mitigation measures. The selected mitigation measures and test settings were chosen such that the effects on the mechanisms could be fully understood. These experimental results are presented as well. Figure 1.3 summarizes this research strategy and provides an outline.

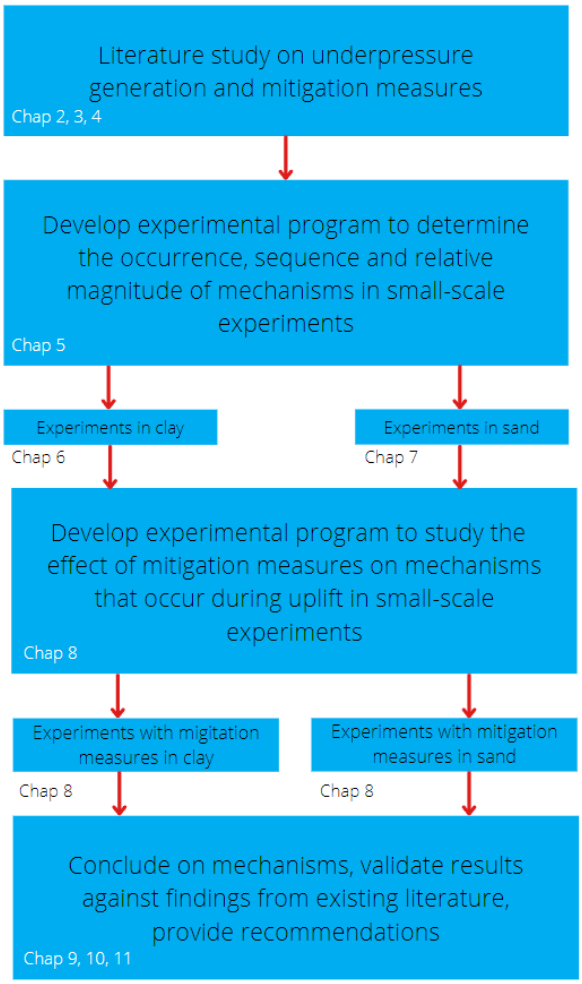


**Figure 1.3:** Research strategy and thesis outline.

## 1.4 Scope

This research is focusing on underpressure generation around the mud-mat/soil interface of pre-piling templates. As mud-mats are temporary foundations, permanent foundations are not under consideration. The mechanisms that occur during the uplift of permanent foundations might be comparable. However, this research focuses on temporary foundations. Solely steel mud-mats are considered. Other construction materials such as composite or concrete might result in differential values for adhesion or friction. Some pre-piling templates rest on the seabed with ring-shaped mud-mats, such as the pre-piling template in Figure 1.2b. The underpressure that is generated underneath foundations

with an opening for the pile installation is supposed to be lower due to shorted drainage paths compared to circular shallow foundations. Therefore only circular foundations are covered. In practice, the pre-piling template settlement should be limited, hence the level of the foundation invert coincides with the mudline in this study. It is known that underpressures are generated during uplift both in cohesive and non-cohesive sediments. Whether the same mechanisms occur that contribute to this suction is unestablished. The research will make a distinction between the mechanisms that occur in clay and sand. The pile installation procedure will be assumed as quasi-static. Considering cyclic loads and pore pressure generation due to pin-pile installation and waves acting on the pile is not within the scope of this study as it does not prove any valuable insights into the pore pressure changes without properly understanding underpressure development.

## 1.5 Thesis outline

Chapter 2 describes the necessary background information on mud-mats under pre-piling templates to understand the research. After informing the reader about the current state of the literature on underpressure generation, information on shallow foundations and pre-piling templates is presented. Lastly, the scope is further refined.

In Chapter 3, the mechanisms that take place during the compression and uplift of shallow foundations are described and explained in depth. Here, the distinction between the four mechanisms that lead to a resisting force during uplift is made.

Based on the distinguished mechanisms, Chapter 4 presents the existing calculation methods to quantify either the uplift force or the pore pressure changes due to foundation uplift. Both an approach to quantify the pressure differences altogether and a distinction of the mechanisms where each effect can be calculated separately are presented. Presenting the existing calculation methods helps the reader to better understand the current state of research on underpressure generation and the tools that geotechnical engineers utilize to quantify for example pore water flow.

Chapter 5 describes the experimental program. After that, the test set-up is explained in depth and discussed. The functionality of the test bench and pore pressure sensor is described. The reader should understand the steps that were taken to end up with the results that are presented in the following Chapters after reading this Chapter and how to interpret the graphs.

The results of the experimental program are presented in Chapters 6 and 7. Force-displacement graphs or stress-quasi strain are presented, as well as observations from each graph and explanations. Trends over the different tests are compared. Preliminary conclusions on the occurrence of the mechanisms are made.

After studying the mechanisms that contribute to underpressure generation, several mitigation measures are presented in Chapter 8. Experimental results with selected mitigation measures in place are shown. The conclusions from this Chapter, in combination with the results from Chapters 6 and 7, contribute to making well-argued recommendations for a design method to quantify the uplift force during pre-piling template retrieval.

In Chapter 9 the results are discussed and compared to other small-scale tests, centrifugal or field tests, and numerical work. A conclusion will be drawn in Chapter 10. Recommendations for further research are provided in Chapter 11. The recommendations provide the reader with several directions for further research on underpressure generation during uplift. Next to that, recommendations for a test on flexible foundation are presented.

# 2

# Background mud-mats

This Chapter provides the reader with the required background knowledge to understand this research and emphasizes the relevance of the research on uplift of temporary foundations. A brief overview of the literature on breakout of objects from the ocean bottom is presented, as during object breakout mechanisms similar to foundation uplift can occur. Next, this Chapter provides the reader with more information on offshore temporary shallow foundations and associated complexities. The current standard (ST) and recommended practices (RP) from DNV are presented and the different considerations that determine pre-piling template design are presented. Lastly, the scope of the research is further refined.

## 2.1 Breakout of objects from the ocean bottom

Research regarding breakout investigates the retrieval of objects such as sunken vessels from the ocean bottom, see for example the research of Al-Shamrani, 1997; Das, 1991; Guha, 1979; Lee, 1972; L. Liu, 1969; Roderick and Lubbad, 1975, and Vesic, 1969. Those works consider objects of an arbitrary shape and foundations that are (partially) embedded, as displayed in Figure 2.1. All research concludes that the force required to lift the object is higher than the submerged object weight. Shallow foundations resting on the seabed are not the only objects that are subjected to underpressures in the soil body due to an uplift force. Embedded plate anchors under rapid loading show pore pressure variations both at the upper side and base of the anchor. However, the uplift of embedded objects is not within the scope of this research, as mud-mats under pre-piling templates are designed to settle as little as possible. Next to that, different failure mechanisms during uplift become predominant and top suction might influence the soil behavior. Irregular object shapes such as the geometry of a sunken vessel are likely to result in the accumulation of underpressures, leading to an uneven distribution. This complicates the modeling of the expected underpressures. Nevertheless, the mechanisms that lead to negative pore pressure generation underneath these objects during upwards movement are comparable with pore pressure development under mud-mats. Further Chapters, except for Chapter 4, will only consider shallow foundations.

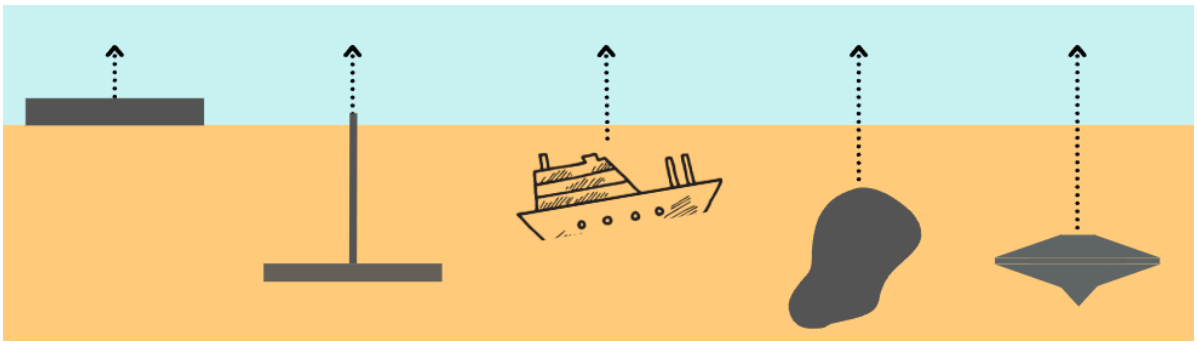

**Figure 2.1:** Variety of objects that can be buried in the seabed and need to be retrieved, from left to right: shallow foundation, buried plate or strip anchor, sunken and embedded vessel, boulder, spudcan.

## 2.2 Shallow foundations

Shallow foundations require to remain stable on ground level. The bearing capacity of onshore shallow foundations under compression has been thoroughly investigated in the past, however not all theories for shallow foundations are applicable to offshore conditions (Verruijt, 1982). Large dynamic loads, rapidly changing geomorphology, large expenses, and increased uncertainties associated with offshore geotechnical surveys and foundation installation complicate foundation design. Next to that, shallow foundations exhibit different behavior under uplift or compression, as further explained in Section 3.2.

Mud-mats are equipped for both permanent and temporary offshore applications. Large permanent mud-mats under jacket structures and manifolds transfer and distribute loads from the subsea structure to the underlying soil. Permanent mud-mats remain on the ocean bottom for over $20$ years, dependent on the design lifetime of the structure. Thereafter, (partial) decommissioning of the structure can take place (Ersdal, 2005). The settlement that occurs due to (primary or secondary) consolidation, pore pressure dissipation, and a higher probability of extreme load cases for permanent shallow foundations make the soil behavior differ greatly from temporary foundations.

Skirts, vertical circumferential steel plates, can be included in shallow foundation design to withstand additional horizontal loads, as well as to increase the vertical capacity due to wall friction. Suction can develop in the soil confined within the skirts, the soil plug, which increases uplift capacity. This alters the failure mechanism. The skirts cause the drainage paths to increase significantly and the entrapped water above the soil plug in combination with gapping effects plays a big role in the uplift response. (Li et al., 2014; Randolph and Gourvenec, 2011) In this research, solely unskirted foundations will be considered.

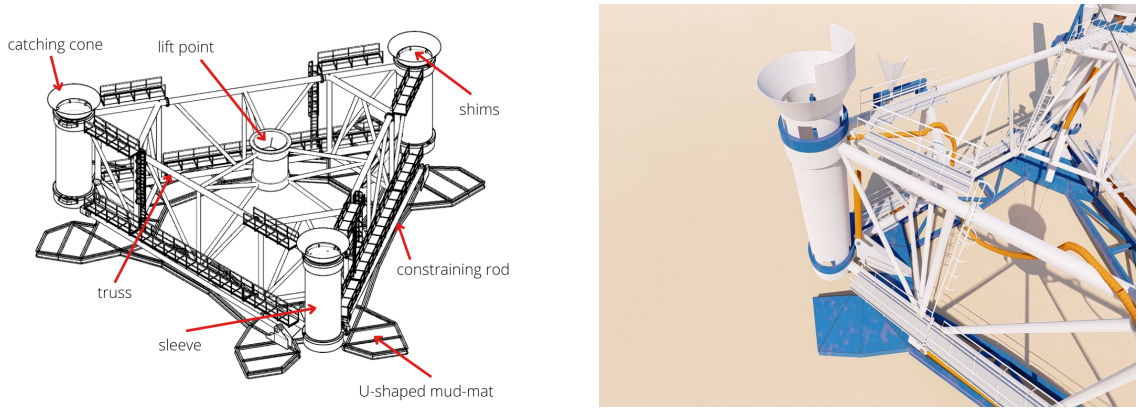


**(a)** Schematic of pre-piling template with mud-mats.

**(b)** Three-dimensional model of a pre-piling template.

**Figure 2.2:** Computer renders of a pre-piling template (TWD, 2018).

## 2.3 Pre-piling templates

A pre-piling template is constructed to aid in pile or anchor installation. A template is either attached to jack-up legs or resting on the seabed during pile installation to guarantee stability. The jack-up legs can be used as a positioning guide. If placed on seabed, mud-mats prevent the pre-piling template from sinking into the soil[1] and enable the template to transfer loads to the soil. The pre-piling template ensures the correct location, center-to-center distance, and orientation of the piles, within predefined tolerances. (DNV, 2021c) Next to that, the pre-piling template speeds up the installation process. A pre-piling template usually consists of three or four mud-mats and pile sleeves, connected with hydraulic cylinders and constraining members to a truss. Hydraulic cylinders allow the mud-mat to be placed on sloped surfaces and distribute forces over the foundation area. Mud-mats are either used as a raft foundation or as a mat through which the pile is installed, see for example Figure 2.2 where U-shaped mud-mats are selected. Pile installation methods include the driving, drilling, and oscillating of foundation piles into the subsoil (Dean, 2010). Pre-piling template retrieval is either for repositioning, removal for maintenance, or decommissioning. Mostly, the templates are uplifted for repositioning.

[1] It is especially relevant to prevent excessive settlements in soils with low bearing capacity such as clays. Soft soils in offshore conditions are often described as mud, hence the term mud-mat.

### 2.3.1 Design procedure for pre-piling templates

The foundations of the pre-piling template are part of the bigger system and interplay occurs with the different structural components. To understand the totality of the pre-piling template design, the most common steps are presented:

1. Determine load cases: wave or current load on the template and pin-piles, as well as the pile dynamics. Consider both individual forces from the pin-pile on the template for the governing case and the combination of all piles in a multiple-pile model. Following the standard from DNV, the ultimate limit state and accidental limit state are to be considered. (DNV, 2019a)
2. Perform a tolerance study for the positioning of the pre-piling template and the pile installation.
3. Incorporate the chosen piling method in the design of the sleeves and constraining members.
4. Design the closing mechanism around the pin-piles, e.g. shims or rollers to ensure the pile verticality.
5. Design the mud-mats. Offshore shallow foundation capacity is often assessed with interaction diagrams. Combinations of horizontal, vertical, and momentum forces are investigated to obtain the maximum load combinations a foundation can withstand. Next to that, the mats should cope with local seabed slopes. Consider the forces on the mud-mat for the lowering through the wave-slamming zone. Also consider pre-installed scour protection of pin-piles.
6. Design a leveling system for the pre-piling template.
7. Design the connections of the mud-mats to the frame of the template.
8. Design the lifting point(s).
9. Design a monitoring plan for pile installation to determine pile stick-up height, orientation, and template levelness.

**DNV guidelines**

DNV recommends and prescribes guidelines regarding (the lifting of) foundations. DNV-ST-N001 (DNV, 2021c) states that when templates are liable to settle in clay or silt, the provision shall be made for jetting or other means to overcome adhesion during subsequent extraction. DNV-RP-N103 (2021b) postulates that due to the suction generation, one will have to overcome a reversed bearing failure in the soil to lift the submerged weight of the structure. This leads to the statement that a *suction factor* of $2$ should be taken into account. The suction factor is defined here as the force that is required to retrieve the object from the seafloor divided by the submerged object weight in $N$. The foundation design should be able to sustain suction for additional overturning or uplift capacity to ensure operational stability. However, this is not a requirement for a pre-piling template as the overturning moment is carried by the structure as a whole. It is recommended to fix the lifting force within safe limits and then gradually increase the overpressure until the soil resistance is exceeded, rather than the other way around. (DNV, 2021b)

**Constraints in pre-piling template design**

Next to the constraints enforced by local geotechnical considerations, other technical aspects play a role in template design. One should take into account the maximum crane capacity and uplift speed of the vessel operating the template. The load control during uplift is adjustable in real-time, however is limited based on equipment specifications. Next to that, large expenses are associated with operation time due to vessel utilization. Vessel size limits the size of the template and consequently the mud-mats. Next to that, the template should be sea fastened for safe transport to the construction site. Long skirts along the mud-mat periphery introduce difficulties during transport, as the mud-mats cannot be placed directly on the support deck. During transport, the template is often placed on a specifically designed transport frame, such that the mud-mat is not in contact with the deck. Another major influence on template design is constructability. For example, realizing many perforations in a mud-mat to mitigate suction is labor-intensive. Fabrication time and material demands influence the total cost of the template. Contractors aim for a minimal weight of the structure, as this impacts material usage and the required crane capacity. In short, the procedure of installing pin-piles by means of utilizing a pre-piling template should be cost-efficient in terms of material use, installation duration, and energy requirements. (TWD, 2019a)

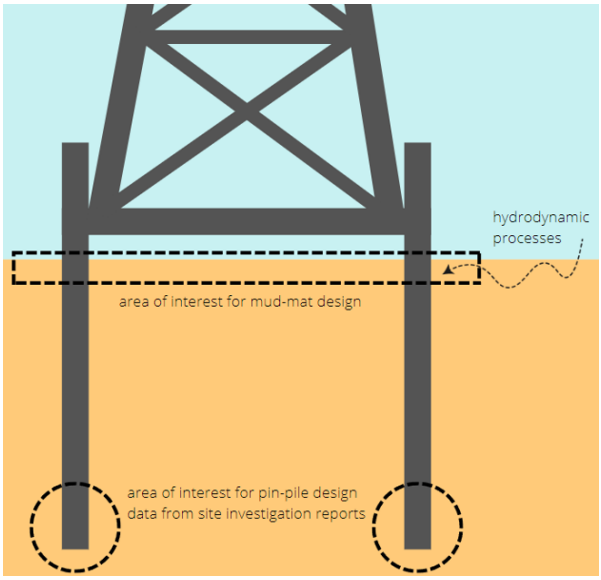


**Figure 2.3:** Little site investigation data from the upper layer on which the mud-mat is placed is present for template design.

### 2.3.2 Uncertainties in mud-mat design

Site investigation for offshore jacket structures mostly includes one borehole CPT[2] per jacket location. CPT data provides the foundation engineer with the required data for the pile design. The focus lies on the deeper layers, for pile end bearing capacity estimations, see Figure 2.3. However, solely the upper layer is of interest for mud-mat design. Additional uncertainty is introduced by the large heterogeneity of the soil due to the geomorphological processes which lead to soil mobility of the upper layer. This also causes CPT to often be deemed inaccurate in the top meters of the soil. The state of the soil (e.g. stress state, pore pressures, and void ratio) at the start of uplift, after disturbances due to the landing impact of the pre-piling template and the pin-pile installation, is unknown. Furthermore, boulders, solid coral, or irregular bathymetry can add to the uncertainties of the site and soil conditions.

## 2.4 Refining scope

The previous Sections describe the differences between mud-mats under pre-piling templates and other foundation types and object breakouts. Acknowledging these differences helps in defining the final scope and further research decisions. The following model abstractions are proposed as a further refinement of the scope.

- Circular mud-mats: Shallow foundation geometries include rafts, strips, and circles, Underpressure generation during uplift under a circular foundation is the predominant load case, compared to rafts and strips of equal foundation area.
- No skirts: Only unskirted foundations are analyzed, as the load transfer and mobilized failure mechanisms under skirted foundations differ from regular foundations. Next to that, skirted foundations for pre-piling templates are rarely designed as the hydraulic cylinders and truss carry the major part of the horizontal load.
- No interaction with other mud-mats under a template: As jackets increase in size, pin-piles are placed further apart and templates increase in size. This entails that mud-mats are positioned further apart too.
- Homogeneous soil: The diameters of mud-mats are typically within the range of $4$ to $12$ meters, thus the assumption of homogeneous soils is rigorous, however necessary to make any valuable conclusions.

[2]Cone Penetration Tests (CPT) are a common tool in geotechnical engineering for determining soil characteristics over depth. The characteristics include shear strength, frictional resistance, and in special cases pore pressure measurements over depth

- Fully saturated soil: Suction generation in unsaturated soils is associated with capillary effects and sorption, which cannot be observed in saturated soils. Any gas presence is neglected. the pores are assumed to be fully filled with pore water.
- Fully flat ocean bottom: The uplift load is distributed uniformly across the foundation and the uplift force is applied perpendicular to the foundation invert and seabed.
- Incompressible grains: The soil skeleton is deformable and can be subjected to volume change, the individual grains however cannot.
- Constant water temperature, viscosity, and density: Salinity is assumed to not influence the water characteristics, the same goes for temperature effects or density.

## 2.5 Terminology

The terminology in this research concerning foundation uplift should be defined to avoid ambiguities.

| | |
|---|---|
| Breakout | The whole process during which an object is removed from the ocean bottom, from the start of applying upwards force to placement on the vessel |
| Breakout time | The time duration from the start of the uplift procedure until the crane is solely lifting the submerged weight of the pre-piling template |
| Detachment | Total loss of contact between the soil grains and the foundation |
| Failure mechanism | A mechanism that develops within the soil body, consisting of planes along which the soil has the tendency to shear |
| Foundation | The mud-mats under pre-piling templates, not the pin-piles that are to be installed |
| On bottom time | The time during which the mud-mats are in contact with the ocean bottom, including the pile installation, excluding the breakout time |
| Operation duration | Duration of pin-pile installation |
| Suction | Negative excess pore pressure in the soil body |
| Underpressure | Negative pressure changes that occur in the soil or water body due to the foundation uplift |
| Uplift procedure | Upward force application, which could induce soil deformations, until the structure is lifted above the water level |

# 3

# Mechanisms

As stated in Chapter 1, underpressure generation during foundation uplift under shallow foundations is problematic for rapid foundation retrieval. One should recognize the effects of mud-mat installation on the soil to understand the negative (pore) pressure development during uplift. Next to considering the underpressure generation, it is of interest to study the underpressure relief, which can lead to foundation breakout. This Chapter examines mechanisms known from existing literature to map the current knowledge on soil behavior under shallow foundations subjected to compression and uplift.

## 3.1 Mechanisms that occur during foundation installation

Initially, foundations under compression are considered. The mechanisms expected during shallow foundation installation as presented in Figure 3.7 are in consecutive order. Considering the full installation, one starts with lowering the pre-piling template onto the ocean bottom. Due to foundation placement, soft soils can be remoulded and sandy soils might fail, see Section 3.1.1. Friction along the sides and bottom of the mud-mat upon settlement is observed, as further explained in Section 3.1.3. Next to that, adhesive bonding takes place. As the foundation is in contact with the ocean floor, loads can either be transferred to the soil skeleton or the pore water. Consolidation theory describes the changes in pore pressures and subsequent settlement. The degree of pore pressure dissipation is dependent on the soil type. Excess pore pressures dissipate but might be regenerated under cyclic loading (Verruijt and Merwehoofd, 1994). Cyclic operational loads on the mud-mat depend on the pile installation method. The total installation duration depends on local environmental and geotechnical conditions, equipment, and installation method. Pile installation can be delayed by problems such as pile run[1] or pile refusal[2]. (Dean, 2010) This influences the on bottom time and changes the geotechnical parameters at the start of the uplift, as described in Section 3.1.4.

### 3.1.1 Landing impact

DNV-RP-N103 (DNV, 2021b) states that the effects of the foundation landing should be taken into account for foundation design. This is to prevent the foundation from failing upon its' self-weight. Next to that, the landing impact should be considered to add to the forces that are required for foundation uplift. For sandy seabeds, extensive scour of sand underneath flat unskirted foundations should be avoided, which could be achieved by reducing the lowering speed upon approaching the seabed. The structural integrity of the foundation should also be guaranteed as the pre-piling template is landing on a hard seabed. (DNV, 2021a) If the installation is performed under controlled conditions by use of a heave compensator and low rate of descent towards the seafloor ($< 0.2m/s$), no extra safety margin is needed. (API, 2021)

### 3.1.2 Consolidation theory

The consolidation theory of soils under compression states that a load applied to a foundation is initially carried by the water in the pore spaces and will be gradually transferred to the soil skeleton over time.

[1] Rapid pile penetration due to a strong stratum overlying a soft layer. Pile run can lead to overpenetration of the pile or damage to installation equipment

[2] Pile refusal, or sustained hard driving is the inability to further install pile due to boulders or an extremely hard stratum. Pile refusal can lead to underpenetration of the pile or damage to installation equipment and pile

A mechanical model of a spring in a water-filled piston is often taken as an analogy, see Figure 3.1. The response of the soil is highly dependent on the permeability of the medium. As water commences to flow through the porous skeleton, it obeys Darcy's law. Terzaghi and Biot propose equations to model this coupled problem based on Darcy's law, see Section 4.2.1. (Biot, 1941; Selvadurai, 2021)

The expected magnitude of pore pressures and settlements depends on the dimensionality of the equipped equation. One-dimensional consolidation theory underestimates settlement rates as it excludes horizontal dissipation of pore pressures (Davis and Poulos, 1972). After consolidation is complete, creep will occur. However, due to the temporary placement of the mud-mat on the ocean bottom, creep is not within the scope of this research.

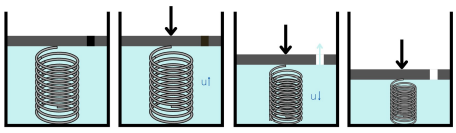

**Figure 3.1:** Mechanical model of a spring in a piston, analogous to a consolidating soil.

### 3.1.3 Bottom friction

Bottom friction is mobilized as horizontal forces act on the foundation. Inevitably, friction develops along the sides of the foundation as the foundation settles into the soil. Ninomiya et al. (1972) state that there is a relationship between settling time and side friction. As minimal mud-mat settlement is presumed in this research, side friction is disregarded. Bottom friction impacts the development of a failure mechanism, see Section 3.3 for a further explanation of how failure mechanisms occur.

### 3.1.4 Template operation

During operation, the pre-piling template is subjected to dynamic loading due to pile installation and environmental forces acting on the pile and template. In-situ time of a template ranges from $3$ to $48\ hours$. Roderick and Lubbad (1975) state that increasing an objects' in-situ time will increase both the breakout time and force, which is confirmed by experiments. Note that they consider permanent foundations. They hypothesize that this may be due to thixotropic strength regain of the disturbed sediment, most predominantly in clayey soil. Thixotropy of soil is the return to a stronger state after softening by remoulding under constant water content and constant volume conditions over time. Another hypothesis for increased breakout force with longer on bottom time is a larger degree of consolidation, and thus an increased excess pore pressure dissipation. (DNV, 2021a) Lastly, researchers propose that adhesion increases upon a longer duration of contact, see Section 3.2.2.

## 3.2 Mechanisms that contribute to underpressure generation during foundation uplift

This Section proposes a distinction of **four mechanisms** that contribute to a resisting force to uplift. Although these mechanisms are derived from literature, a similar distinction has not been made before. Figure 3.7b shows an overview of the mechanisms. Figure 3.2 shows how the mechanisms would appear in reality. Depending on the soil conditions, the mechanisms are expected to occur and impact the total underpressure that develops.

1. Negative pore pressures are generated as the upward load is initially carried by the pore water.
2. Adhesive bonding occurs between the soil and the foundation, depending on the cohesion.
3. The pore volume increases due to unloading by a combination of shear and tension and induces additional negative pore pressures.
4. A void between the foundation and soil must be filled with water causing a viscous drag along the foundation invert, which leads to an underpressure.

Finn and Byrne (1972, 1978) state that during the removal of a foundation from the subsoil, the **water takes the** instantaneous **uplift load**, see Section 3.2.1. Especially cohesive soils adhere to the foundation invert. This causes the soil to stick to the foundation invert, which adds to the resisting force. The pore volume increases due to **adhesion** of the soil to the foundation invert, as described in Section 3.2.2. In the work of Deshpande (2016), a distinction is made between two processes in tension tests of saturated soils: dilatancy and application of the tensile force. Soil dilatancy can drive the soil to a looser state, as does the application of tension. The combination of shear and tension as the soil is **unloaded** is further explained in Section 3.2.3. Foda (1982) states that the upwards movement of the soil with a

foundation is a consequence of viscous drag by pore fluid flow. This is argued to be incorrect as the soil movements are driven by adhesion and unloading effects. Inevitably, the development of negative pore pressures is in reality a combination of both water pressures developing and grain rearrangement. Lastly, a resisting force leads to an **underpressure** due to gap formation between the soil and the foundation invert. This contributes to the total resisting force, as pore fluid might be sucked out of the soil, see Section 3.2.4.

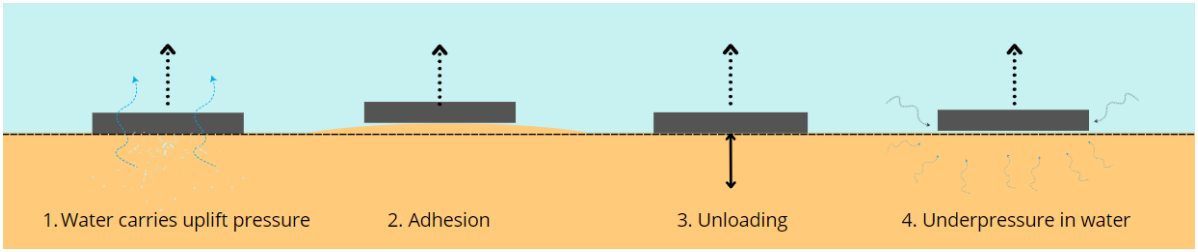


**Figure 3.2:** Four mechanisms that contribute to a resisting force during the uplift of shallow foundations.

### 3.2.1 Mechanism 1: Water carries uplift pressure

Finn and Byrne (1972, 1978) postulate that the uplift pressure is transferred to the soil by a reduction in pore pressure. This entails that the upward load during lifting is fully carried by the water until the contact is lost, as long as no water flow is induced. This is similar to compressing a foundation, where the foundation load is initially carried by the pore water, as long as the loading conditions remain undrained. Selvadurai (2021) calls the tension state during unloading and the subsequent water flow to increase the negative pore pressure to zero ”unconsolidation”. The magnitudes of excess pore pressure under compression and uplift loading along the foundation interface are similar, for equal load rates. These negative pore pressures contribute to the suction force that resists uplift.

Terzaghi’s principle distinguishes effective stresses ($\sigma'$) and pore pressures ($u$) as different contributions to the total stress ($\sigma$) in the porous medium: $\sigma = \sigma' + u$. Terzaghi’s equation, applied to the initial stage where the water sustains the total upward load, results in negative total stress, effective stress, and pore pressure at the foundation invert. The change in effective stress due to load application is close to zero. (Byrne and Finn, 1978)

Purwana et al. (2005) also suggest, when studying spudcan foundations, that at the foundation base the uplift load is translated mainly to the soil by pore pressure changes rather than by changes in effective stress. Results from earlier experimental work show that the total stress and pore pressures measured by sensors develop simultaneously and are of similar magnitude. It was found that for foundations with circular cross-sections, the highest pore pressure is observed in the center. This is expected as the flow paths to relieve the suction are the longest in the center of the foundation.

Note that this mechanism is not the opposite of consolidation, as water still tends to flow toward the area of the lowest pressure. The difference between compression and uplift is the location of the low-pressure area and the direction of water flow to dissipate the excess pore pressures. The spring analogy for consolidation holds for compression, see Figure 3.1, for uplift however it does not. A body of water cannot sustain pure tensile loads, and neither does a soil skeleton consisting of non-cohesive particles.

### 3.2.2 Mechanism 2: Adhesion

As the steel mud-mat comes into contact with the soil, adhesive bonding takes place. Adhesion can be understood as a boundary layer effect. Cohesion refers to the tendency of particles or surfaces to stick to each other due to intermolecular forces and mechanical effects. Adhesion and cohesion are different in that adhesion refers to the adhering of *dissimilar* molecules, while cohesion refers to the clinging of the *same* molecules. Adhesion occurs only in cohesive soils with at least $10$ to $20\%$ clay mineral[3] content. The level of adhesive bonding is thus dependent on mineralogy. (Spagnoli et al., 2019) The total soil volume increases slightly if adhesion causes the upper layer of the soil skeleton

[3]A soil is identified as a clay if the particle size is less than $0.002mm$. Clay soils do not necessarily consist of clay minerals. Clay minerals are layered secondary silicates of colloidal size. Their chemical composition and their charge can vary (Blume et al., 2016).

to move along upwards with the foundation. This will increase the pore volume, as the soil grains will not change in volume. This might result in additional negative pore pressures. Both due to the sticking and the increase in negative pore pressures, a resisting force is generated.

Vesic (1969), among the first researchers to study the breakout of objects from the ocean bottom, writes that the development of adhesion is a physico-chemical process that is parallel to the regeneration of shear strength of soils. Longer on bottom times are associated with larger values of adhesion. (Ninomiya et al., 1972). That clay adheres to steel surfaces is established and defined as problematic by Sass and Burbaum (2009) while studying the sticking of clay to the cutting wheel of tunnel boring machines. Burbaum and Sass (2017) also found that an increase in adhesion stress is the result of reduced water content. They demonstrate that adhesion depends on both clay mineralogy and pore water pressures. Non-cohesive soil, usually with higher permeabilities compared to clay, however, build up no adhesive forces. Material properties such as the roughness of the steel foundation are of minor influence on adhesion development. (Burbaum and Sass, 2017)

### 3.2.3 Mechanism 3: Unloading

Unloading of the foundation causes the grains close to the mud-mat interface to rearrange to a looser state. This results in larger pores and increased porosity. The unloading mechanism can be subdivided into a part shear and a part tension. A dilative effect is observed in dense granular sediments subjected to shearing. Very dense materials have the tendency to expand, which will lead to the suction of water into the pores. During the change in particle assembly, the particles slide with respect to each other which causes mechanical energy to dissipate. (Verruijt, 2001) Generally, sediments in offshore conditions in the upper layer tend to be in a loose state. Despite that, the sediment under the foundation is compressed due to the mud-mat loading. Strain energy is stored in the consolidated soil skeleton, showing elastic behavior upon unloading (Selvadurai, 2021). Note that an increased pore space entails that the hydraulic permeability increases. This suggests that less suction would be expected. That is however not the case as the water is not yet present at the area of suction and has to flow from the surrounding area to reduce the negative pore pressures.

The tension effect results in an increase in pore volume as well. Pure tension in a soil sample can however not be studied. A comparison with triaxial extension testing is made to gain further insight into soils under tensile loads. Yan et al. (2016) consider isotropic consolidated saturated clays in triaxial extension tests. The conclusion is drawn that during unloading, shear stresses generate positive pore pressure[4]. The contribution of the total mean stress is negative. The distinction between excess pore pressure generation due to a change in mean total stress and a change in deviatoric stress follows from Henkel's theory[5]. Immediately after unloading, the negative excess pore pressures exceed the positive pore pressures. For triaxial extension tests, the following can be concluded:

**Change in mean total stress** This is also called isotropic stress, which leads to negative excess pore pressures

**Change in deviatoric stress** This is the remaining part of the stress tensor, after subtraction of the isotropic stress, which leads to positive excess pore pressures

### 3.2.4 Mechanism 4: Underpressure in water

Ninomiya et al. (1972) are the first to describe a mechanism where a viscous force needs to be overcome for a cohesive soil to fill a void between the sediment and the foundation invert. Ten years later, Foda (1982) and Mei et al. (1985) state that after an object loses contact with the soil, an underpressure in the gap between foundation and mudline develops, although they consider sandy soils. This underpressure draws water into the gap. The water to fill the gap can originate from the surrounding water or the underlying soil if the permeability is sufficiently high. When the gap flow primarily starts to come from the periphery of the gap, the drag force from the porous medium vanishes, and the underpressure is reduced. At this instant, the forces that resist uplift are overcome.

It remains uncertain how this underpressure in the gap is exactly generated. If an object moves through a water body at high speeds, turbulent drag is predominant as fluid is pushed away. Under lower

[4]Although Yan et al. (2016) state that a change in deviatoric stress results in positive excess pore pressure, this depends on the characteristics of the medium and the combination of shear and tension. Changes in deviatoric stress in a granular material will result in negative excess pore pressure.

[5]Henkel's theory requires information about the stress states, which is often not available in offshore conditions. Especially the stress states at the mud-mat interface at the instant the uplift has commenced are hard to predict, see Section 2.3.2.

speeds, skin friction or viscous drag occurs. Fluid is dragged along the object as it moves upwards. Initially, when assuming a uniform tiny gap, the distance between the foundation and the soil is small, thus high water velocities are anticipated. Following fluid dynamics theory, the inertia of the moving fluid in a small gap is insignificant compared to the viscous force under this circumstance. Therefore, the fluid motion in the tiny gap may be regarded as a creeping flow. (Zhou et al., 2008)

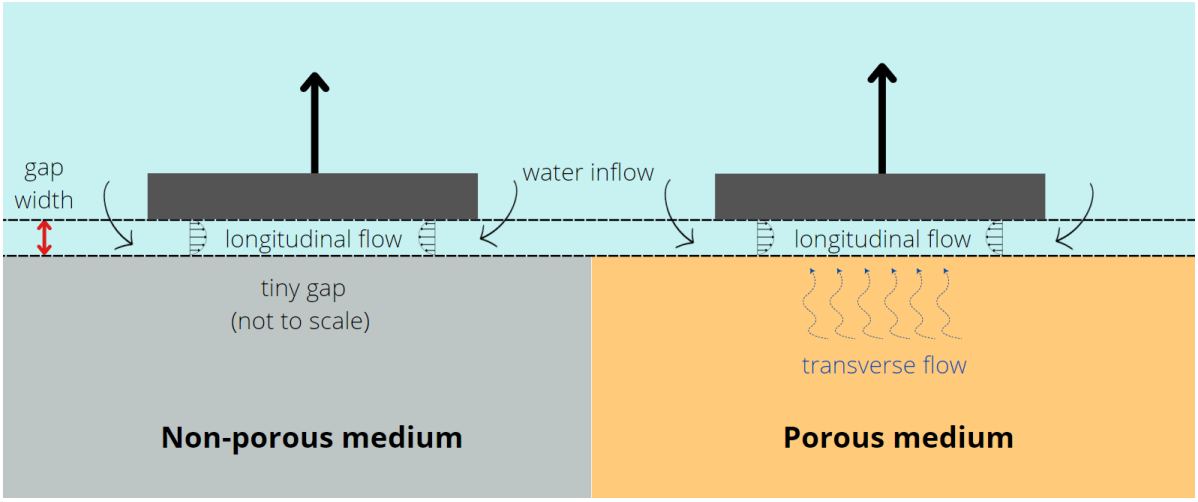


**Figure 3.3:** The longitudinal flow into the gap between the foundation and a non-porous or porous medium following detachment during uplift. Transverse flow only occurs in porous media.

Hypothetically, when a foundation detaches from a non-porous medium, such as a steel plate, a resisting force due to the underpressure would still be observed. However, in that case, no water flow from the underlying medium is present such that the void is solely filled with water from the surrounding water body. Figure 3.3 shows the flow into the gap for both a non-porous and porous medium, assuming a flat mudline after foundation detachment.

**Upward foundation displacement**

The foundation displacement until the maximum underpressure would be reached is a combination of the soil displacing due to adhesion and unloading effects, combined with the creation of a small void that needs to be filled. If the adhesion is reduced to zero, the uplift displacement is driven by the volume increase due to soil unloading and the occurrence of a tiny gap, see Figure 3.4.

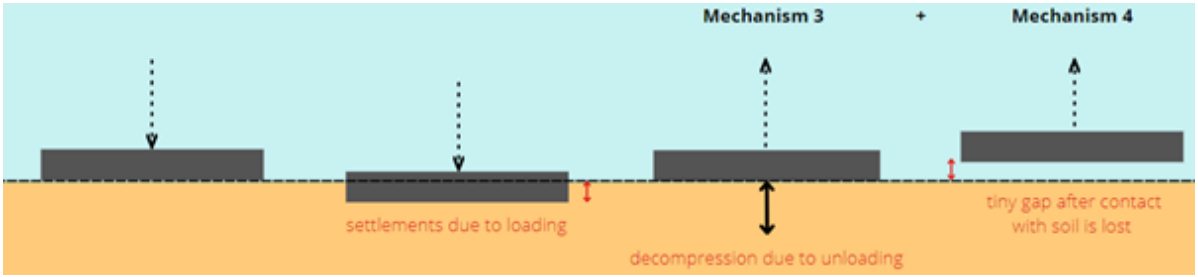


**Figure 3.4:** Displacements that occur during compression and uplift, if no adhesive bonding is present.

## 3.3 Mechanisms that lead to foundation breakout

Soil failure should be considered to assess the bearing capacity of a foundation and to understand how the underpressure is relieved. A mud-mat can fail during installation, operation, and retrieval. Especially the loss of contact during uplift is relevant for this study. The theory of foundations under compression is equipped to estimate failure under uplift.

Foundations fail due to the soil not being able to sustain the load. An ultimate failure mechanism will develop within the soil body. The Prandtl failure mechanism consists of three triangles with planes

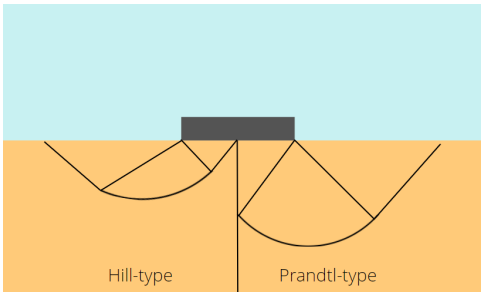


**Figure 3.5:** Hill and Prandtl type failure mechanisms for foundation under compression (modified from Mana et al., 2013).

at an angle of $45°$ and two wedges. In all the zones, the stress state is assumed to be critical. Hill-type failure mechanisms consist of four triangles. These failure surfaces are not under $45°$ inclination but are dependent on soil properties such as the friction angle. Figure 3.5 shows both mechanisms. (Verruijt, 2001, Mana et al., 2013) Note that the failure mechanisms are not taking into account any (change in) pore pressures.

If negative pore pressures develop within the soil body as the foundation is lifted from the seabed and the magnitude of suction is sufficiently high, a full reverse end bearing mechanism can be sustained. If the effective stress is reduced to zero before the full mechanism develops, either a crack within the soil or a partial gap between the foundation invert and mudline is generated. Which failure mechanism develops is highly dependent on the possibility of pore water flow (Li et al., 2014). Following Liu (1969), the soil can fail in one or a combination of the three ways. Figure 3.6 shows the mechanisms that lead to foundation breakout.

**a** Adhesion force failure: a crack at the foundation inverts develops.
**b** Shear stress failure: a failure mechanism develops within the soil body.
**c** Soil tension failure: the tensile strength of the soil is overcome.

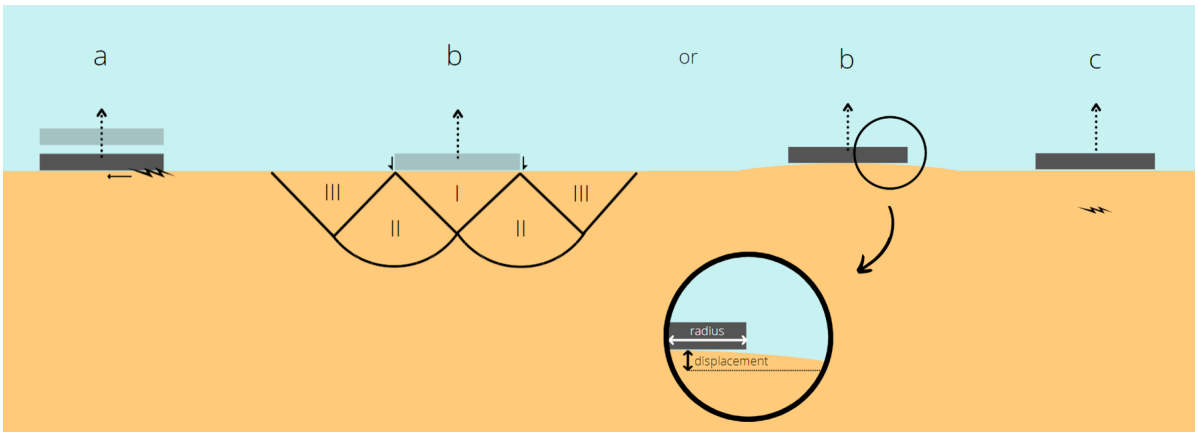


**Figure 3.6:** Failure mechanisms of foundations under uplift: (a) Crack propagation, (b) Reverse end bearing mechanisms (left) or Hemispherical contraction (right), (c) Tensile failure.

### Crack propagation

If the ocean bed is rigid and adhesion between the soil and foundation is low, it is unlikely that the soil will move upwards with the foundation during uplift. Suction can develop, as the tensile force will be transferred to the pore water. As the pore sizes are expected to remain mostly unchanged, the magnitude of the suction will be lower than in soft seabeds. Figure 3.6a shows the crack propagation. It is hypothesized that rapid suction generation occurs, until the total loss of adhesion. This indicates failure. To which extent water is allowed to flow towards the area of negative pore pressures depends on the hydraulic permeability, uplift velocity, and mineralogy of the sediment type.

**Reverse end bearing**
The reverse end bearing failure mechanism is equal to the ultimate bearing mechanism, see Figure 3.5, but opposite in direction. The reverse end bearing mechanism is most evident in skirted foundations, as the suction is sustained more easily. It could theoretically also be mobilized during the undrained uplift of unskirted shallow foundations. The soil underneath the plate moves upward with the foundation by sustaining adhesion at the foundation invert. This mechanism is highly dependent on soil cohesion. Figure 3.6b shows the theoretical shape of the failure plane and the upwards movements of the soil.

Some soils stick to the mud-mat invert after foundation retrieval. Roderick and Lubbad (1975) show that some silty clays move upwards along with the foundation. The soil mass in their experiments has a conical shape. The model foundation size (50 mm) is substantially smaller than mud-mats under a pre-piling template ($4$ to $12m$). In reality, mud-mat uplift could never result in such sediment displacements as adhesion is not sufficiently high to carry a considerable amount of soil upwards.

**Hemispherical contraction**
If the reverse end bearing mechanism does not fully develop, a breakout hemispherical contraction-type mechanism can develop. This indicates partial gap formation, starting at the circle periphery, where failure propagates inwards with upwards foundation movement. Water flows to the regions of negative pore pressure. Figure 3.6b shows how the seabed displaces. These displacements occur until the suction is relieved and the contact between the foundation and soil is lost. Once a partial gap forms, a transverse water flow is likely to speed up the underpressure relief. This could temporarily lead to an additional resisting force, see Section 3.2.4. The effective foundation area decreases with gap formation, causing the load transfer to the soil to change as well. Cavity expansion theory could be equipped to model the loss of adhesion and for obtaining an equation for the changes in radial stresses. (Chen et al., 2012; Zhou et al., 2008)

**Tensile capacity**
The uplift problem could be considered pure tensile failure if shear is disregarded. The tensile strength of the sediment would than dictate the foundation capacity. The tensile strength of clay is highly dependent on the consolidation pressure. (Tamrakar S et al., 2013). The tensile capacity of the soil is limited by the tension cut-off. The tensile strength is an outcome of extrapolating the test results from the compressive regime, however, this leads to large uncertainties. Li et al. (2019) state that the tensile strength of the soil depends significantly on porosity. Rodríguez (2006) states contradictory that the influence of void ratio on tensile strength becomes insignificant when the soil is close to saturation (as cited in Li et al., 2019).

## 3.4 Conclusion
This Chapter proposes that suction does not exist by itself but is a combination of four mechanisms. The resisting force that needs to be overcome in excess of the submerged weight of the pre-piling template, is not purely a change in pore pressure. A change in the pressure in the water body develops as the foundation loses contact with the underlying sediment. Figure 3.7 summarizes the mechanisms that occur in a soil body as a foundation is installed and describes the soil behavior as a foundation is removed from a seabed. It is clear that the soil behavior during compression differs from the behavior during uplift. Whether these mechanisms can be observed and whether their respective sequence can be proved will be studied in physical experiments, executed as described in Chapter 5.

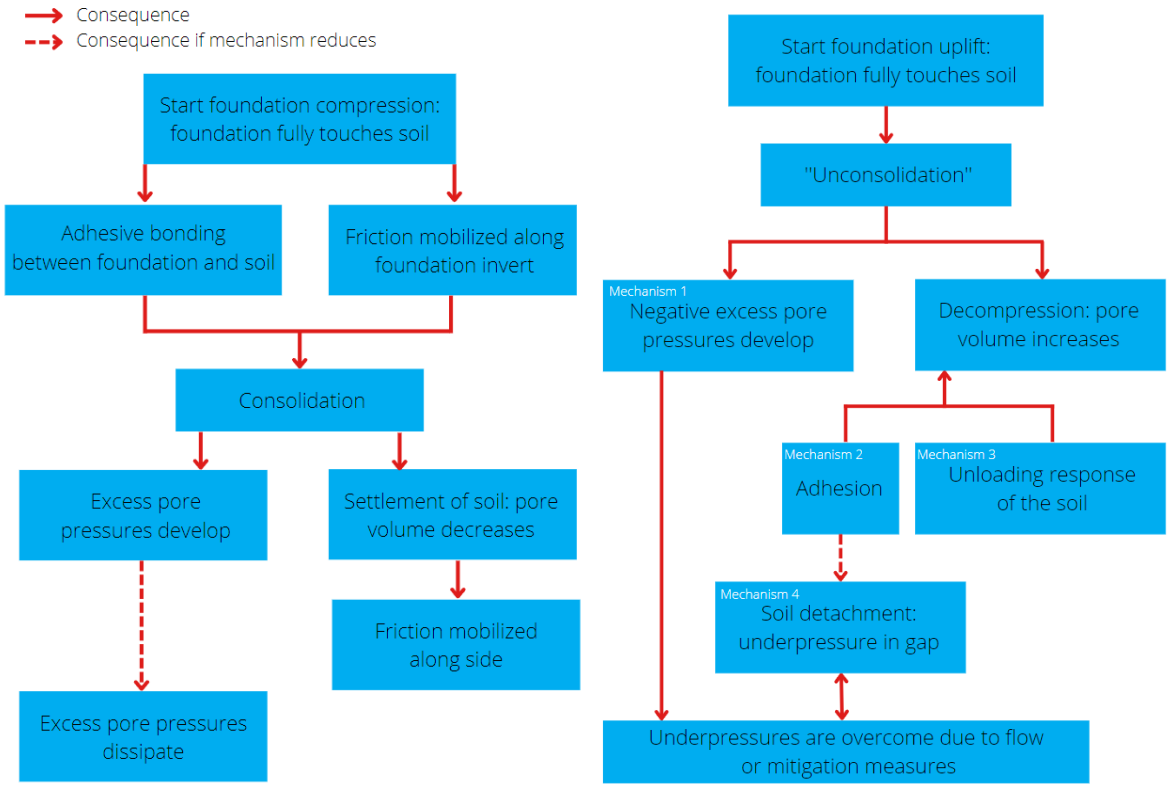


**Figure 3.7:** Overview of mechanisms that occur during compression (left) and uplift (right) of offshore shallow foundations.

# 4

# Existing calculation methods

The background of mud-mats under pre-piling templates is covered in Chapter 2 and Chapter 3 listed the mechanisms that occur during a sequence of mud-mat installation and removal. In this Chapter, the reader will be informed about the state of the literature regarding the modeling and quantifying of suction and underpressures. This Chapter is part of the research to explore the current methods that geotechnical engineers employ to study foundations (under uplift) and quantify stresses within the soil. The experiments will aid in determining whether these equations are suitable and accurate tools to model the underpressures. Methods from literature and offshore standards that quantify the breakout force, breakout time, and pore pressure changes are presented. Next, calculation methods to model the separate mechanisms that contribute to the underpressure are presented.

## 4.1 Object breakout from seabed

Efforts to quantify both breakout force and breakout time from early literature on underpressure generation are presented. Note that the equations are not necessarily drafted for temporary shallow foundations. The formulas are also equipped for arbitrary shapes that are buried and need to be removed from seabed. The intended purpose is indicated for each equation for clarity.

### 4.1.1 Uplift capacity

Prandtl composed an equation to estimate the ultimate bearing capacity of shallow foundations, which was extended by Brinch Hansen and others. This equation, Equation 4.1, is derived for strip foundations under compression. The equation includes factors for the soil cohesion, surcharge, and unit weight of the soil. Additional factors can be included to model inclined loads, rectangular foundation areas, or sloping soil surfaces. (Verruijt, 2001; Verruijt and Merwehoofd, 1994)

$$q = cN_c + q_0 N_q + \frac{1}{2}\gamma B N_\gamma \tag{4.1}$$

As stated in Section 3.3, the same equation can be utilized for foundations under uplift. Chen et al. (2012) propose a simpler version, Equation 4.2, to calculate the uplift capacity of offshore mud-mats. The undrained shear strength $s_u$ is supposed to be equal to the soil cohesion $c$. This equation includes the factor $\alpha$ to indicate to which extent a full reverse end bearing mechanism ($\alpha = 1$) can develop. A cavity contraction mechanism, see Section 3.3, is indicated by $\alpha = 0$. This factor mainly captures the 'sticking' of the soil to the mud-mat. The equation only holds for embedded foundations, as $h$ represents the depth of the foundation. See also the work on the vertical bearing capacity of perforated mud-mats of White et al. (2005) in which the variation of $N_c$ is elaborately discussed.

$$q_u = s_u N_c - \gamma' h \alpha \tag{4.2}$$

The uplift capacity of foundations located on the seabed can be calculated with Equation 4.3. In this equation, the load inclination and shape factor are included. Mitigation measures that reduce the effective foundation area such as perforations can be included to obtain a reduced uplift capacity. (Tapper et al., 2015)

$$q_u = s_u N_c i_c s_c \tag{4.3}$$

In their study, the term $N_c$ denotes the undrained bearing capacity factor which depends on cohesion, foundation shape, skirts, load directionality, and perforations. $N_c$ captures the indistinguishable contributions in the resistance to uplift of the various mechanisms.

**DNV Standard**
DNV-ST-N001 (2021c) states that for the retrieval of an object that is placed on the seabed, forces due to suction should be calculated. The equation from the following DNV Sections *may* be used to calculate suction forces. The effect of the landing on the sea bottom for high set-down velocities should be taken into account when designing lifting equipment. This effect is quantified with the total dynamic mass, design soil resistance, and soil displacement. This adds to the suction forces and submerged structure weight.

**DNV Recommendations**
DNV-RP-C212 presents a more detailed version of the Brinch Hansen equation, in addition to making a distinction between drained or undrained, and a constant or a linearly increasing shear strength. The following equations are presented in the corresponding paragraphs in DNV. (2021a)

***5.4.6*** Bearing capacity for fully drained conditions

$$q_u = \frac{1}{2}\gamma' b_{eff} N_\gamma s_\gamma d_\gamma i_\gamma + (p'_0 + a) N_q s_q d_q i_q - a \tag{4.4}$$

***5.4.7*** Bearing capacity for undrained conditions – constant shear strength

$$q_u = N_c s_u (1 + s_{ca} + d_{ca} - i_{ca}) + p'_0 \tag{4.5}$$

***5.4.8*** Bearing capacity for undrained conditions – linearly increasing shear strength with depth

$$q_u = F(5.14 s_{u0} + \frac{k b_{eff}}{4})(1 + s_{ca} + d_{ca} - i_{ca}) + p'_0 \tag{4.6}$$

### 4.1.2 Breakout force

Whereas the uplift capacity is often equipped to determine whether a foundation will remain stable under tensile loading, the breakout force describes the force necessary to lift and retrieve a foundation from the seabed. Poinc proposes Equation 4.7 to calculate that force for an arbitrary object. $k_p$ is an empirical coefficient that depends on the soil type. (1970, as cited in Sawicki and Mierczyński, 2003) This equation is merely a rough estimate of the breakout force.

$$F_{breakout} = (1 + k_p) W' \tag{4.7}$$

The breakout force can also be calculated as the addition of the force necessary to overcome the uplift capacity and the submerged weight of the structure.

$$F_{breakout} = q_u A + W' \tag{4.8}$$

Craig and Chua (1990), studying undrained spud-can extraction, propose to include the weight of the soil that is displaced by the object. The soil will adhere to the top of the spudcan and will be displaced upwards.

$$F_{breakout} = q_u A + W' + W'_s \tag{4.9}$$

Muga (1968) postulates that the breakout force can be derived with the empirical formula in Equation 4.10. The force is time-dependent. Liu (1969) investigated the problem in the 1960s in a similar manner. Although findings of Liu show a significant scatter, still a trend is clear. Muga's correlation however disagrees with Liu's data.

$$F_{breakout} = 0.2 A q_u e^{0.0054(t-260)} + W' \tag{4.10}$$

### 4.1.3 Suction force

Ninomiya et al. (1972) state that the suction force that resists the uplift of sit-on-bottom type offshore structures in cohesive soils consists of side friction, a viscous force, and bottom adhesion. The viscous force is dependent on the uplift velocity and is required in the calculations as the soil fills the void space resulting from the upward foundation movement. The equation Ninomiya et al. present to calculate the suction force depends on many constants that have to be derived experimentally. Although this distinction of mechanisms that contribute to a downward force upon foundation uplift is a first of its kind, the proposed equation does not prove to be practically applicable.

### 4.1.4 Breakout time

Previous research also aims to quantify the amount of time required to retrieve an arbitrary object from the ocean bottom. This breakout time can be calculated with Equation 4.11, which shows a dimensionless correlation between the breakout force and the breakout time. (L. Liu, 1969)

$$\frac{F_m}{F_r} = 1.5 \left( \frac{T}{T_{in-situ}} \right)^{-0.07} \text{ for } 10^{-3} < \frac{T}{T_{in-situ}} < 10 \tag{4.11}$$

Where:
$F_m$ is the mean soil holding strength
$F_r$ is the static soil resistance due to shear and tension
$T_{in-situ}$ is the soil in-situ time
$T$ is the allowed pull-out time

Roderick and Lubbad (1975) present Equation 4.12 in which $R_0$ is the force ratio required for breakout in time $T_0$. Both Equation 4.11 and 4.12 are not verified by other researchers.

$$T = T_0 e^{(R_0 - R)/m} \tag{4.12}$$

Where:
$R_0$ is the breakout force ratio
$R$ is the ratio of the force over the submerged object weight
$T_0$ is an arbitrary reference time
$m$ is the slope of the $R$ versus $ln(T)$ plot

## 4.2 Mechanism 1: Water carries uplift pressure

The nature of this mechanism is the changes in pore pressure corresponding to the changes in force, as Equation 4.13 describes. The force in the crane will gradually increase to lift the structure from the seabed. As described in Section 3.2.1, the analogy to the consolidation of foundations under compression can be made to partially understand this uplift mechanism. Equations from consolidation theory are presented to model changes in pore pressures as the stress in the soil body changes.

$$\Delta u = \frac{F}{A} \tag{4.13}$$

It is hypothesized that Equation 4.13 changes to Equation 4.14, for a reduced foundation area that is still fully in contact with the soil.

$$\Delta u = \frac{F}{A_{eff}} \tag{4.14}$$

### 4.2.1 Consolidation

In this Section, the equations to model soil consolidation under compression are presented for the three-dimensional scenario. These equations form the basics of the theory of Sawicki (1995) to model pore pressures under foundations under uplift. Next to that, the dissipation of excess pore pressures could be modeled with the consolidation equations, for the soil behavior of foundations under compression or tension.

**Biot's theory**
Biot (1941) presents a three-dimensional formula to model the coupled consolidation problem. Equation 4.15 quantifies pore pressure dissipation as well as soil deformation. This equation is considered complex and relatively few solutions have been obtained. (Davis and Poulos, 1972)

$$\frac{du}{dt} = c_v \nabla^2 u + \frac{1}{3}\frac{d\theta}{dt} \tag{4.15}$$

In this equation, $c_v$ is the consolidation coefficient, $u$ is the pore pressure, and $\theta$ is equal to the addition of the principal stresses: $\sigma_x + \sigma_y + \sigma_z$. The consolidation coefficient is dependent on the hydraulic conductivity $k$, see Equation 4.16. $\nabla$ represents the LaPlace operator, making this equation a partial differential equation, see Equation 4.17.

$$\text{for the general case: } c_v = \frac{k}{\gamma_w m_v} \tag{4.16}$$
$$\text{for the one-dimensional case: } c_{v1} = \frac{kE'}{\gamma_w}\frac{(1-\nu')}{(1-2\nu')(1+\nu')}$$

$$\nabla^2 = \frac{\partial^2}{\partial x^2} + \frac{\partial^2}{\partial y^2} + \frac{\partial^2}{\partial z^2} \tag{4.17}$$

The simplified diffusion theory of consolidation assumes $\frac{d\theta}{dt}$ to be zero, reducing Equation 4.15 to Equation 4.18. This is assumed to be true for a constant load if $\sigma$ remains unchanged. The simplified equation can be solved as an ordinary diffusion equation.

$$\frac{du}{dt} = c_v \nabla^2 u \tag{4.18}$$

To solve the differential equation, the initial and boundary conditions have to be defined. Davis and Poulos (1972) state that for consolidation the initial pore pressure equals the mean stress, $u(t=0) = {}^{\theta}/_{3}$. If the Poisson's ratio of the soil is equal to $0.5$, the initial pore pressures equal the applied surcharge. Verruijt (1982) incorporates the compressibility of the water and soil in the initial pore pressures.

**Sawicki's theory**
Selvardurai (2021) presents a modified Terzaghi equation, which includes the bulk moduli of the porous skeleton and the solid material, see Equation 4.19.

$$\sigma = \sigma' + \left(1 - \frac{K_D}{K_S}\right) u \tag{4.19}$$

Similarly, Sawicki (1995, 2003) introduced an equation in which the ratio of the compressibility of the pore fluid over the compressibility of the solid material is included. Sawicki's theory is derived from the mass balance equation for the pore fluid. The reader is referred to the articles for the derivation. Equation 4.20 shows the obtained partial differential equation.

$$\zeta \frac{\partial u}{\partial t} = \nabla^2 u + \xi \frac{\partial \sigma}{\partial t} \tag{4.20}$$

In the theory, the compressibilities are included in the constants $\zeta$ and $\xi$, see Equation 4.21. The initial porosity at the start of uplift is required to calculate the development of pore pressure over time and space.

$$\zeta = \frac{\gamma_w(\kappa^S + n_0\kappa^D)}{n_0 k} \tag{4.21}$$
$$\xi = \frac{\gamma_w \kappa^S}{n_0 k}$$

Equation 4.20 reduces to Equation 4.22 for the one-dimensional case after rewriting.

$$\frac{\partial^2 u}{\partial z^2} - \zeta \frac{\partial u}{\partial t} + \xi \frac{\partial \sigma}{\partial t} = 0 \tag{4.22}$$

**Undrained conditions**
As stated previously, the maximum suction occurs in undrained conditions. Sawicki's theory for the one-dimensional case reduces to Equation 4.23 if the hydraulic conductivity $k$ is very small. This indicated undrained conditions.

$$\frac{du}{dt} = \frac{\xi}{\zeta}\frac{d\sigma}{dt} \tag{4.23}$$

The magnitude of the uplift force needs to be known to calculate how the pore pressure changes over time due to changes in vertical stress. If the force is assumed to increase linearly, the total stress can be calculated with Equation 4.24. The parameters $d$ and $b$ are the water depth and foundation thickness respectively. Parameter $a$ is a coefficient calculated by dividing the uplift force rate in $kN/s$ over the foundation area in $m^2$.

$$\sigma_z = -at + \gamma_w d + (\gamma_b - \gamma_w)b \tag{4.24}$$

The parameters that are utilized in the equations derived from consolidation theory are expected to not solely influence this mechanism. For example, the compressibility coefficient also affects the unloading behavior.

## 4.3 Mechanism 2: Adhesion

The adhesion strength is most commonly experimentally derived. Either a foundation is left to settle, after which the surrounding soil is removed to omit side friction and the pulling force is measured (Ninomiya et al., 1972) or a specially designed adhesion test device is employed (Sass and Burbaum, 2009). How the adhesion develops over time remains unknown. Calculating adhesion is not yet attempted as the micromechanical behavior of cohesive sediments is largely unexplored and highly dependent on mineralogy. Mei et al. (1985) aim at modeling loss of adhesion. Despite attempts to simplify calculations, the numerous resulting equations are difficult to use in practice. The reader is referred to the paper for the equations and the derivations.

## 4.4 Mechanism 3: Unloading

Triaxial tests are equipped to study soil behavior by imposing loads in three directions. Triaxial extension tests can be performed to model the soil in the wedge underneath the foundation from Prandtl's failure mechanism if an upward load is applied, see Figure 3.6 (Byrne and Finn, 1978). Yan et al. (2016) state that triaxial extension tests can be divided into three stages according to their unloading path:

- Relief triaxial extension.
- Common triaxial extension.
- Average stress for constant triaxial extension.

Yan et al. (2016) compare the first stage of a triaxial extension test to foundation uplift. A constitutive model to capture the soil behavior is required to calculate the stresses and pore pressures at this stage. In their work, the Modified Cam Clay model is equipped. $p$ is the mean stress, $p'$ is the effective mean stress, and $q$ is the deviatoric stress. The pore pressure in the $p-q$ and $p'-q$ space is the difference between the total and effective mean stress.

$$\Delta u = \Delta u_p + \Delta u_q \tag{4.25}$$

Initially, the excess pore pressure is negative upon unloading. The excess pore pressures become positive over time. The Modified Cam Clay accurately predicts this.

## 4.5 Mechanism 4: Underpressure in water

Foda also adapts Biot's consolidation theory: Together with Mei (1980, 1981, see also Mei et al., 1985), Foda proposes a boundary layer approach to obtain a 'small-time' solution for the coupled Biot's equation. Initially, the water is modeled to flow out of the porous seabed to fill the void that is left by a displaced foundation. Water flows towards the area of largest underpressure. After a certain gap width

between the seabed and the foundation invert is reached, a longitudinal flow becomes predominant in relieving the underpressure. The porosity and the elasticity of the seabed influence the water flow. Chang et al. (2015) take a different approach to model this flow from and near a rigid porous bed: They apply Stokes flow to the gap, equip Brinkman equations to the viscous effect of pore flow within the porous medium and Song and Huang's complete interfacial conditions to the bed interface.

The equations to model the underpressure in water in a tiny gap are complicated. Lubrication theory is used to model flow in a pipe, analogous to the flow in the tiny gap. In work from Zhou et al. (2008), again Stokes' equation, see Equation 4.26, is altered. The pressure over time and radius is dependent on the longitudinal flow velocity and the position along the gap width (z-coordinate). Presenting boundary conditions for this second-order partial differential equation is not within the scope of this research.

$$\frac{\partial u(r,t)}{\partial r} = \mu \frac{\partial^2 v_r(r,z,t)}{\partial z^2} \tag{4.26}$$

## 4.6 Conclusion

In this Chapter, multiple methods to calculate breakout force, breakout time, and pore pressure changes due to uplift are presented, as well as equations to calculate the effects of the mechanisms that contribute to pressure differences. The equations as presented in the DNV assume a reverse end bearing mechanism. In practice, this can not develop under a shallow unskirted foundation. These equations are thus conservative. Some researchers assume pore flow within the soil body, although it depends on the load rate whether this can occur in fine-grained, cohesive sediments during uplift. The reported equations in this Chapter to quantify the mechanisms separately do not allow for a superposition to obtain an accurate value for the expected maximum peak force. This is due to the fact that the underpressure generation is not linear over time. It is expected that there's an interplay of mechanisms. Table 4.1 shows an overview of the presented approaches and whether they accurately capture the mechanisms. The last column indicates the most relevant parameters from each equation for the uplift problem. After analyzing the experimental results, an assessment to include or exclude parameters in a calculation method is made in Chapter 10.

**Table 4.1:** Calculations methods that are listed in this Chapter. It is indicated for each method whether the distinction between mechanisms is made in the equations. The last column indicates the relevant parameters for underpressure estimations.

| Calculation methods | Water carries the uplift pressure | Adhesion | Unloading | Underpressure in water | Relevant parameters |
|---|---|---|---|---|---|
| Brinch-Hansen | No | Yes | Yes | No | $s_u$, $N_c$ |
| DNV | No | Yes | Yes | No | $s_u$, $N_c$ |
| Ninomiya et al. | No | Yes | No | Yes | $A$, $v$ |
| Liu | No | No | Yes | No | $T_{in-situ}$ |
| Biot | Yes | No | Yes | No | $c_v$, $E'$ |
| Sawicki | Yes | No | Yes | No | $\zeta$, $\xi$ |
| Zhou et al. | No | Yes | Yes | Yes | $r$, $k$, $E$ |

# 5 Experiments

It is concluded from literature that multiple mechanisms contribute to the force that resists foundation uplift. The postulation that *suction* is better described as a combination of several mechanisms needs to be verified. An experimental program is designed such that the following questions can be answered:

- Which mechanisms can be observed and distinguished in physical experiments that contribute to underpressures during uplift?
- What is the sequence of these mechanisms or do the mechanisms occur simultaneously?
- What is the relative magnitude of these mechanisms?

## 5.1 Goals and hypotheses

Goals for the experimental program and hypotheses are drafted for each of the mechanisms, as displayed in Table 5.1. This aids in designing an adequate experimental program. It is expected that the behavior of *drained* and *undrained* soils under uplift largely differs due to differential pore pressure generation, permeability effects, and adhesion. The tests will thus be executed both in clay and sand to get a proper understanding of the mechanisms in different soil types.

## 5.2 Experimental program

An experimental program is designed to work towards the goals and verify the hypotheses, as presented in Table 5.1. Relevant comparisons between graphs will be made to gain insight into the mechanisms, these are displayed in Table 5.2. In Chapters 6 and 7 the presented results are sorted by the parameters, for clarity. The program is designed such that all tests can be executed in the laboratory of TWD with the available test bench, with adjustments to the mud-mat and test bench settings, as displayed in Figures 5.1 and 5.4. See Appendices A.3 and A.4 for the specifications of the test bench and mud-mats.

**Table 5.1:** Goals and hypothesis for the mechanisms.

| | Mechanism 1: Water carries uplift pressure | Mechanism 2: Adhesion | Mechanism 3: Unloading | Mechanism 4: Underpressure in water |
|---|---|---|---|---|
| Goals | · Verify that pore pressure follows force rate<br>· Derive magnitude of pore pressures<br>· Obtain time when either underpressure relief occurs or skeleton starts deforming | · Verify that adhesion contributes to the development of a resisting force in cohesive soils<br>· Derive magnitude of adhesive strength<br>· Observe whether adhesion increases over time | · Verify that an increase in void ratio occurs and causes underpressures<br>· Derive magnitude of resisting force due to unloading<br>· Investigate whether unloading adds to the deformations (due to adhesion) | · Verify that still a resisting force is observed if there is solely a tiny gap between the soil and the foundation invert<br>· Derive magnitude of resisting force due to the underpressure<br>· Investigate whether underpressure leads to water getting sucked out of the soil |
| Hypothesis | · Pore pressures develop with increasing force rate, until the pore water starts to flow | · Adhesion is only prevalent for suction development if the tensile strength of the soil is larger than the adhesive strength at the foundation invert<br>· Loss of adhesion occurs at the periphery of the foundation and propagates inward [1] | · If there is no adhesion between the foundation and the soil, still a resisting force due to the unloading behavior of the soil is expected | · After the foundation loses contact with the soil, still, a resisting force is present |

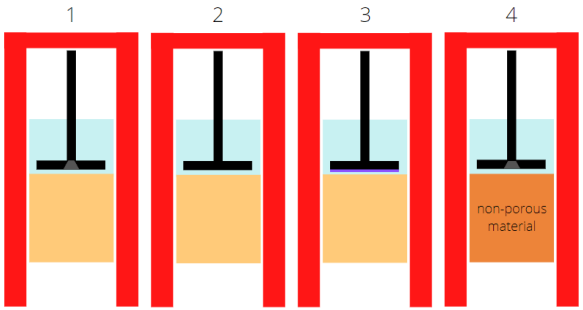


**Figure 5.1:** Set-ups to study the mechanisms that are equipped in the experiments. (1) Water pressure sensor, (2) No pressure sensor, (3) Adhesion reduction layer, (4) Non-porous material.

[1]Note that as the foundation is installed in water to imitate offshore conditions, it cannot be observed at which exact moment this occurs

**Table 5.2:** Comparisons between tests to draw conclusions on mechanisms.

| Mechanism | Variable | Range | Comparison |
|---|---|---|---|
| Mechanism 1: Water carries uplift pressure | Load rate | Vary load rate between $1$ and $800N/s$ | Compare force, displacement, and water pressures and maximum values, *do negative water pressures follow the uplift force?* |
| Mechanism 2: Adhesion | Area | Test with $150$ and $200mm\varnothing$ mud-mat | Compare force and displacement, *does the adhesion depend on the area?* |
| | Preload | Vary preload between $50$ and $1000N$ | Compare force, *is the adhesion-dependent on the normal force during compression?* |
| | Settling time | Vary settling time between $20\ sec$ and $14\ hours$ | Compare force, *is adhesion time-dependent?* |
| Mechanism 3: Unloading | Interface layer | Apply interface layer (cellophane and grease) to foundation invert, test on steel plate | Compare force, *is adhesion eliminated or reduced with interface layer and grease?* |
| | Interface layer | Apply interface layer to foundation invert, test on soil | Compare force and displacement with and without interface layer and grease |
| | Preload | Vary preload between $50$ and $1000N$ | Compare force-displacement graphs, *does the unloading effect increase with higher preload?* |
| | Settling time | Vary settling time between $20\ sec$ and $30\ min$ | Compare force and displacement, *does soil relaxation occur, and does this diminish the suction?* |
| | Step-wise uplift | Apply uplift until the submerged weight of the structure is reached, wait for $1\ min$ and continue pulling | Compare force, *does the underpressure decrease due to the partial unloading effect that allows for pore pressure dissipation?* |
| Mechanism 4: Underpressure in water | Gap width | Vary gap width between $0$ and $15mm$, test with water on steel plate | Compare force and water pressures, *is there a resisting force and underpressure during uplift due to a tiny gap*? |
| | Gap width | Vary gap width between $0.5$ and $15mm$, test with water on soil | Compare force, *is the resisting force, if present, dependent on gap size?* |
| | Area | Test with $150$ and $200mm\varnothing$ mud-mat | Compare force, *does the length of the flow path influence the resisting force?* |

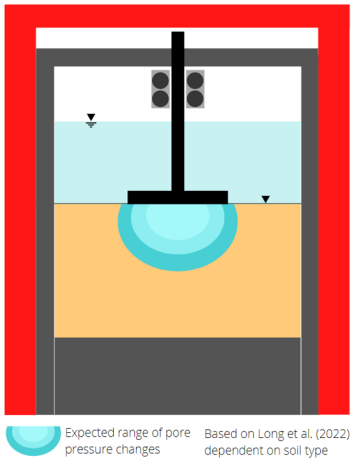


**(a)** Schematic test set-up.

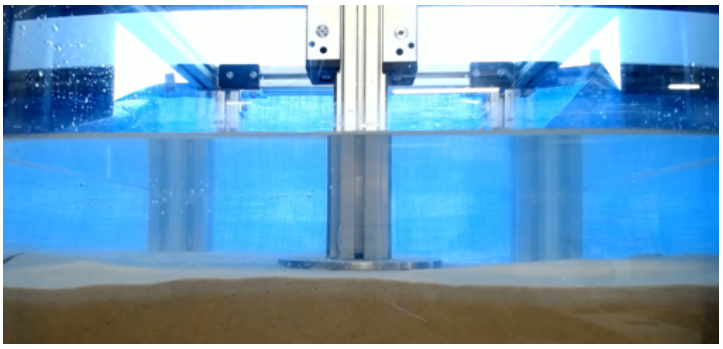

**(b)** Picture from mud-mat on sand sample.

**Figure 5.2:** Experimental test set-up.

## 5.3 Set-up

Small-scale experiments are executed during which a mud-mat is pressed into the soil, to mimic pre-piling template placement. The experiments are performed in the laboratory of TWD, Rotterdam. A small-scale laboratory set-up has advantages compared to on-site testing:

- Controllable parameters
- Good visibility on set-up and test execution
- Tests are easier to reproduce
- Tests are faster to conduct

The tests are performed in a water-tight Plexiglass container that is supported by aluminum rods. This frame ensures that the container walls do not bend and that the seams remain in place. The dimensions of the container are $500mm$ x $500mm$ x $500mm$. This container is placed on the test bench and filled with either clay or sand. The thickness of the soil sample is $160mm$. After filling the container with soil, the sample is wetted until fully saturated and the water column height on top of the soil sample remains unchanged. The height of the water column is $100mm$. The foundation plate is attached to a stiff aluminum rod, that can be attached to and detached from the test bench with bolts and nuts in one connection point. There is no bolt clearance in this connection and no movement is allowed. Water pressures are recorded for selected tests. As the water pressure sensor is located in the middle of the plate, two additional aluminum rods are added to transfer the load from the test bench to the plate. The rods are attached with countersunk bolts through the foundation plate. A roller system is designed to ensure pure vertical movement and to avoid moment generation in the test bench. The foundation will only move upwards and downwards through the rollers. The friction that is generated from the rollers against the rod is negligible. In between tests, the soil sample was flattened and leveled, to guarantee the perpendicularity of the load from the test bench and the ground level. Figure 5.2 shows the set-up. It is ensured that the positions of the ground level and water level remain constant throughout all tests.

The foundation is lowered until the contact with the seabed is recorded in the load cell by a sudden increase in force. The force is allowed to increase to $20N$ and is tared. At that instant, a preload is applied which represents the load of the weight of the pre-piling template that is transferred to that mud-mat. For a predefined amount of time, the mat remains on the seabed, under constant load. Limited mud-mat settlement might occur, depending on the preload and the settling time. After the settling time has elapsed, the mud-mat is lifted from the seabed, in a force-controlled manner. The instant the foundation reaches its original position, the movement stops, data recording is finalized and the test method is closed. The forces that act on the system are displayed in Figure 5.3.

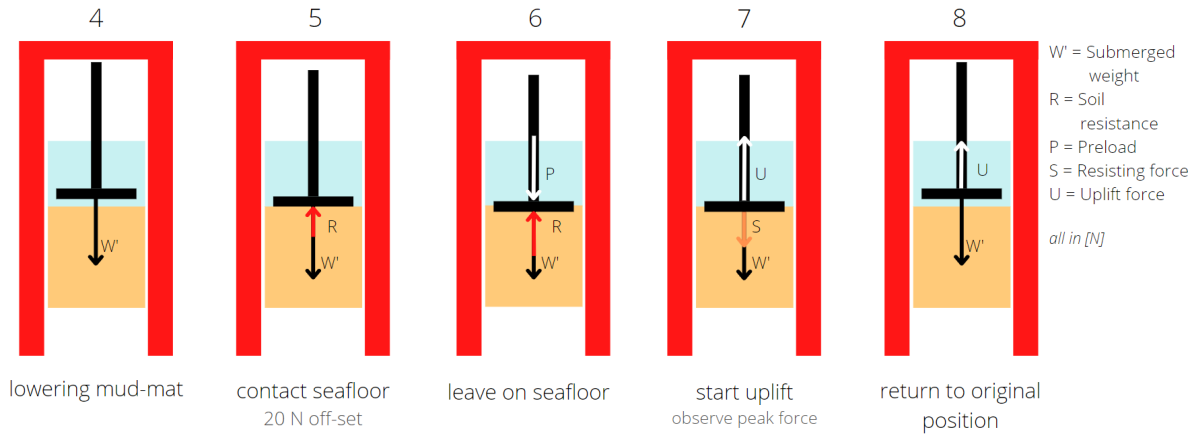


**Figure 5.3:** Steps of one test in a free body diagram, numbering coincides with Figure 5.8a.

A variety of mud-mat types are equipped in the experimental program. Complying with Tables 5.1 and 5.2, the mud-mat diameter is adjusted and an adhesion reduction layer is added to the underside for the corresponding tests. This effectiveness of the interface layer is discussed in Chapter 6.

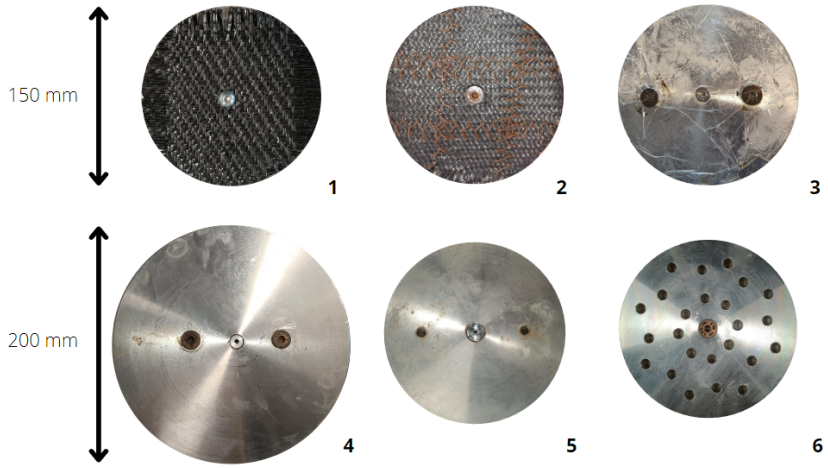


**Figure 5.4:** Overview of mud-mats equipped in the experiments. (1) Geotextile, (2) Perforated with geotextile, (3) Adhesion reduction layer, (4) Regular large, (5) Regular small, (6) Perforated.

### 5.3.1 Soil sample

Both a clay sample and a sand sample are prepared for testing. This fine sand consists of $99\%$ quartz and particle sizes range from $0.1$ and $0.3mm$. DINOloket was consulted to verify that the clay sample actually contains clay minerals, see Figure A.1. As clay is found in the upper layer, it can be assumed that the sample is in fact clay. Next to that, adhesion at the foundation invert is observed. As described in Section 2.3.2, the soil properties of the upper layer in reality are subjected to large scatter. Next to that, it is difficult to predict the exact soil conditions at the start of the uplift. Either no tests are performed on the upper meter of soil or measurement results are considerably heterogeneous, such that soil properties remain hard to estimate. The soil equipped in the experiments is comparable to sediments and associated uncertainties in offshore conditions. In between tests, the sand and clay is redistributed and leveled to flatten the surface. Effects due to reloading the soil such as reconsolidation are disregarded. Each test is repeated three times to reduce uncertainties. The test procedure is listed in Appendix A.6.

### 5.3.2 Functionality test bench

The mud-mat is lifted from the seabed shortly after installation by the test bench as this research aims to study the removal of temporary foundations. This lifting procedure is force-controlled, as a crane

would lift a pre-piling template. However, the test bench in the laboratory does not fully apply loads in a force-controlled manner. An iterative mechanism in the software of the test bench attempts a certain displacement, measures the force needed to obtain this displacement, and adjusts the rate. Despite that, when adjusting the speed in $N/s$, the initial attempted loading rate is altered. In the input window, the user can set a nominal speed, which is the trial speed. This determines the adjustments of the load rates. The adjustments of load rates influence the shape and smoothness of the graph of force over time. During the lowering of the foundation, the speed is kept at a constant rate. This installation rate is $500mm/min$ for every test. Similar to for example the research of Li (2014), the installation rate is higher than the lifting rate. The hold speed is required as input if the force should be kept constant. The hold speed influences the frequency of the oscillations, see also Figure 5.8b.

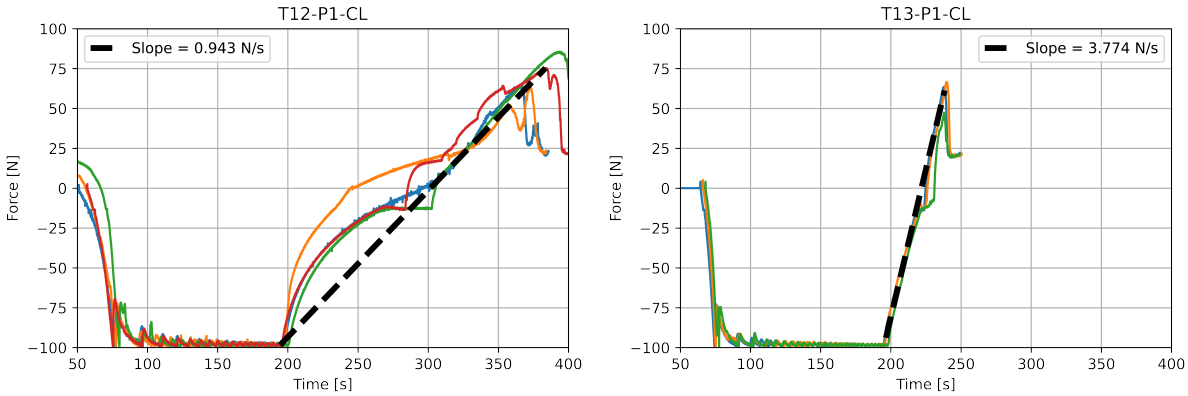


**(a)** Compare load rate and force

**(b)** Compare load rate and force

**Figure 5.5:** Load rates and forces of T12-P1-CL ($1N/s$) and T13-P1-CL ($4N/s$)

**Applied load rate and actual load rate**

The applied load rate is not equal to the actual load rate. Figure 5.5 shows the comparison of actual load rates for applied load rates of $1$ and $4N/s$. It can be observed that the secant load rate does not equal the applied load rate. Table 5.3 displays values for different applied loading rates and actual load rates. It can be seen that the normalized error between the applied rate and the actual average load rate decreases for higher load rates. Figure 5.6 shows there is a clear correlation between the uplift velocity in $mm/s$ and the applied load rate in $N/s$.

**Table 5.3:** Comparisons between applied load rate and actual load rate.

| | 1 N/s | 4 N/s | 40 N/s | 400 N/s |
|---|---|---|---|---|
| Average load rate during uplift | 0.6138 N/s | 2.282 N/s | 25.7620 N/s | 359.584 N/s |
| Normalized error between applied and average load rate | 0.386 | 0.430 | 0.356 | 0.101 |
| Secant start uplift to peak | 0.943 N/s | 3.774 N/s | 25.015 N/s | 352.777 N/s |
| Average duration uplift to peak | 182.1037 s | 43.471 s | 6.2911 s | 1.558 s |

### 5.3.3 Pore pressure sensor

A water pressure transducer is installed into the foundation, see Appendix A.1 for the specifications, after drilling a $16mm$ hole. The transducer is controlled with an Arduino microcontroller, see Appendix A.2. Two modules are installed on the microcontroller: a real-time clock and a memory card module. This allows the user to add a timestamp to the sensor output file which is compared to the timestamp that is automatically added to the load cell output. As the time difference can be obtained, the water pressure graph can be shifted, such that the data matches in time, and comparisons could be made. As stated above, the water pressure sensor is a pressure transducer. This entails that the numeric value that is read from the sensor on the microcontroller is in bits and should be converted to voltage, see Equation 5.1, which in turn can be converted to pressure ($kPa$). Equation 5.2 shows the conversion

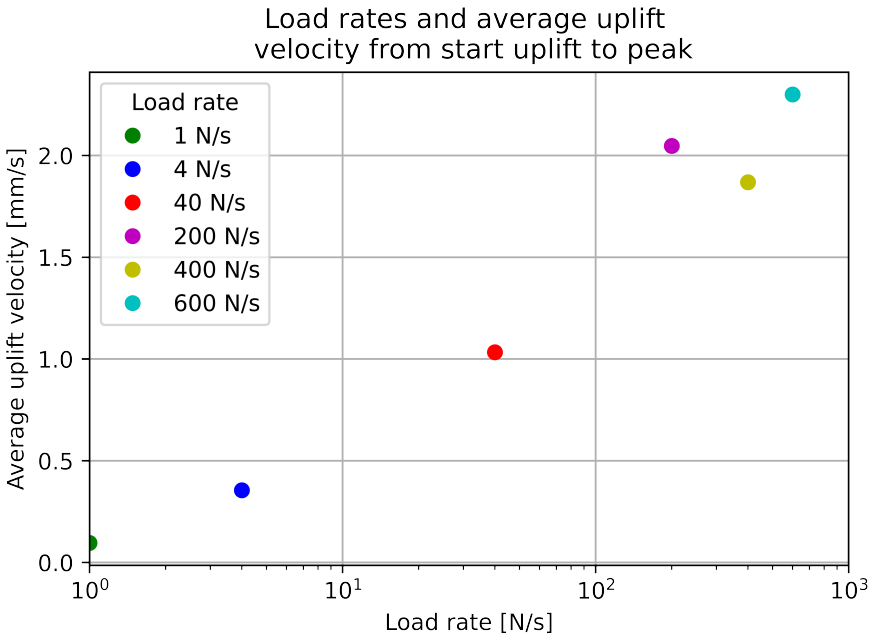


**Figure 5.6:** Correlation of load rate and uplift velocities in clay.

formula that is adjusted from the formula provided by the sensor manufacturer. The offset is the lowest recorded voltage if the sensor is not yet installed in water. The sensor was calibrated with a water column and porous stone to ensure the correct functioning. Water pressure measurements of the foundation with the sensor were taken at various water depths.

$$V = V_{read} * {}^{5}/_{1024} \tag{5.1}$$

$$u = (V - OffSet) * 225 \tag{5.2}$$

### 5.3.4 Functionality pore pressure sensor

The pressure transducer detects changes in pressure by a diaphragm that alters positions. This results in varying voltage. The sensor measures changes in voltage when the transducer is connected to and disconnected from a power source. After connecting to a power source, the voltage needs to be divided through the circuit, which explains the increase in voltage. After stabilization, the removal of the foundation can be recorded, however precise values for the decrease of the excess pore pressure as the foundation settles are not detected. Some noise is detected in the measurements. Following Igoe et al. (2010), a porous stone is installed to ensure that the sensor is measuring pore water pressures. No sediment is acting on the transducer sensing face. This porous stone is embedded in the foundation. The saturation of the stone is assured by ensuring that the stone was submerged at all times during testing. There is a small delay due to the presence of the porous stone. The instant when the foundation removal leads to pore pressure changes can still be approximated. Although the water pressure sensor is best equipped for taking measurements in a stationary situation, the pore pressure changes in this dynamic environment prove to be accurate in determining the detachment and giving an indication of the magnitude of the suction.

## 5.4 Data presentation

The results from the experiments are presented and discussed in Chapters 6 and 7, for clay and sand tests respectively. As indicated, each test is repeated three times. Tests are repeated if the correspondence of three tests with the same conditions is insufficient. If the test results show no large discrepancies, the average of three graphs is taken. Presenting the average of three tests results in more evident

figures. Figure 5.7 shows a test with slight differences between test runs that were acceptable and a test that was rejected. These discrepancies could be caused by coincidental adjustments to the set-up. Force and displacement measurements over time are obtained from the load cell and the test bench. All force-displacement graphs show the average of three tests, the test numbers are indicated above the graph. The respective force-displacement, force-time, and displacement-time graphs for the three tests are presented in Appendices C, D, and E. If trends are studied (for example the dependency of the peak force and the settlement), the data for each test repetition is indicated with small markers, and the average is indicated with a large marker.

As the weight of the foundation does not change throughout the tests, the force will be tared at the start of the test. In the post-processing, any weight of soil that is on top of the foundation is subtracted, such that the force goes to zero after the resisting force is overcome, remaining constant during the return to the original position. The displacements are shifted such that the sea bottom level after compression, as the uplift starts, equals zero.

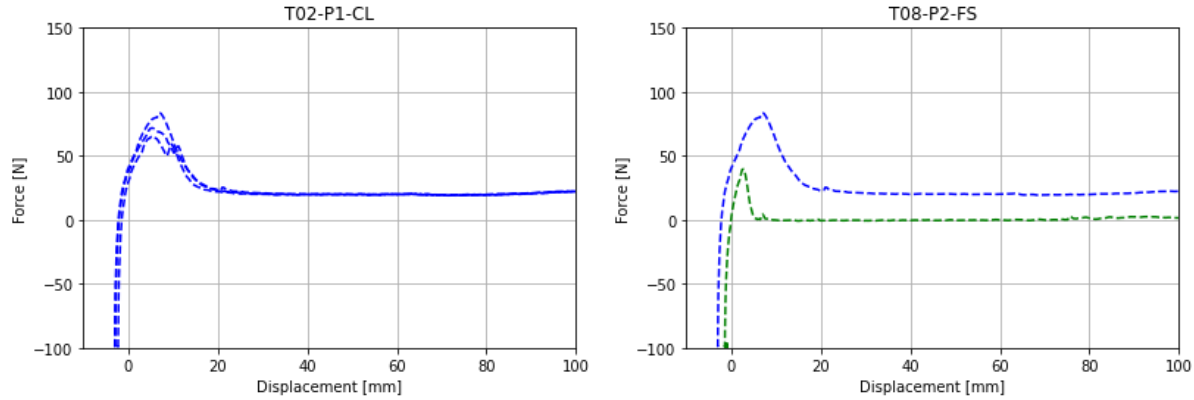


**(a)** Acceptable discrepancies.

**(b)** Unacceptable discrepancies.

**Figure 5.7:** Example of test results that are acceptable and unacceptable.

The stages that are inputted in the test bench for the base case are displayed in Figure 5.8a. The numbers in this Figure coincide with the stages. Figures 5.8b explains how these stages are exemplified in the graph and how to read and compare the values. The force and displacements before uplift starts are relevant, as the magnitude of the preload will alter the mechanisms and settlement might correlate to peak forces. Regardless, only the measurements after uplift[2] has started are discussed in further chapters. Most tests are compared to the base case: T1-P1-CL and T1-P1-FS. The input for the base case is presented in Table 5.4. All tests are numbered in a similar manner: TX-PY-QQ, where X denotes the test number, Y the primary mechanism under investigation, and QQ the soil type in which the foundation is installed. Appendix B lists all tests and conditions.

[2]Uplift is defined as the reduction of the compression force and the subsequent tensile force to achieve the breakout of the foundation. Once the force in the load cell is positive, tension is applied on the foundation.

Calculations:-

Stages:-
1:- Wait for operator

2:- Zero Extension

3:- Start Recording Data 0.000

4:- Go to Force -20.000 N
Rate Control:- Standard
Speed:- 100.000 mm/min
Record Data:- No
Ramp Down:- No

5:- Tare force

6:- Go to Force and Hold -600.000 N
Time:- H:0 M:2 S:0
Rate Control:- Standard
Speed:- 100.000 mm/min
Hold speed:- 1.000mm/min
Record Data:- Yes
Ramp Down:- No

7:- Return to Start Position
Rate Control:- Load Rate
Unidirectional Rate:- No
Speed:- 400.000 N/s
Record Data:- Yes
Ramp Down:- No

8:- Stop Recording Data 0.000

9:- End of test

**(a)** Test stages test bench for the base case.

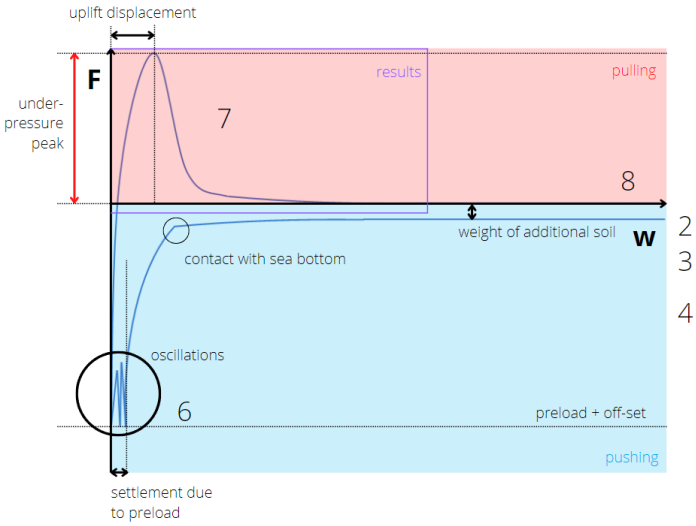


**(b)** Typical force and displacement development with additional information.

**Figure 5.8:** Typical force and displacement graph in (a) with numbering corresponding to the stages in the test bench in (b).

**Table 5.4:** Parameters for the base case test in clay and sand.

| Sample name | Mud-mat diameter [mm] | Mud-mat type | Uplift velocity [N/s] | Settling time [min] | Preload [N] | Soil type | Uplift load increment |
|---|---|---|---|---|---|---|---|
| T01-P1-CL | 150 | unperforated | 400 | 2 | 100 | clay | linear |
| T01-P1-FS | 150 | unperforated | 400 | 2 | 600 | fine sand | linear |

# 6

# Experimental results clay

All experiments in clay are performed according to Table 5.2, as described in Chapter 5. In this Chapter, the results of the clay tests are presented. First, the mechanisms and how they are studied in clay with the equipped test set-up will be explained. Next, the results are shown graphically and the observations with corresponding explanations are presented for each parameter that is adjusted.

## 6.1 Mechanism 1: Water carries uplift pressure

Pore water pressure changes are required to start the instant that load is applied to the foundation to prove that the uplift pressure is carried by the water. Pore water pressure measurements are collected during the tests. Figure 6.1 shows the pore pressures next to the force data during uplift. It can be concluded that the water pressures change as the uplift is commenced. The negative excess pore pressures develop rapidly, after which the pore pressures become positive. Note that overcoming the peak force does not necessarily equal the loss of adhesion.

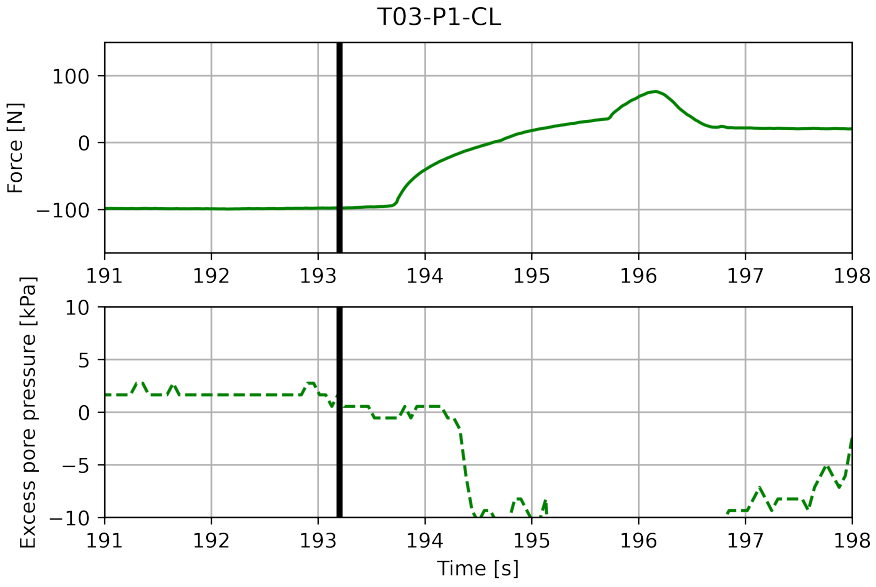


**Figure 6.1:** Water pressures and force over time ($200N/s$), the vertical black line indicates the start of the uplift.

## 6.2 Mechanism 2: Adhesion

The resisting force will increase as the clay particles adhere to the foundation invert. It is hypothesized that adhesion is dependent on the foundation area, preload, and settling time. Experiments with saturated clay without a water column were performed to study the change in the mudline due to compression. Although this does not mimic offshore conditions, adhesion of the clay to the foundation invert was observed. The force-displacement graphs from those tests are not presented here.

## 6.3 Mechanism 3: Unloading

The soil is expected to undergo a volume change during the unloading. Section 3.2.3 proposes that this volume change is due to shear and tension. As clay barely dilates under shear, predominantly tension on the soil causes the pore spaces to increase. An interface layer is added to cover the full foundation bottom to remove the adhesive effect between the subsoil and the foundation. The interface layer should ensure that the soil is not dragged upwards along with the foundation invert. Completely eliminating the bonding force between the foundation and the soil is impossible in the equipped set-up. Next to the addition of this layer, a step-wise uplift is applied to the foundation to study changes in pore volume. The foundation is lifted until its self-weight, is suspended for a predefined amount of time and moved further upwards. This pull to the self-weight of the foundation can alter the unloading soil response, potentially allowing excess pore pressure to be reduced in between load steps. Note that the skeleton deformations might not be fully reversible, as remarked by Selvadurai (2021).

## 6.4 Mechanism 4: Underpressure in water

Lastly, the delay for water to flow into the space between the foundation and the soil after detachment is analyzed. This mechanism is isolated by placing the foundation on the seabed for a brief moment. After lifting the foundation to create a tiny gap, the foundation is left hanging to ensure that the underlying soil is fully detached. Thereafter, the foundation will return to its' original position. It will be investigated whether there is any resisting force due to this underpressure in water. The area where the foundation was placed is not assumed to have a smooth surface after lifting. This can disturb the flow in the tiny gap. As soon as detachment has commenced, the water starts filling the void.

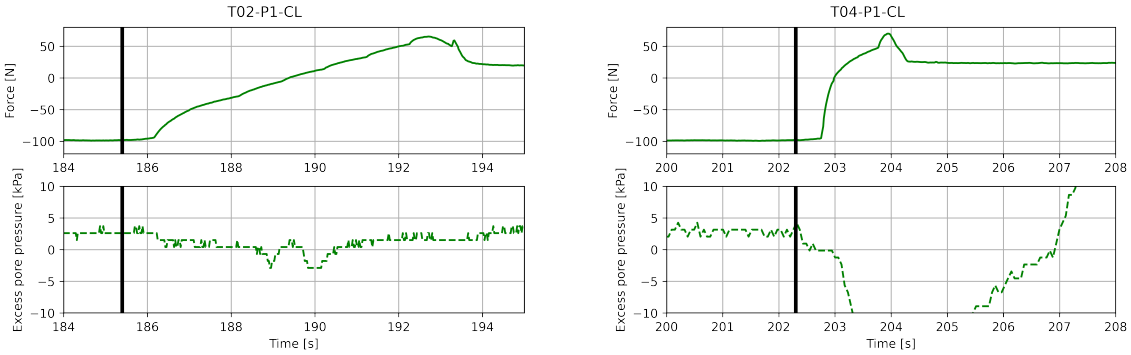


**(a)** Water pressures and force over time.

**(b)** Water pressures and force over time.

**Figure 6.2:** Water pressures of T02-P1-CL ($40N/s$) and T04-P1-CL ($600N/s$).

## 6.5 Effect load rate

DNV (2021c) states that it should be noted that the pull-out resistance in cohesive soils will increase with increasing loading rate, which should be accounted for. The load rate is varied to prove whether it influences pressure differences. The question arises whether the water pressure develops simultaneously with the force and whether the pore pressures increase with increasing force rate. In this case, the quasi-strain in Figure 6.4 is the settlement normalized by the diameter of the foundation. This allows making a comparison with different foundation diameters. Lastly, the effect of the load rate on the underpressure that is generated in the gap between the clay and the foundation is studied in Figure 6.5.

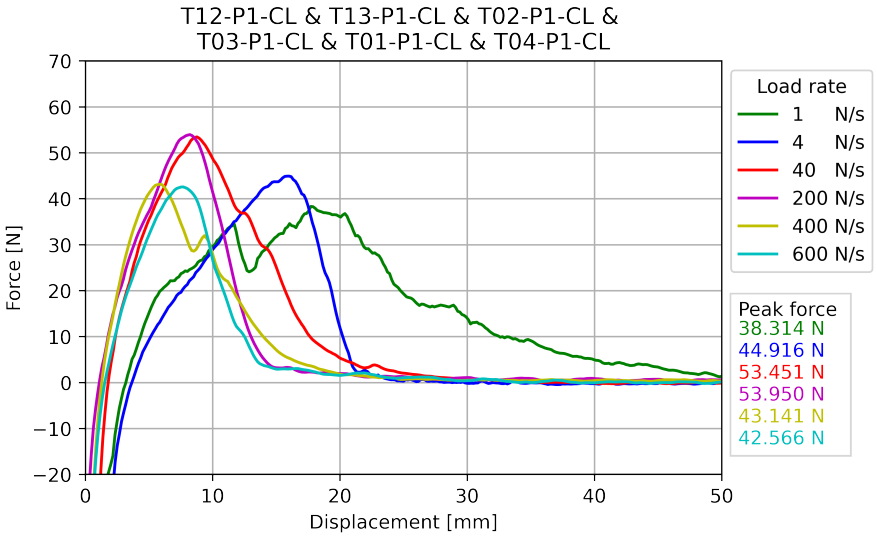


**Figure 6.3:** Influence of load rate on forces and displacements.

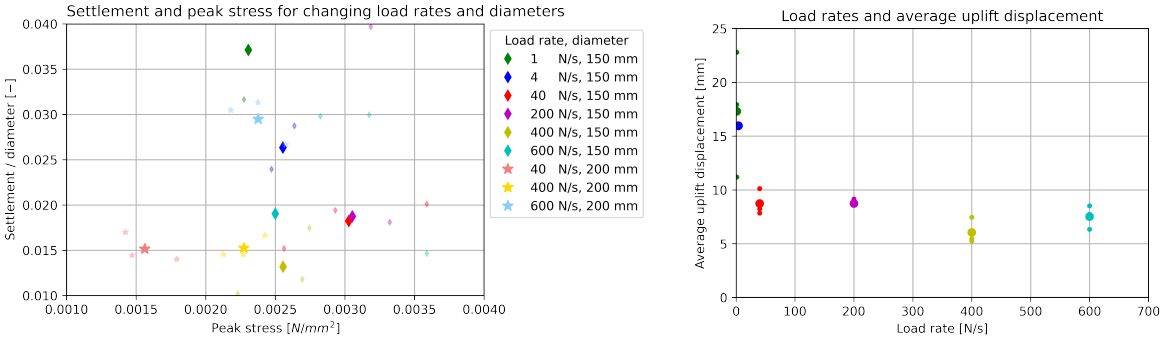


**(a)** Influence of load on the peak stress.

**(b)** Influence of load rate on the uplift displacement.

**Figure 6.4:** Influence of load rate on the uplift displacement and uplift displacement in clay.

**Table 6.1:** Observation and explanation of the comparison of the load rates.

| Observation | Explanation |
|---|---|
| The water pressures in Figure 6.2 show that the values for peak water pressures increase with increasing load rates.<br>Higher velocities do not result in higher peak forces, as is visible in Figure 6.3 | The pore water carries the uplift pressure in the initial stage of uplift and is dependent on the load rate.<br>This could be explained by the impermeability of the clay. The pore water barely flows towards the area of the largest underpressure. |
| It can be observed from Figure 6.4a that the scatter in settlement increases for the foundation of the smaller diameter. Next to that, there is no clear trend between the settlement and the peak stress. | This can be explained by larger diameter foundations being less sensitive to uneven leveling of the seabed, as any heap of clay will easily be distributed over the foundation area. |
| Smaller uplift displacements are observed for higher load rates. | As the uplift is slower, the soil has the possibility to move upwards along with the foundation invert. Higher load rates can lead to faster loss of adhesion. |

Figure 6.5 shows an increase in peak force and uplift displacement for slower tests in clay with a gap of $3mm$.

It cannot be guaranteed that the complete detachment of the clay has occurred. It thus cannot be concluded that there is a load rate dependency of the peak force due to the underpressure in water.

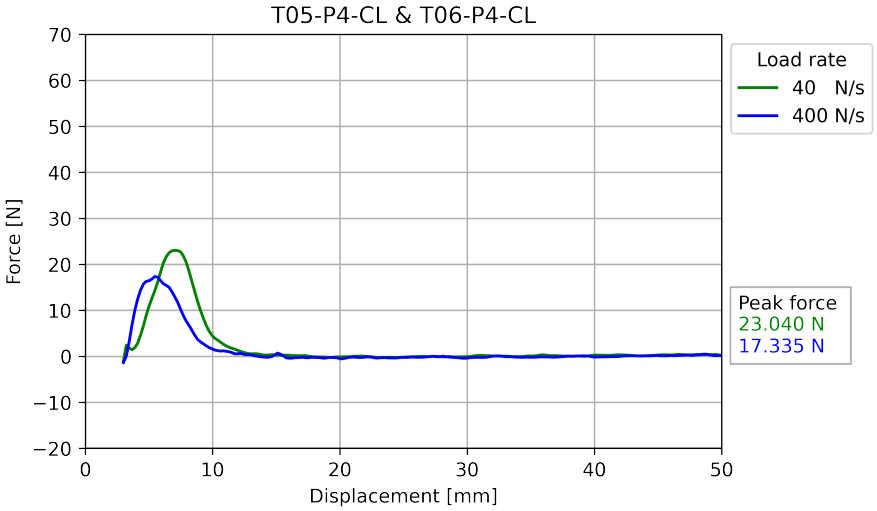


**Figure 6.5:** Influence of load rate on forces and displacements with a gap of $3mm$.

### 6.5.1 Effect load rate with interface layer and no gap

Next, the effect of the load rate on the adhesion of the interface layer to the plate is studied, by creating full contact between the foundation and a steel plate. The loading rates are varied to investigate whether it affects the adhesion force of the interface layer, see Figure 6.6.

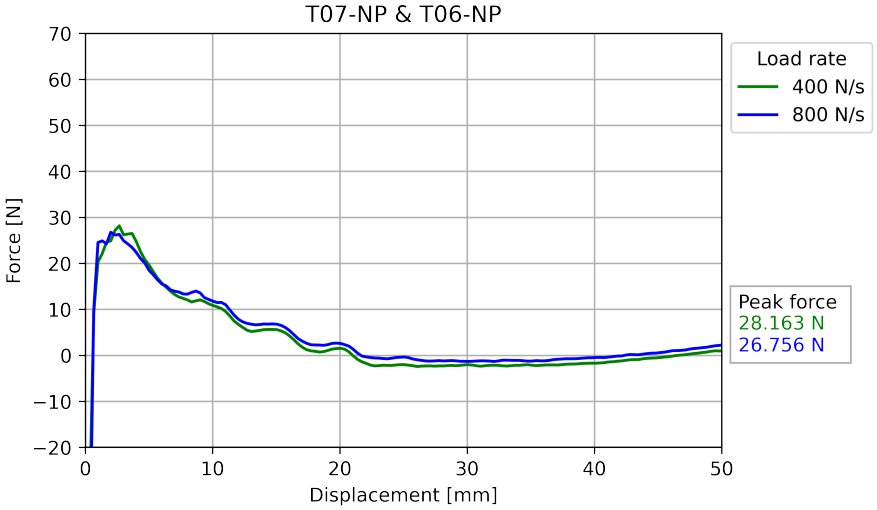


**Figure 6.6:** Influence of load rate on forces and displacements with an interface layer on a steel plate without a gap.

**Table 6.2:** Observation and explanation of the load rates with an interface layer on a steel plate without a gap.

| Observation | Explanation |
|---|---|
| There is a peak in the resisting force. | This entails that there is an adhesive force, regardless of the intermediary interface layer. |
| The peak resisting force shows little difference if the loading rate is doubled. | This suggests that the adhesion of the interface layer is not dependent on the load rate. |

## 6.6 Effect area

The contact area with the soil increases as the foundation diameter increases. More adhesion is expected for larger foundation areas. Stresses are displayed in Figure 6.7 to make a comparison of the peak forces of the different diameters. The quasi-strain is the foundation displacement divided by the foundation diameter.

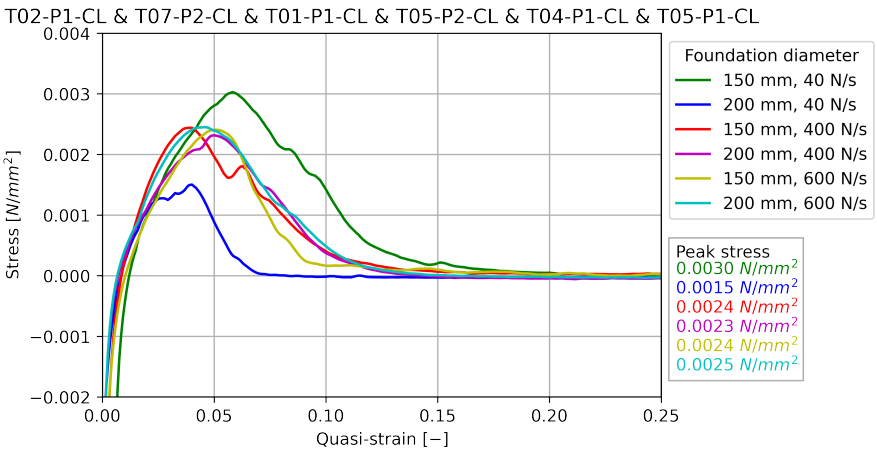


**Figure 6.7:** Influence of area and load rates on stresses and strains.

**Table 6.3:** Observation and explanation of the comparison of the areas.

| Observation | Explanation |
|---|---|
| It can be observed that for the load rate of $40N/s$, the smaller diameter leads to a higher peak stress value. For higher load rates, however, the different diameters lead to comparable peak values. | This can be explained by adhesion. The load rate is sufficiently low to allow the soil to be dragged upwards along with the foundation invert, adding resistance to uplift. The fact that the peak stress is not sensitive to the change in foundation area can be explained by the small relative difference in diameter between the two equipped foundations. |
| The quasi-strains at the peak stress for $40N/s$ are significantly different for both foundation diameters. | This can be explained by adhesion depending on both the load rate and the foundation area. |

## 6.7 Effect preload

Positive excess pore pressures can develop in clays during compression. It is hypothesized that increasing normal pressures lead to increased pore pressures and pore volume changes upon unloading which could lead to higher underpressures. Figure 6.8 shows the forces and displacements graphs and Figure 6.9 the trend of peak forces and settlements.

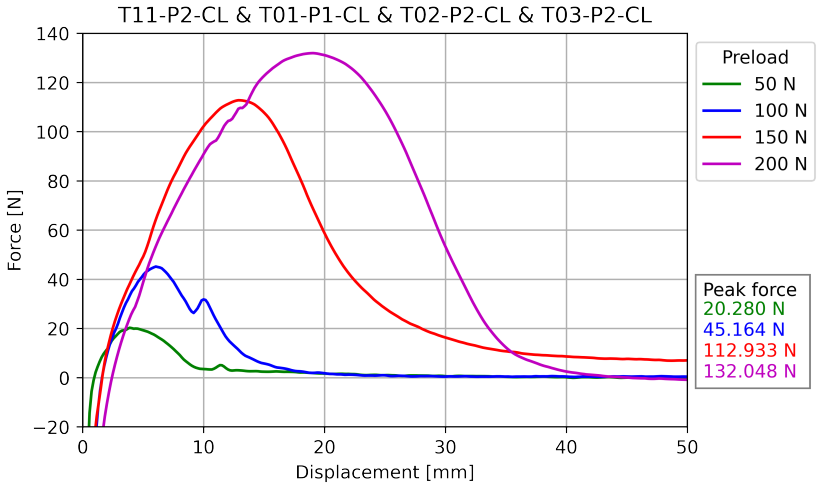


**Figure 6.8:** Influence of preload on forces and displacements.

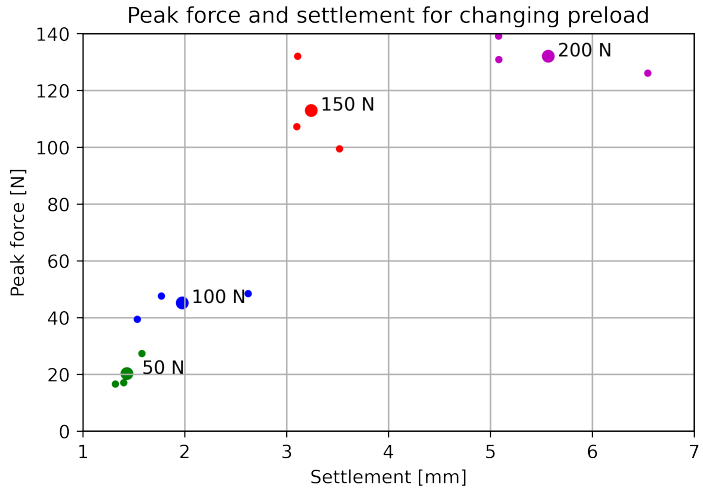


**Figure 6.9:** Influence of preload on peak force and settlement.

**Table 6.4:** Observation and explanation of the comparison of the preloads.

| Observation | Explanation |
|---|---|
| It can be observed that higher preloads lead to increased peak forces. | This is due to the increased changes in pore volumes and pore pressures that are the effect of unloading. |
| Figure 6.9 shows a clear trend between the settlement and peak force, which both increase with increasing preload. | This shows that pore volumes and pressures at the start of uplift largely influence underpressure generation. |
| The uplift displacements increase with the preload. | This is likely the effect of adhesion. The adhesive binding in combination with the negative pore pressures is sufficiently strong to lead to the soil being dragged along with the foundation. |

### 6.7.1 Effect preload with interface layer

Again the effect of the preload is studied, now with the addition of the interface layer. The conditions of the tests of the same preload are identical, except for the set-up itself. In tests T02-P3-CL and T04-P3-CL, the underside of the foundation is greased and covered with the interface layer. Figure 6.10 shows the comparison of the different preloads and the set-up without and with the interface layer.

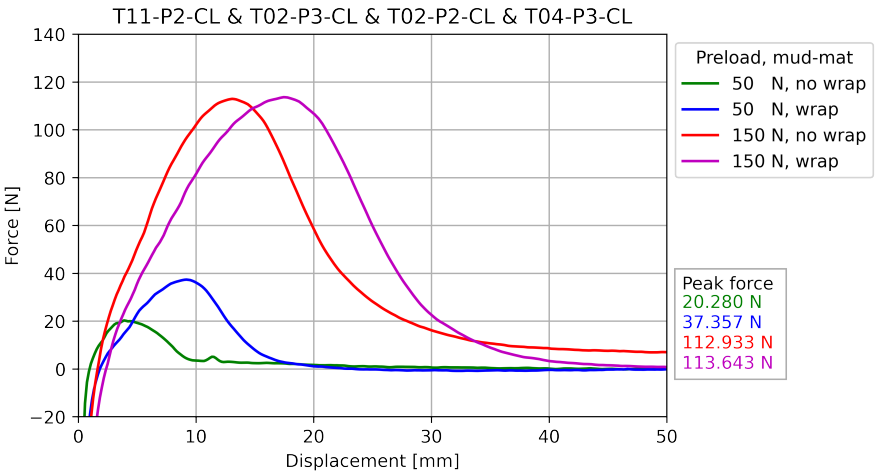


**Figure 6.10:** Influence of interface layer on forces and displacements.

**Table 6.5:** Observation and explanation of the comparison of the preloads with an interface layer.

| Observation | Explanation |
|---|---|
| The peak resisting force increases for a higher preload. | See Table 6.4. |
| The interface layer has a moderate effect on the peak force value. The uplift displacement increases due to the application of the wrap. | This can be explained by improper attachment of the interface layer to the foundation invert, leading to either water or clay being dragged upwards. |

## 6.8 Effect settling time

It is hypothesized that adhesion increases over time. This would be due to pore pressure changes, as the positive excess pore pressures dissipate over time due to the load. Time influence is important to distinguish as the development of pressure differences under temporary foundations varies from permanent foundations. Figure 6.11 show the forces over various settling times. $14\ hours$ is a realistic duration for a mud-mat of a pre-piling template to be placed on the seabed.

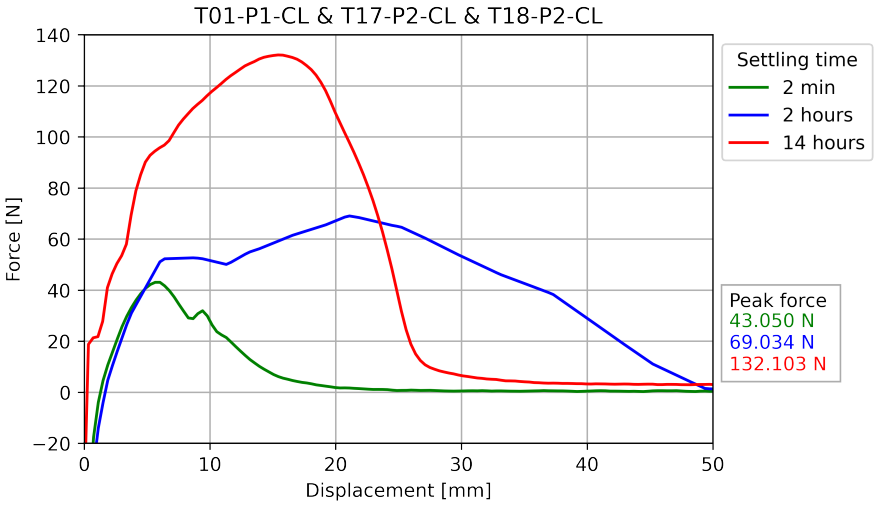


**Figure 6.11:** Influence of settling time on forces and displacements.

**Table 6.6:** Observation and explanation of the comparison of the settling times.

| Observation | Explanation |
|---|---|
| It is observed that increased settling times lead to higher peak values. | This can be explained by decreased excess positive pore pressures and increasing settlement. The pore volume decreases due to the occurring consolidation. However, the consolidation that can occur within $14\ hours$ is small. This indicates that there is likely an increase in the adhesive bonding of the clay to the foundation invert. |

## 6.9 Effect interface layer

### 6.9.1 Effect interface layer on steel

The effectiveness of the addition of an interface layer to the foundation invert to remove adhesion is investigated by testing on a steel plate in water. The foundation is pressed onto a steel plate and remains there for a predefined 'settling time', similar to the experiments on a soil sample. This prevents turbulence in the water from disturbing the uplift. The foundation on the steel plate with and without the interface layer is compared, Figure 6.12 shows the results for this test. There is no difference between the adhesion between the steel plate and the mud-mats with or without the interface layer. The interface layer thus has minimal adhesion-reducing properties.

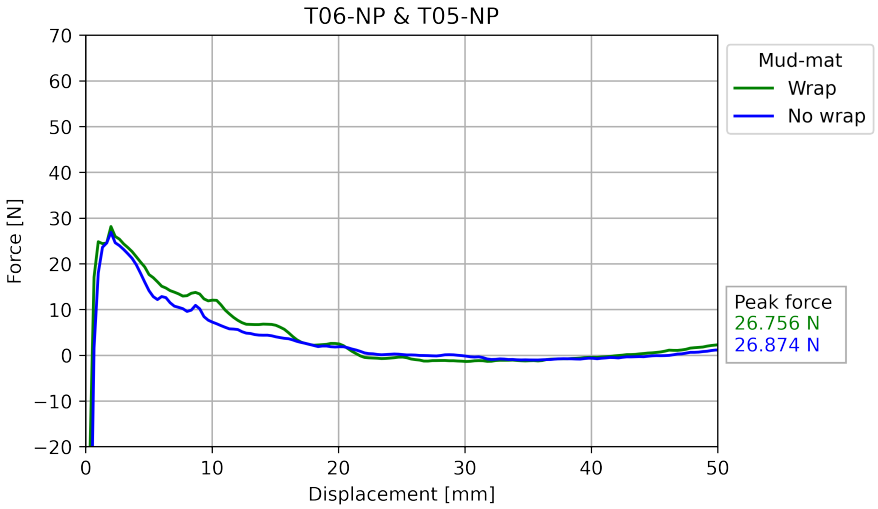


**Figure 6.12:** Influence of interface layer on forces and displacements on a steel plate without a gap.

### 6.9.2 Effect interface layer on clay

Two tests are compared to check whether the interface layer aids in reducing adhesion in clay. As can be observed in Figure 6.13, the peak force and uplift displacement appear to decrease due to the addition of the wrap. This is contradictory to the observations from Figure 6.10. The discrepancy can be explained by the interface layer collecting water, which moves along with the foundation out of the water. This intrusion results in a quantifiable additional weight, as this is carried upwards along with the foundation. The self-weight of the foundation, including this water, is shifted to zero which alters the peak force. The effectiveness of the interface layer is thus questioned.

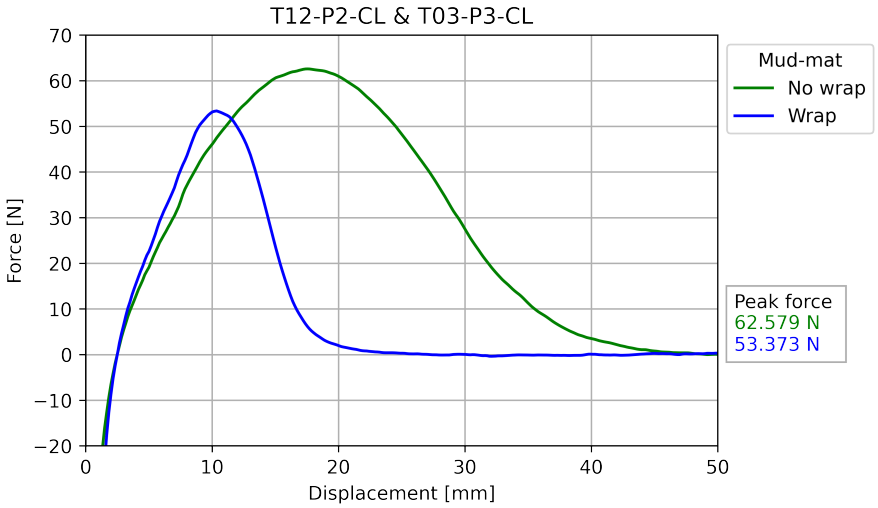


**Figure 6.13:** Influence of interface layer on forces and displacements on clay without a gap.

## 6.10 Effect step-wise uplift

In practice, pre-piling templates are occasionally lifted from the seabed in steps. This was recommended in 1979 by Pliskin (as cited in Craig and Chua, 1990). First, the full weight of the pre-piling template is lifted until it is carried by the crane. The mud-mats remain in contact with the seabed. The template is left suspended in the crane for a predefined amount of time. The template is fully lifted after that period has passed. This is expected to prevent large suction forces and should lead to reduced breakout time.

In this research, this is imitated by setting the force to zero the instant the foundation is placed on the seabed. After the application of the preload and settling, only the weight of the foundation is lifted. The force is increased to zero, thus not yet overcoming all underpressures. After one minute the mud-mat is lifted to return to its' original position. Figure 6.14 shows the comparison of the base case and the tests in which the mat is lifted in steps.

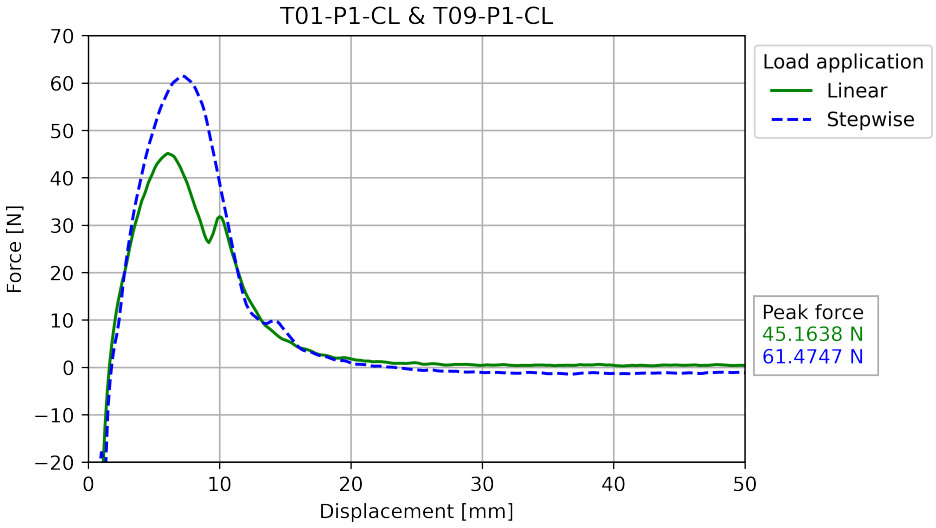


**Figure 6.14:** Influence of load application and diameter on forces and displacements.

**Table 6.7:** Observation and explanation of the comparison of the load application.

| Observation | Explanation |
|---|---|
| Lifting in steps does not reduce the peak force, the peak stress increases for a foundation of similar size compared to linear uplift. | This can be explained by a fault in the settings in the test bench. The test bench aims to keep the displacement constant in between the lifting steps, however, this causes the forces to become more negative. This entails that after the lifting until the self-weight of the structure, again a preload is applied. This could not be avoided, as keeping the force constant led to many oscillations in both the force and displacement. This would introduce cyclic loading to the soil. In both cases, keeping either the force or the displacement constant over time, it was recorded that the pore pressures increase compared to linear uplift. |

## 6.11 Effect gap width

The width of the tiny gap between the foundation and underlying medium is expected to influence the magnitude of the resisting force. The width is varied from $0.5$ to $3mm$. The water is flowing around the foundation, along the foundation invert, to reduce the underpressure. Note that if the gap is considerably large, the effect of the tiny gap cannot be studied. If the gap is larger than $10mm$, it can solely be observed that there is a negligible viscous drag. Figure 6.15 shows the results for both a steel plate and clay. Note that the load rates differ, however, this will have little influence on the peak force, as can be seen in Figure 6.6. The foundation diameters differ as well, however from Figure 6.7 it can be deduced that for the equipped load rates this is not an influence on the soil response.

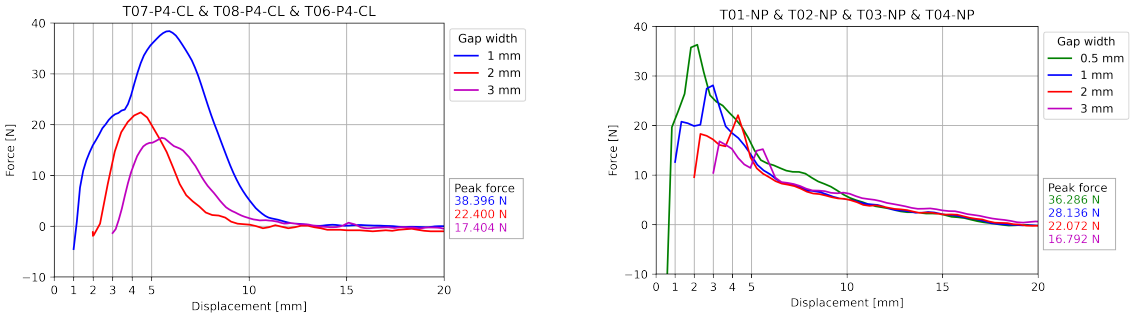


**(a)** Influence gap width clay, $400N/s, 150mm\varnothing$.

**(b)** Influence gap width steel, $800N/s, 200mm\varnothing$.

**Figure 6.15:** Influence of the gap width on the peak forces in clay and steel.

**Table 6.8:** Observation and explanation of the comparison of the gap widths.

| Observation | Explanation |
|---|---|
| Increasing the gap width reduces the peak force the foundation experiences during uplift, both in clay and steel. | This can be explained by the friction that the water encounters when flowing around the foundation, which is higher in the case of a smaller gap. |
| In clay, higher peak force values are observed for similar gap widths compared to the steel plate. | This is likely caused by the incomplete detachment of the clay during the development of the tiny gap. This however cannot |

## 6.12 Conclusion

The tests with the mud-mats of changing diameter are executed in clay with changing test bench conditions. The results are analyzed. An initial comparison with tests on a steel plate is made. The findings can be summarized:

- The pore pressure starts to reduce the instant the uplift has commenced. It can be concluded that the pore water carries the uplift pressure in clay. It is observed that the pore pressures are of a larger magnitude for faster load rates.
- Adhesion from the clay to the foundation invert is present and influences the underpressure development. The underpressure is dependent on the preload and settling time. These factors also highly influence the magnitude of the excess pore pressures and the pore volume at the start of the uplift. Increased settlements were recorded for longer settling times and increased preloads. This could alter the adhesion.
- The unloading behavior of clay is hard to distinguish from the adhesion. It was not possible to draw conclusions regarding unloading based on the tests with an adhesion reduction layer or step-wise uplift.
- The underpressure in the water due to the gap between the foundation and an underlying medium is observed in tests performed with a steel plate. The peak force due to the underpressure is dependent on the width of the tiny gap. It could not be guaranteed that the foundation was fully detached from the mudline.

# 7 Experimental results sand

After presenting the experimental results in clay in Chapter 6, the data for the experiments conducted in sand are shown in this Chapter. The occurrence of the mechanisms in sand is expected to differ from clay. No adhesive properties of sand are present (Verruijt, 2001). Next to that, dilatancy in non-cohesive sediments is expected to have a significant influence on the pore volume changes. Lee (1972) states that underpressures are solely present in sands in the lifting rates are sufficiently high. Den Hartog (2017) states that underpressures are present in sand by making the comparison to blade cutting theories. First, the observability of the four mechanisms in sand is examined. Next, the results are presented, as well as the corresponding observations and explanations.

## 7.1 Mechanism 1: Water carries uplift pressure

Similar to the mechanism in clay, the water is expected to instantly carry the upwards load upon application. One cannot make the same assumptions in sand and clay when comparing this mechanism to the spring-dashpot analogy, see Figure 3.1. As the hydraulic conductivity is significantly lower in clay, the negative pore pressures in clay can develop more easily. After suction is generated in sand, pore water will start to flow to reduce the negative pore pressures. Thus this mechanism is still expected to occur however for a reduced amount of time and to a reduced extent. Figure 7.6 shows the forces and the pore pressures over time for different preloads. It can be observed that the pore pressures start to change the instant the uplift force is applied, suggesting that this mechanism exists.

## 7.2 Mechanism 2: Adhesion

Next, the adhesion is discussed. As the cohesion in sandy soils is zero, the adhesion of the sand to the foundation invert is expected to be absent. Still, the sand particles will remain in contact with the mud-mat if suction is not yet overcome. This can be explained by *apparent cohesion*, which is the suction force of pore water that keeps sand particles together. However, the term apparent cohesion is more frequently used in unsaturated soil mechanics (e.g. in Ravindran and Gratchev, 2022). In the experiments, no *adhering* of sand to steel was observed. The dependency of suction and thus the apparent cohesion on area, preload, and settling time is studied.

## 7.3 Mechanism 3: Unloading

The unloading effect is expected to be more dominant in granular soils such as sand due to the tendency to dilate. This is due to lowered inter-particle bonding forces in sand, thus adding less resistance to shear and subsequent dilatancy. The unloading behavior in the sand will induce shearing and tensile forces, both leading to an increase in pore space. This will add to the total negative pore pressures that develop. It is expected that the pore volume change due to this mechanism in combination with the underpressure in water is the predominant driver in generating a resisting force to uplift in sand.

## 7.4 Mechanism 4: Underpressure in water

As the adhesion is zero in sand, the loss of contact in sandy soils will occur in a different manner than in clay. This will impact the development of a void between the foundation and the soil. As the water

will aim to find the path of least resistance, the water in the center of the void could originate from the soil instead of the surrounding water body. Figure 7.1 shows the force and pore pressure peak for the uplift with a gap. It is observed that the transducer records an underpressure due to the filling of the void. It is examined with the experiments whether water gets sucked out of the soil. Chapter 6 showed that the underpressure can also occur if there is no porous medium from where the water can originate. Comparing the resisting forces in steel and sand due to the underpressures allows for determining whether the resisting force is permeability-dependent.

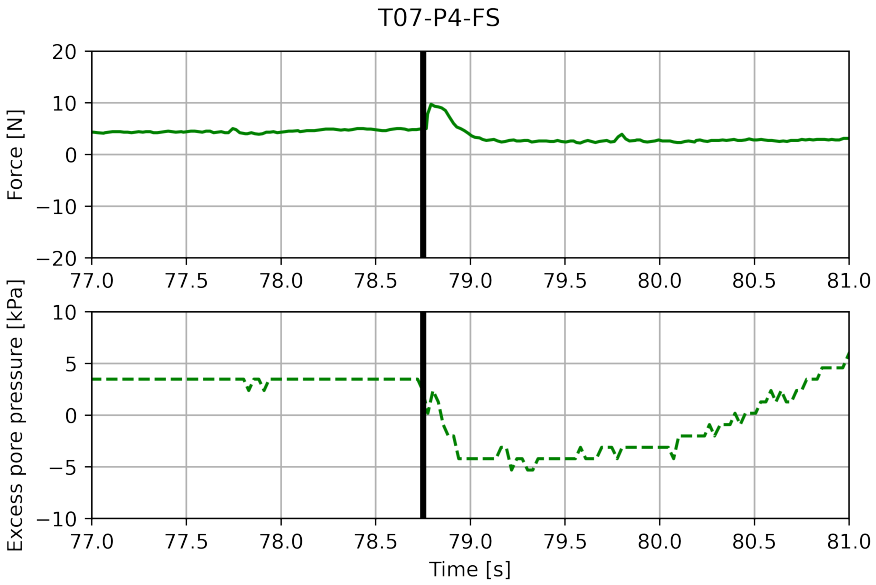


**Figure 7.1:** Water pressures and force over time ($1mm$ gap width).

## 7.5 Effect load rate

The effect of different load rates on pressure differences is studied. Reduced forces for slower load rates are expected. Figures 7.2 presents the development of the force for different load rates. Figure 7.3 shows the trend for peak forces for the different load rates.

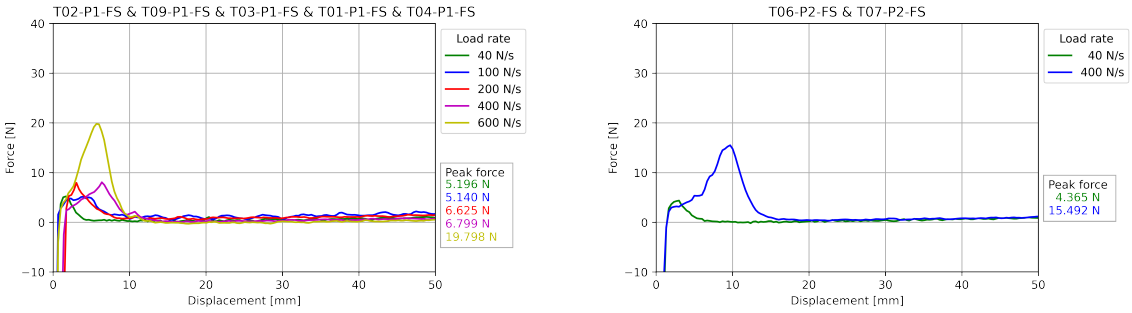


**(a)** Preload of $600N$.

**(b)** Preload of $1000N$.

**Figure 7.2:** Influence of load rate and preload on forces and displacements.

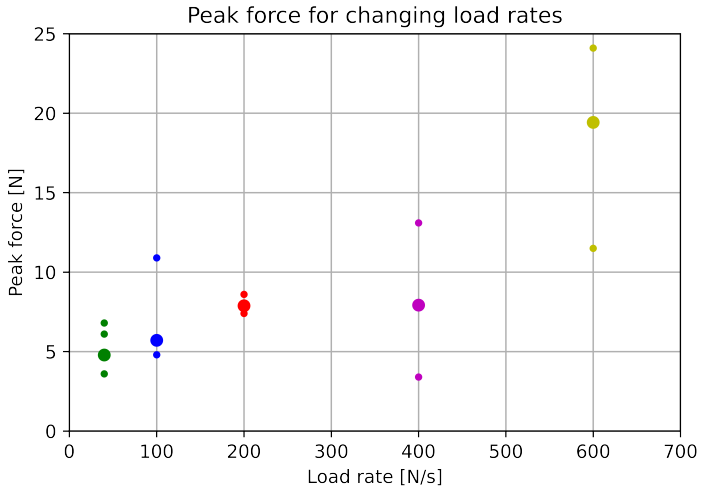


**Figure 7.3:** Influence of load rate on peak forces for a preload of $600N$.

**Table 7.1:** Observation and explanation of the comparison of the load rates.

| Observation | Explanation |
|---|---|
| It can be observed that the peak force is increasing with increasing load rate from Figures 7.2 and 7.3, irrespective of applied preload. It is observed that the peak force values in sand are reduced more than $50\%$ compared to the peak in clay for $600N/s$, see Figure 6.3. The reduction in peak force is substantially larger for other load rates. | Faster load rates lead to increased peak forces due to the reduced amount of time water has to relieve the negative pore pressures. |
| There is a small increase in uplift displacement if the load rate increases. | This can be due to the occurrence of a tiny gap, which adds to the resisting force. Due to the increasing load rate, the water has less time to reduce the underpressure in that gap. |

### 7.5.1 Effect load rate with gap

A small gap is created between the soil and the foundation, similar to the tests described in Section 6.4. The load rate is varied to examine the effect of the load rate on the resisting force due to an underpressure in water. The foundation diameter is adjusted as well. The quasi-strain is the displacement divided by the corresponding foundation diameter.

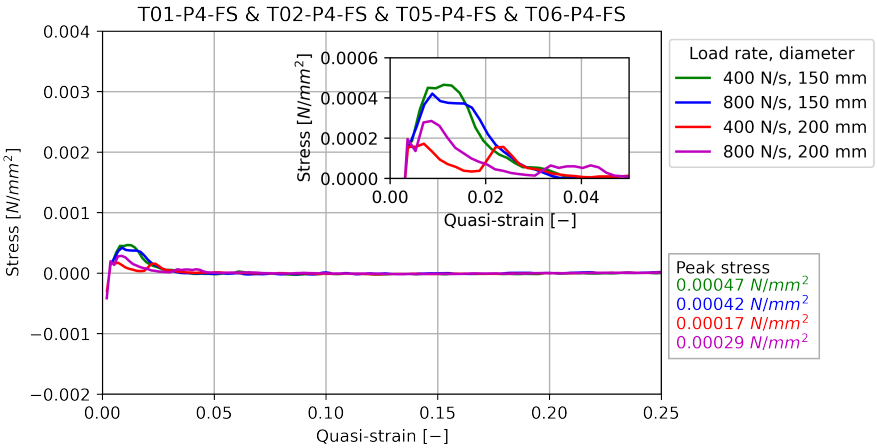


**Figure 7.4:** Influence of load rate with a gap of $0.5mm$.

**Table 7.2:** Observations and explanation of the comparison of load rate and area with and without gap.

| Observation | Explanation |
|---|---|
| There is no distinct effect of the load rate on the generation of the underpressure in the gap. | This can be explained by the fact that the underpressure is not dependent on the load rate. |
| It can be observed that the stresses under the smaller foundation are higher, both from Figures 7.4 and 7.5. | It would be expected that the smaller diameter would lead to reduced underpressure, as the longitudinal flow has to cover less distance to the mud-mat center. The fact that the larger foundation has reduced resisting stress could indicate that the area of the foundation is beneficial, as water will be sucked out of the porous medium more easily. |

## 7.6 Effect area

As larger foundations could lead to higher instantaneous positive excess pore pressures, the underpressure that develops underneath the mud-mat is expected to increase compared to smaller foundations. See Table 7.2 for the observation and explanation.

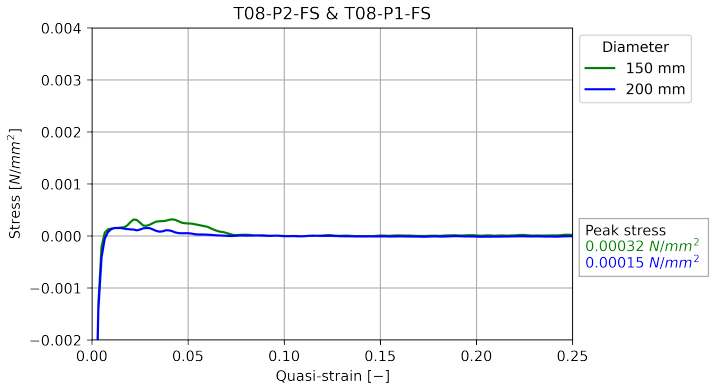


**Figure 7.5:** Influence of area on stresses and strains.

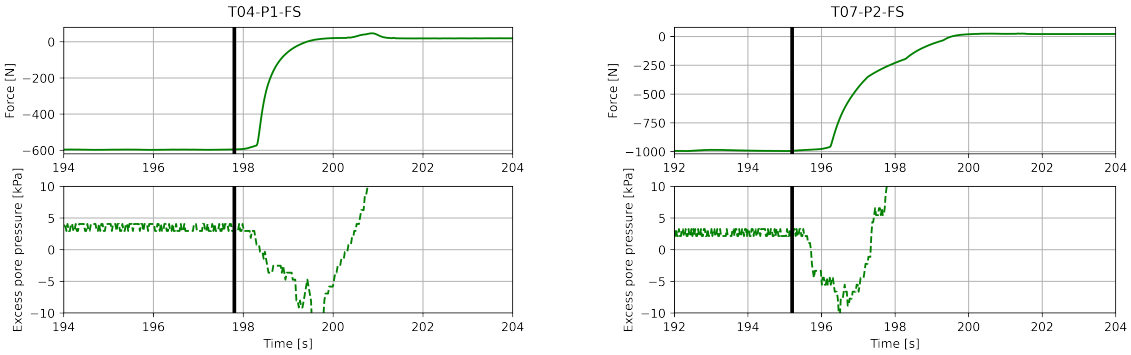


**(a)** Water pressures and forces over time.

**(b)** Water pressures and forces over time.

**Figure 7.6:** Water pressures of T04-P1-FS (preload of $600N$) and T07-P2-FS (preload of $1000N$).

## 7.7 Effect preload

Next, the effect of the preload on underpressure development is studied. Increased preload will result in a denser soil state. This can cause larger pore volume and pore pressure changes upon unloading. Figure 7.6 displays the pore pressures for different preloads. Figures 7.7 and 7.8 show the effect of the preload on the force, stress, and settlement.

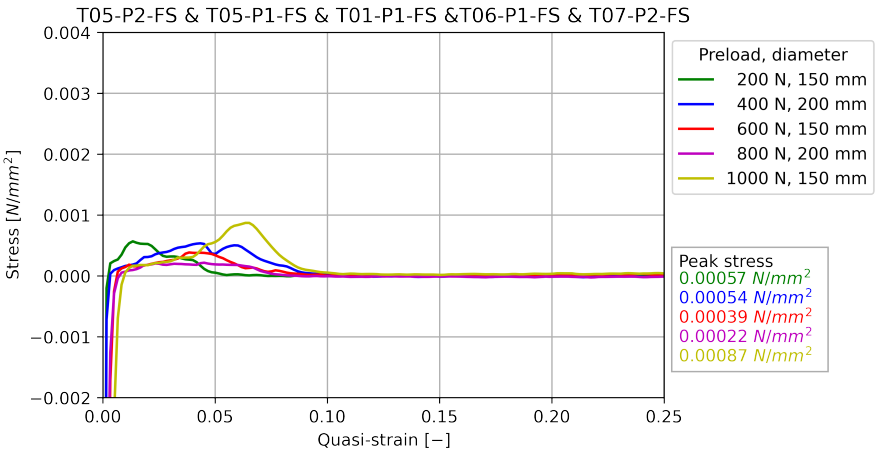


**Figure 7.7:** Influence of preload and diameter on forces and displacements.

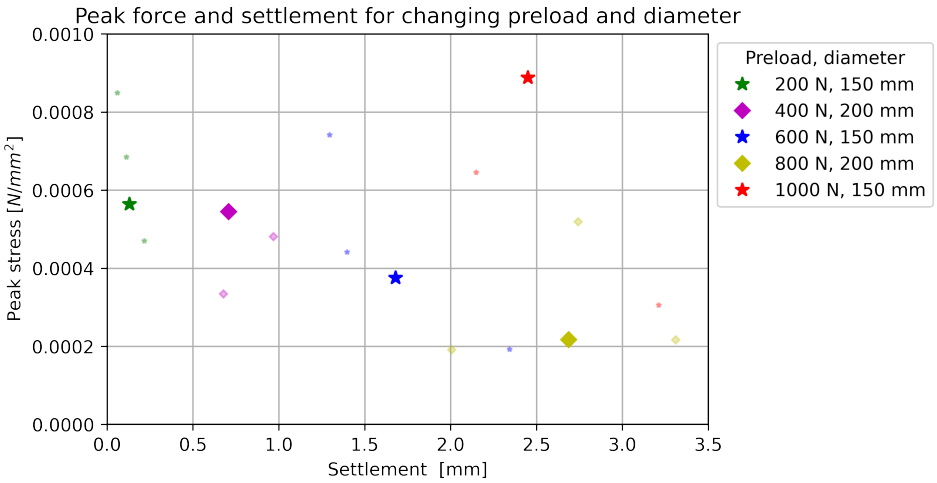


**Figure 7.8:** Influences of preload and diameter on peak stress and settlement.

**Table 7.3:** Observation and explanation of the comparison of the preloads.

| Observation | Explanation |
|---|---|
| Increased preload leads to higher settlement upon compression.<br>Higher preloads lead to reduced peak forces, except for a preload of $1000N$. Figure 7.6 shows however that the pore pressures for the preload of $1000N$ are reduced compared to a preload of $600N$. | This is because the preload causes the soil skeleton to compact.<br>Higher settlements and thus the reduced pore volumes do not lead to higher peak forces and stresses. It can be hypothesized that the increased pore volume changes upon unloading lead to water getting sucked out of the soil into the tiny gap more easily. |

## 7.8 Effect settling time

The settling time is adjusted after executing tests with variable load rates and preload. Increased settling time might allow for further soil skeleton rearrangement. Figure 7.9 shows the effect of changing settling time.

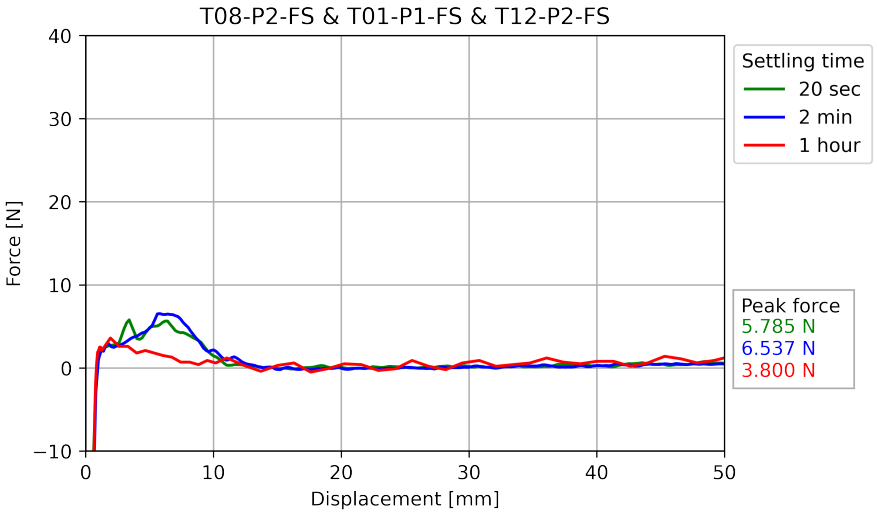


**Figure 7.9:** Influence of settling time on forces and displacements.

**Table 7.4:** Observation and explanation of the comparison of the settling times.

| Observation | Explanation |
|---|---|
| It can be observed that the increased settling time leads to a reduced peak force and uplift displacement. | This could be explained by stress relaxation as the effective stresses reduce due to the increased settling time. This might allow for more rapid suction relief as dilatancy occurs more easily. |

## 7.9 Effect interface layer

Although no adhesion is present in sand, the interface layer is added to the foundation to isolate the unloading effect. Figure 7.10 shows the result of the tests with this interface layer.

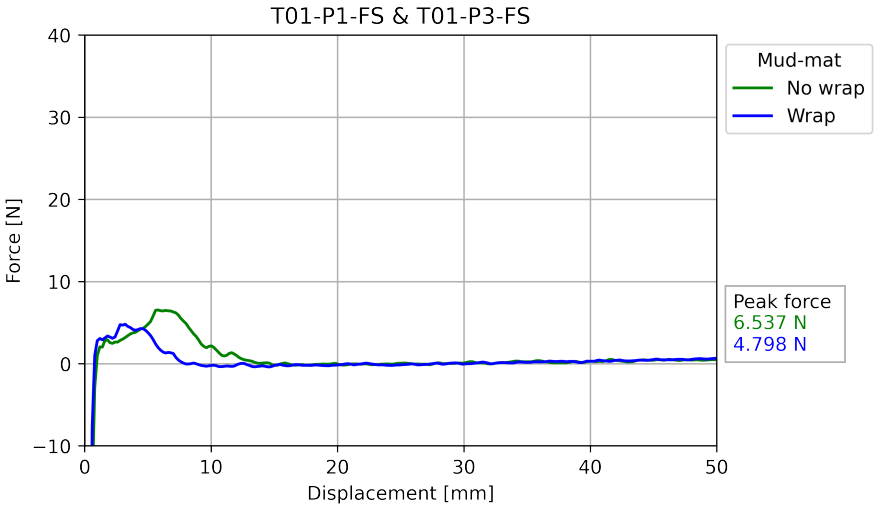


**Figure 7.10:** Influence of interface layer on forces and displacements.

**Table 7.5:** Observation and explanation of the comparison of the interface layer.

| Observation | Explanation |
|---|---|
| The interface layer reduces the peak force. The uplift displacement decreases due to the interface layer. | This can be explained by the interface layer facilitating the loss of underpressures in or near the soil. |

## 7.10 Effect step-wise uplift

The step-wise uplift was not advantageous to reduce the uplift force in clay. In sand, again experiments are performed with linear and step-wise uplift so the effect of adjusting the load application in sands can be evaluated, see Figure 7.11.

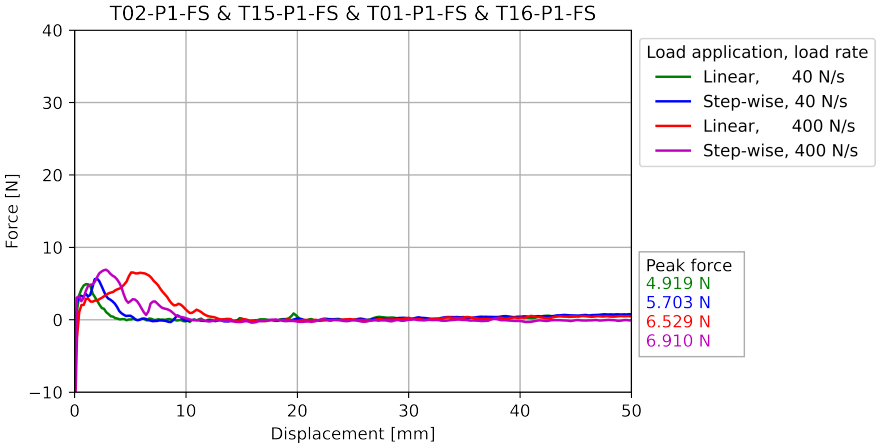


**Figure 7.11:** Influence of load application on forces and displacements.

**Table 7.6:** Observation and explanation of the comparison of the load application.

| Observation | Explanation |
|---|---|
| Step-wise uplift results in similar peak forces compared to linear uplift. | This can be explained by the additional compression of the sand due to the step-wise uplift being negligible. The pore water can easily flow and the underpressure in water can still occur despite the step-wise uplift. |
| Reduced load rates lead to reduced uplift displacement, also in the case of step-wise uplift. | See Table 7.1. |

## 7.11 Effect gap width

Lastly, the gap width between the sand and the mud-mat is varied to study the generation of underpressures in the water body. Whereas in clay, the gap width was not ensured due to the adhesive properties of the sediment, in sand a proper gap between the sea level and the foundation invert can be guaranteed. Figure 7.12 shows a variety of gap widths and corresponding forces over displacements.

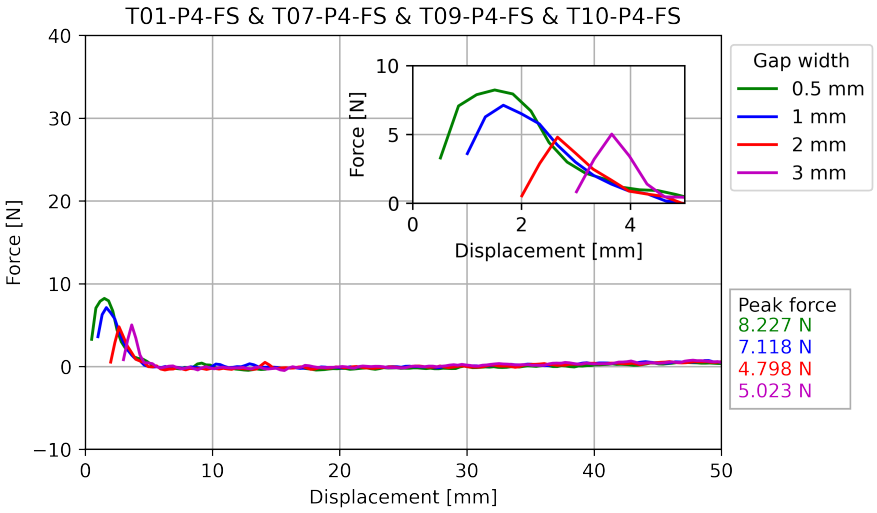


**Figure 7.12:** Influence of gap width on forces and displacements.

**Table 7.7:** Observation and explanation of the comparison of the gap widths.

| Observation | Explanation |
|---|---|
| It can be observed that there is a peak force visible for all gap widths. | This can be explained by the occurrence of an underpressure in the gap between the soil and the foundation. |
| The peak force is dependent on the gap width. An increased gap width leads to a reduced peak force. The displacement needed to reach the peak force is not dependent on the gap width. | This can be explained by the resistance the water flow encounters to fill the void left by the foundation. The flow experiences less ”wall” friction from the foundation invert and sand grains in wider gaps. |

### 7.11.1 Effect porous medium

Figures 6.15b, 7.12, and 7.13 are compared to study the effect of the underlying porous medium on the underpressure in the tiny gap. The magnitude of the peak force in steel is significantly higher compared to sand, as the only difference between these tests is the underlying medium. This allows for concluding that water is sucked out of the soil body to relieve the underpressure in the gap.

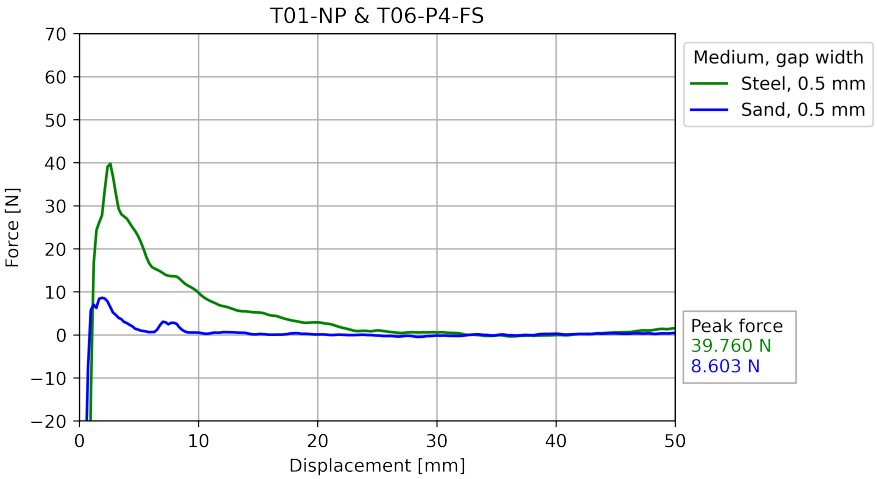


**Figure 7.13:** Influence of underlying medium on forces and displacements.

## 7.12 Conclusion

It is shown that the magnitude of the peak force and peak pore pressure in sand is small compared to the peak in clay. This is due to the differences in mineralogy and permeability of clay and sand. Although the underpressure peaks in sand are less distinctive, pressure differences during uplift still occur. The findings of this Chapter can be summarized:

- Water partially carries the uplift pressure. The pore pressure sensors show that the pore pressure changes the instant that the upwards force is applied. There is a load rate dependency of the peak force. This suggests that the permeability of the sand allows water to flow toward the area of the highest negative pore pressure. The pore water has less time to flow and quickly relieve suction upon more rapid uplift.
- The *adhesion* of the sand to the foundation is not due to any physico-chemical bonding, as the mineralogy of non-cohesive sediments does not allow for this. Negative pore pressures hold the grains together. Any soil displacements are a combination of the ”*cohesion*”, the unloading displacement, and movement of the ground level due to water getting sucked out of the soil.
- The unloading effect is difficult to distinguish, as the changes in pore volume are not observable with the current set-up.
- After the foundation detaches, a resisting force is observed. This is due to the underpressure in the gap between the foundation and the sand. Flow alongside the foundation invert in combination with water from the sand reduces this underpressure, after which the peak force is reduced. It is proven that water is sucked out of the soil. The respective volumes of water originating from the soil body or the water body are not derived.

# 8

# Mitigation measures

The previous Chapters discussed the mechanisms that occur during uplift of shallow foundations. Chapter 6 and 7 show that the proposed four mechanisms, as listed below, contribute to a resisting force during uplift. The experimental results aid in designing further tests with mitigation measures in place. Understanding how the mitigation measures impact the different mechanisms aids in effectively reducing the resisting force for different mud-mat designs. The existing mitigation measures known from literature are presented. The impact on the underpressure generation is hypothesized for each measure, following the numbering below, and the advantages and disadvantages are listed. Next, the test results of the mitigation measures in both clay and sand are presented and discussed. Thereafter, the effectiveness of the mitigation measures is evaluated.

1. Water carries uplift pressure
2. Adhesion
3. Unloading
4. Underpressure in water

## 8.1 Perforations

Perforations to reduce underpressures are commonly used in practice. As water can easily flow through the perforations, the negative pore pressures in the soil are relieved more rapidly compared to an unperforated foundation. It has been extensively investigated whether it is more effective to have many small perforations, compared to fewer large perforations. Next to that, it has been studied whether perforated mud-mats still provide sufficient bearing capacity (see Arts, 2017; Li et al., 2014; R. Liu et al., 2020; Tapper et al., 2015). White et al. (2005) conclude that a large number of small perforations is optimal in reducing the pressure differences. Next to that, they found that the uplift resistance decreased proportionally with the perforated area and that perforations resulted in a shallower failure mechanism upon uplift. The perforation ratio, the perforated area over the total foundation area, largely impacts the settlement. Table 8.1 shows the advantages and disadvantages of perforated mud-mats, which are relevant within the scope of this research.

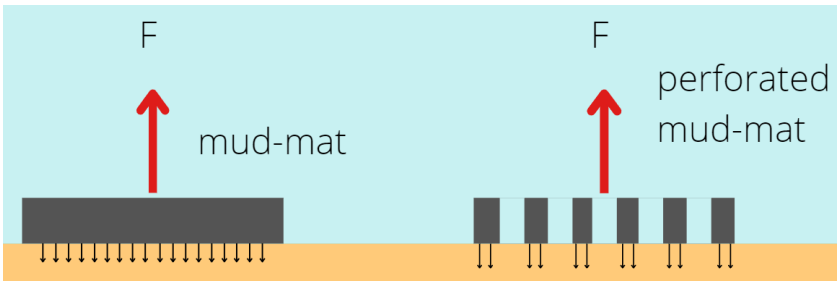


**Figure 8.1:** Loads on an unperforated mud-mat are more evenly distributed compared to a perforated mud-mat.

**Effect on mechanisms in clay**

1. Perforations reduce the total area that can contribute to pulling water from the pore spaces. This entails that the remaining perforated foundation area carries the uplift force. This will likely lead to higher stresses and increased instantaneous pore pressure changes, see Figure 8.1. However, the negative excess pore pressure will be quickly relieved due to shortened drainage paths.
2. A reduced foundation area implies less adhesive effects in soft soils. However, as the shallow foundation settles into cohesive soil, an arching effect between the perforations will occur, as visualized in Figure 8.2. (White et al., 2005) This will lead to increased side friction. The contact between the soil and the foundation is expected to be lost more rapidly compared to an unperforated foundation. Hemispherical contraction can thus occur more easily between the perforations.
3. A reduced stress increase is expected when pressing a perforated foundation into the soil, compared to an unperforated mud-mat. The stress is distributed more unevenly along the foundation invert. The excess pore pressures that occur due to foundation loading can easily dissipate due to the perforations. The perforations will alter the unloading effect, resulting in a reduction of the pore volume change upon unloading and thus the underpressure.
4. The tiny gap that forms after complete loss of contact between the soil and the foundation will quickly fill with water through the perforations. There is no expected resisting force due to underpressure in the gap in the case of a perforated mud-mat. The perforations do result in a differential hydrodynamic response upon foundation movement near seabed. (Rosingh, 2018).

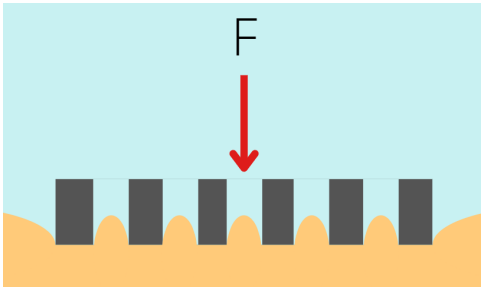


**Figure 8.2:** Arching effect due to perforations might influence the bearing capacity.

**Effect on mechanisms in sand**

1. Similar to clay.
2. Sand does not have adhesive properties.
3. As the perforations lead to reduced soil confinement, increased stress relaxation is expected to occur during operation. The unloading effect in sand will be reduced due to the perforations.
4. Similar to clay. The chance that the underpressure in the gap will result in water getting sucked out of the soil is close to zero.

**Table 8.1:** Advantages and disadvantages of mud-mats with perforations.

| Advantages | Disadvantages |
|---|---|
| Shortened drainage paths | Realizing many perforations is labor-intensive |
| Reduced adhesion | Reduced bearing capacity |
| Reduced effect due to underpressure in the gap between the soil and the foundation | |
| Reduced effect of trapped water on top of the mud-mat[1] | |

[1]Trapped water adds to the total weight that needs to be lifted. The amount of trapped water depends on mud-mat shape and the presence of borders on top of the mud-mat along the periphery.

### 8.1.1 Experiments with perforations: Load rate

Experiments with a perforated foundation are performed in both the clay and the sand sample to properly understand and validate the hypothesized effects of perforations on the development of the different mechanisms.

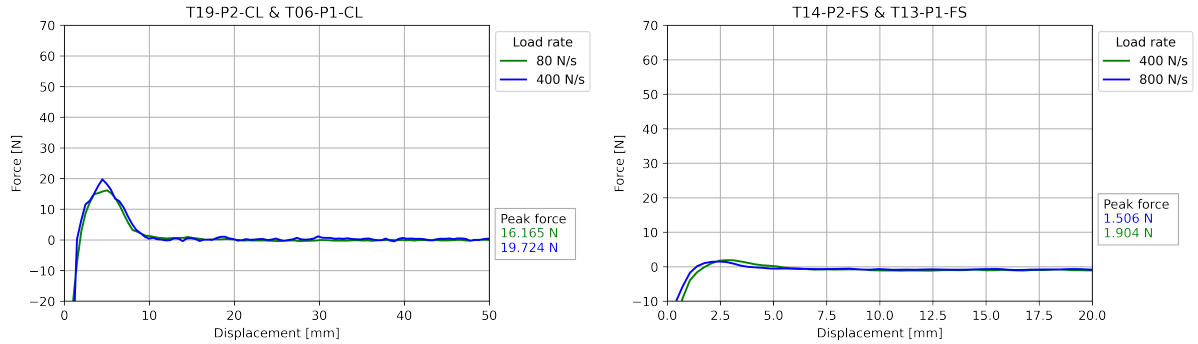


**(a)** Perforated foundation on clay.

**(b)** Perforated foundation on sand.

**Figure 8.3:** Influence of load rate on perforated mud-mats in clay and sand.

**Table 8.2:** Observation and explanation for the effect of the load rate on perforated mud-mats in clay and sand.

| Observation | Explanation |
|---|---|
| There is a small increase in peak force in clay if the load rates increase in Figure 8.3. The peak forces in sand are almost comparable. | This can be explained by the low permeability of the clay. Negative pore pressures are expected to develop due to uplift regardless of the perforations. The effect of the load rate on the force-displacement development in sand is close to zero as there is barely a peak force. |

## 8.2 Geotextile

Geotextile at the foundation invert will serve as a layer with an increased hydraulic conductivity compared to the surrounding soil, see Figure 8.4. This will alter the interface response. It is hypothesized that the geotextile ensures a more rapid underpressure relief as it eases water flow toward the center of the foundation. The friction, adhesion, and (vertical and horizontal) bearing capacity of the mud-mat will alter due to the mounting of geotextile to the foundation. The horizontal sliding capacity can reduce or increase, as the bonding of the soil to the foundation invert will differ.

The geotextile which is equipped in the test setup is a high-strength woven geosynthetic. The textile consists of polypropylene yarns and is selected both for its high durability compared to non-woven geotextile and suitability for offshore application. The textile specifications can be found in Appendix A.5. A picture of the geotextile attached to the foundation invert is displayed in Figure 5.4, mud-mat 1.

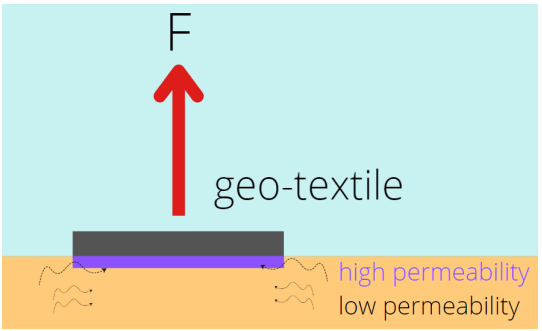


**Figure 8.4:** Geotextile leads to an increased permeability at the foundation invert, the thickness geotextile is not to scale.

**Effect on mechanisms in clay**

1. Pore pressure changes during uplift are altered if geotextile is mounted to the foundation invert. Water can easily flow towards the area of the lowest pressure to relieve the negative pore pressures due to the geotextile interface.
2. The adhesive forces between the geotextile and the underlying soil will differ from the adhesion between steel and clay. As the geotextile is woven, the surface is not smooth and adhesion will not be constant over the foundation bottom. Clogging of the textile openings might occur, which can result in increased adhesive forces.
3. The excess pore pressures can easily dissipate during compression through the geotextile and the unloading effect will be reduced.
4. The underpressure in the void can still occur, as the void between the foundation and the clay is present. The geotextile will allow water to flow close to the foundation invert, causing the void effect to happen more gradually. The peak force will likely be reduced by the geotextile.

**Effect on mechanisms in sand**

1. Similar to clay.
2. Clogging might occur as the finer sand particles will accumulate in the textile openings.
3. Similar to clay, the unloading effect will be reduced. Additional bottom friction might alter the development of a failure mechanism and shear forces within the soil body. Reduced pore volume changes and subsequent pore pressure changes are expected.
4. Similar to clay.

**Table 8.3:** Advantages and disadvantages of mud-mats with geotextile.

| Advantages | Disadvantages |
|---|---|
| Shortened drainage paths<br>Reduced effect of underpressure in the gap between the soil and the foundation<br>Less labor-intensive than cutting perforations | Reduced sliding capacity |

### 8.2.1 Experiments with geotextile: Load rate

**(a)** Foundation with geotextile on clay.

**(b)** Foundation with geotextile on sand.

**Figure 8.5:** Influence of load rate on mud-mats with geotextile in clay and sand.

**Table 8.4:** Observation and explanation for the effect of the load rate on mud-mats with geotextile in clay and sand.

| Observation | Explanation |
|---|---|
| Higher load rates in clay lead to increased peak forces for foundations with geotextile, as visible in Figure 8.5. This is not observable for sand.<br>Both in clay and sand, there is one smooth peak for higher load rates. | This can be explained by the effect of the permeability of the clay. Regardless of the geotextile, negative pore pressures develop due to the rapid uplift.<br>This can be explained by the fact that geotextile is detaching instantly, and no residual ”sticking” to the soil is occurring. |

| | |
|---|---|
| There appear to be two force peaks in clay for low load rates. | This can be explained by the application of the geotextile, as the geotextile is bolted in the center of the foundation. The remaining part of the geotextile is attached with elastics. The outer edge of the geotextile can stick to the clay. This creates a second ”suction peak” during detachment. |

### 8.2.2 Experiments with geotextile: Settling time

**Figure 8.6:** Influence of settling time on mud-mats with geotextile in clay and sand.

**Table 8.5:** Observation and explanation for the effect of the settling time on mud-mats with geotextile in clay.

| Observation | Explanation |
|---|---|
| The peak in clay largely increases due to increasing the settling time from $2$ minutes to $14\ hours$, with geotextile in place. | This can be explained by the adhesion that increases over time. The clay particles will bond with the material of the geotextile. Next to that, the positive excess pore pressures due to foundation compression will be reduced. Settlement increases as consolidation advances. |
| Comparing Figure 8.6 to 6.11 allows for the evaluation of the effectiveness of the geotextile in reducing underpressures for a realistic settling time for a temporary foundation ($14\ hours$). The peak force in clay reduces with % due to the application of geotextile. | This can be explained by the increased permeability of the geotextile. Excess pore pressures can dissipate more easily due to the geotextile, both during compression and uplift. During uplift, the geotextile aids in relieving the negative pressures by allowing water to quickly flow to the center of the mud-mat. |
| Figure 8.6 shows that increased settling times lead to larger settlements for the foundation with geotextile. | The settlements increase due to the ongoing consolidation. Note that the consolidation that occurs within $14\ hours$ is minimal. Settlement recordings from the set-up might be subjected to scatter. |

**Figure 8.7:** Influence of settling time on the settlement of a mud-mat with geotextile in clay.

### 8.2.3 Experiments with geotextile: Step-wise uplift

**Figure 8.8:** Influence of geotextile on forces and displacements during step-wise uplift.

**Table 8.6:** Observation and explanation for the effect of step-wise uplift on mud-mats with geotextile in sand.

| Observation | Explanation |
|---|---|
| The peak force is reduced for the foundation with geotextile if the foundation is lifted from sand in a step-wise manner, see Figure 8.8. | This can be explained by the fact that the geotextile allows water to flow along the foundation invert, as soon as the initial uplift has commenced. |

## 8.3 Bottom water jetting

Jetting systems are most commonly installed in spudcans to break the suction, see Figure 8.9. Large spudcans have a different geometry than mud-mats, see the most right foundation in Figure 2.1. Spudcans are designed to settle to a design depth and upon removal act like buried anchors. As spudcans are lifted from the seabed, a deep failure mechanism develops. Pore pressure changes occur around the spudcan. Either water or air jets can be equipped. A study by Gaudin et al. (2011) has demonstrated that jetting can significantly reduce uplift resistance. Reduced peak forces for extraction are reached if the uplift rate is fast enough to ensure undrained uplift and if a sufficiently high flow rate is

applied with respect to the uplift rate. The amount and location of the jetting nozzles can be optimized for the foundation shape, as is achieved in the study of Jo et al. (2013)

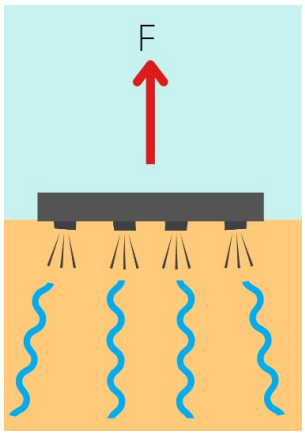


**Figure 8.9:** Jetting nozzles under shallow foundation aid in reducing underpressures during uplift.

**Effect on mechanisms in clay**

1. The underpressure that is generated upon uplift is compensated for by the water flow from the jets. Jetting-induced flow paths allow more rapid suction relief. Next to this, the jetting provides an upwards force, to counter the resisting force.
2. The adhesion is reduced locally, around the nozzle heads.
3. The unloading effect is expected to remain, as the jetting is only commenced when the uplift procedure starts. The jetting does change the soil to a novel stress state, with the largest changes around the nozzle heads. Next to that, the failure mechanism that develops will alter, depending on the nozzle placement. Local failure of the soil is likely to occur.
4. The void between the foundation invert and the clay is filled with the water from the jets, resulting in completely diminishing the underpressure effect. Water will not be sucked out of the soil.

**Effect on mechanisms in sand**

1. Similar to clay.
2. Sand does not have adhesive properties.
3. Similar to clay.
4. Similar to clay.

**Table 8.7:** Advantages and disadvantages of mud-mats with jetting systems.

| Advantages | Disadvantages |
|---|---|
| Shortened drainage paths | Expensive to install and keep operational |
| Reduced adhesion | Risk of clogging of the nozzles |
| No underpressure in the gap between the soil and the foundation | Risk of channel formation, thus overcoming suction only very locally |
| Jets apply an upwards force | Many nozzles are required to be effective in case of a large footing |

## 8.4 Electro-osmosis

A method to reduce suction forces in the soil body during uplift which is not often suggested in literature is electro-osmosis. Electro-osmosis drives water in a porous medium. A direct-current electric potential is applied between electrodes in a soil sample. Water molecules are transported and dragged along with the potential. The fact that clay minerals are charged contributes to this mitigation method. In the 1950s this technique was equipped mostly for dewatering purposes. Roderick (1975) is the first to describe electro-osmosis for the purpose of bottom breakout. Later, electro-osmosis was tested to reduce the adhesion of clays to the machine during tunnel driving (Spagnoli et al., 2011).

**Effect on mechanisms in clay**

1. Water will be subjected to a potential and drag will be exerted on the water molecules that aim to follow the uplift force as the electric potential and uplift force are applied simultaneously. This is tested in the experimental program of Roderick (1975). The water will not carry the uplift pressure.
2. Adhesion will be reduced, although the efficiency of reducing adhesion is dependent on clay mineralogy (Roderick, 1975; Spagnoli et al., 2019).
3. Unloading behavior of the clay will be altered by the application of an electric potential, as the electro-osmosis will cause a net flow to the cathode. The displacement of clay particles due to this water flow is hard to estimate and might depend on electrode positioning.
4. An underpressure in the gap between the foundation and the clay can still occur. The ongoing water flow in the water body due to the electrical field can ease the relief of this resisting force.

The functioning of electro-osmosis in sand has never been studied. This is because sand is not a suitable material as the sand minerals do not have a negative surface charge and sandy soils have large pores. The application of an electrical field in sand would not cause a significant flow of water toward the cathode.

**Table 8.8:** Advantages and disadvantages of the application of electro-osmosis.

| Advantages | Disadvantages |
|---|---|
| Allows the operator to redirect water flow to a specified location | Inherent problems associated with installing electrodes in offshore conditions |
| Effective in reducing negative pore pressures | Expensive to realize and keep operational |
| Reduces adhesion | Effectiveness depends on electrode configuration |
| | Risk of electrode corrosion |

## 8.5 Adjusted lifting

Thus far, solely the application of a force in the middle of the foundation, perpendicular to the seabed has been considered. Two adjustments in the lifting procedure are suggested in this Section, see Figure 8.10. A way to generate a different soil response by altering the lifting procedure is the application of a tilted force. This is implied if the foundation is installed on a sloping seabed, the upwards crane force is in that case not perpendicular to the foundation. Vesic (1969) considers tilted lifting in his study and suggests that in that case, the mechanism to break the suction differs from perpendicular lifting. Alternatively, eccentric loading could be applied to induce an asymmetric failure mechanism. Li (2015) studied the effect of applying an eccentric load at $^4/_5 r$ and found that the uplift resistance reduced with over $60\%$. Chen et al. (2012) show that the eccentric foundation uplift leads to a pull-out resistance that is even lower than the submerged weight of the structure, as the breakout occurs while the foundation is partly still in contact with the soil. Long et al. (2022) find that the underpressures decrease as the uplift eccentricity increases.

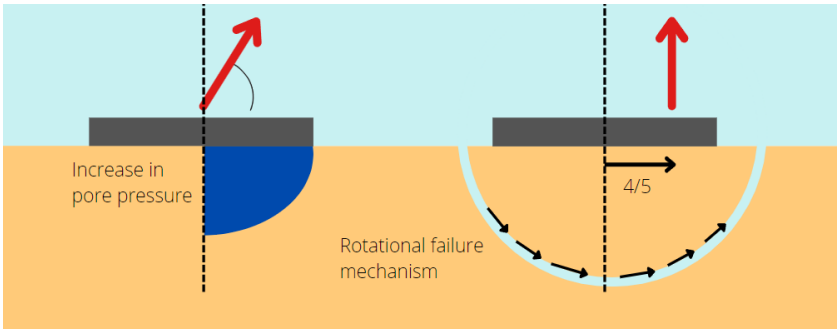


**Figure 8.10:** Tilted (left, following Vesic, 1969) and eccentric lifting (right, following Li, 2015) will alter the generation of underpressures at the foundation invert.

**Effect on mechanisms in clay**

1. Both tilted and eccentric lifting lead to an adjusted distribution of stress along the foundation. Water will still carry the uplift pressure, however, now the accumulation of the negative pore pressure will be more concentrated. The drainage paths to overcome the suction will partially shorten.
2. If an inclined force is applied, the adhesion can be lost more easily since a horizontal force is introduced. In the case of eccentric lifting, the adhesion can be overcome more easily at the zone of the least suction generation.
3. Differential unloading occurs, thus also leading to an altered accumulation of negative pore pressures, likely reducing the magnitude of peak pressure.
4. The underpressure in the gap between the clay and the mud-mat is also unevenly distributed.

**Effect on mechanisms in sand**

1. Similar to clay.
2. Sand does not have adhesive properties.
3. As the failure mechanism is different from centered or perpendicular uplift, the unloading effect will differ along the mud-mat diameter. The shear failure mechanism will be altered, thus also leading to reduced dilatancy.
4. Similar to clay. How the tilted lift influences hydrodynamics is described in the work of Mei et al. (1985). The researchers consider a wedged gap, where one point of the foundation is still touching the seabed.

**Table 8.9:** Advantages and disadvantages of the adjustment of the lifting procedure.

| Advantages | Disadvantages |
|---|---|
| Easy to perform, as the foundation geometry does not need to be adjusted | Distribution of forces in the foundation or pre-piling template is shifted such that the structural integrity might be impacted |
| Eccentric lifting can reduce the pull-out resistances | Adds risk to the lifting procedure in case of an asymmetric sudden breakout |
| | In practice, little sidelead in the crane wire is allowed |

## 8.6 Combinations of mitigation measures: Perforations and geotextile

A combination of two or more of the described mitigation measures can result in a larger reduction in peak force. Up until now, combinations of the mitigation measure are rarely equipped in practice. The only example described in literature dates from 1992. Perforations and geotextile in a skirted foundation are equipped in the Heidrun field, Norway (Lieng and Bjorgen, 1995). The combination of mitigation measures proves to be effective, as a suction reduction of around $50\%$ has been recorded, see Chapter 9. Figure 8.11 shows how the combination of perforations and geotextile is expected to lead to a reduced arching effect. This membrane effect can increase the bearing capacity of the footing while ensuring more rapid suction relief.

The combination of perforations and geotextile at the foundation invert is incorporated into the experimental program of this research. The results for tests in clay and sand are presented in Figures 8.12. Figure 8.13 shows the settlement and peak force for different mitigation measures.

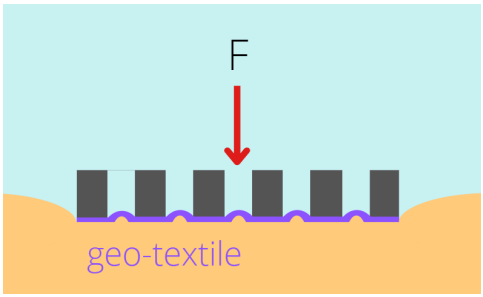


**Figure 8.11:** The arching effect is reduced in case of perforations and geotextile, where the geotextile acts like a membrane.

**(a)** Foundations on clay.

**(b)** Foundations on sand.

**Figure 8.12:** Influence of mitigation measures on forces and displacements in clay and sand.

**Table 8.10:** Observation and explanation for the effectiveness of mitigation measures in clay and sand.

| Observation | Explanation |
|---|---|
| The combination of perforations and geotextile reduces the peak force in clay and sand. The perforations reduce the peak force, as does the geotextile if applied separately. | This can be explained by the increased water flow at the foundation invert and shortened drainage paths, both during compression and unloading. The combination of perforations and geotextile allows water to flow through the holes, which can be easily distributed along the total foundation invert by the geotextile. |
| The uplift displacement is reduced due to all mitigation measures in both sand and clay. | The fact that there is still an uplift displacement recorded and the observation after testing that clay adheres to the geotextile suggests that the adhesion is still present and possibly dominant. |
| In sand, the peak force is largely reduced due to the combination of the perforations and geotextile. The peaks of the geotextile and perforations independently are comparable, although the peak is smoother for perforated foundations. | This is explained by the fact that the water in sand can already easily flow due to its permeability, aided by mitigation measures. The combination of perforations and geotextile is effective in removing all mechanisms that would occur during uplift. |
| No clear trend can be observed from Figure 8.13. It is observed that the combination of geotextile and perforations leads to little settlements and a low peak force. Next to that, both for geotextile and for perforations, increased settlement and reduced peak forces are observed for smaller load rates. The settlement for the perforated foundation with geotextile is lower than the settlement for the base case. | Higher load rates in clay reduce the time water has to flow to relieve the suction. Despite the application of mitigation measures, there is an effect of the load rate on the peak force. The fact that the settlement decreases for a perforated foundation with geotextile can be explained by the compressibility of the geotextile. |

**Figure 8.13:** Influence of mitigation measures and load rates on settlements and peak forces in clay.

### 8.6.1 Experiments with perforations and geotextile: Load rate

**(a)** Perforated foundation with geotextile on clay.

**(b)** Perforated foundation with geotextile on sand.

**Figure 8.14:** Influence of load rate on perforated mud-mats with geotextile in clay and sand.

**Table 8.11:** Observation and explanation for the effect of the load rate on perforated mud-mats with geotextile in clay.

| Observation | Explanation |
|---|---|
| The effect of the load rates is minimal in both clay and sand, in the case of the combination of mitigation measures as displayed in Figure 8.14. | The combination of perforations and geotextile is highly effective in reducing underpressures, such that the effect of the permeability of the soil is of lesser influence on underpressure development. The fact that the load rate does not influence the peak force in clay can suggest that adhesion is still present and dominant in resisting uplift. |

### 8.6.2 Experiments with perforations and geotextile: Preload and settling time

**Figure 8.15:** Influence of preload and settling time on forces and displacements.

**Table 8.12:** Observation and explanation for the effect of preload and settling time on perforated mud-mats with geotextile.

| Observation | Explanation |
|---|---|
| Figure 8.15 shows that the effect of adjusting the preload or the settling time on the peak force is minimal on a perforated foundation with geotextile. There is a slight increase in uplift displacement for larger preloads. | This can be explained by the fact that the peak force is caused by the adhesion in the case of the perforated geotextile foundation. |

### 8.6.3 Experiments with perforations and geotextile: Step-wise uplift

**Figure 8.16:** Influence of load application and mitigation measures on forces and displacements.

**Table 8.13:** Observation and explanation for the effect of step-wise uplift on mud-mats with geotextile in clay.

| Observation | Explanation |
|---|---|
| The step-wise uplift does not prove to reduce the peak force in the case of no mitigation measures, see Figure 8.16. However, due to the application of geotextile (on a perforated foundation), the peak force decreases if step-wise uplift is performed. | The geotextile layer allows negative pore pressures that are generated in the first step of uplift to start to increase to zero. The perforations further ease the excess pore pressure dissipation. |
| The peak force for the foundation with geotextile and the combination of perforation and geotextile is increased due to the step-wise uplift if compared to Figure 8.12a. | This can be explained by the test procedure, see Table 6.7. |

## 8.7 Combinations of mitigation measures: Electro-osmosis and geotextile

Another combination of mitigation measures is the equipping of active geosynthetics. Active geosynthetics represent a new generation of geosynthetic materials, however, are currently not yet studied for application in underpressure reduction under mud-mats. The material is electrically conductive and has the ability to initiate electrokinetic processes as well as to retain the established geosynthetic functions. The electrokinetic phenomena utilized are electro-osmosis and electrophoresis. Electro-osmosis causes water movement through low-permeability materials. Electrophoresis is the technique of separating molecules based on their size (Jones, 2007). All advantages and disadvantages related to electro-osmosis as described in Section 8.4 apply to active geosynthetics as well.

## 8.8 Conclusion

This Chapter presents an overview of existing mitigation measures to reduce peak forces during uplift. The experimental program studied both the effects of selected mitigation measures on the occurrence of the mechanisms and the effectiveness of the measures on the reduction of force that is required to lift the mud-mat. It was found that both the perforations and geotextile affect the mechanisms, separately and as a combined mitigation measure as well. This shows that *permeable foundations* can alter (pore) water flow around the foundation. In both cases, a peak force was still present in clay, likely due to adhesion effects. In sands, the underpressures disappear almost entirely due to the combination of geotextile and perforations.

# 9 Discussion

This Chapter discusses the findings of the research. After discussing the experimental setup and the complexities of observing and taking measurements of the mechanisms in real life, the results are compared with other papers. Lastly, several observations from the experimental results are discussed.

## 9.1 Discussion experimental program

First, it should be stated that the experiments are executed with soil, a natural material that is inherently heterogeneous. Next to that, the soil properties of the clay and sand were not recorded. Recommendations for an improved test procedure and set-up are thus provided in Chapter 11. Nevertheless, the results from the qualitative analysis in this research are valuable in understanding the mechanisms.

### 9.1.1 Test procedure

Although the results presented focus on the uplift procedure, the forces and displacements that are recorded before the uplift procedure starts are of influence on the mechanisms. The settlements between the lowering and uplift of the mud-mat were recorded. The soil was leveled before each test, however, it cannot be guaranteed that the mudline is always fully flat at the start of the test, see Figure 9.1. This alters the taring of the test bench and can explain illogical settlement trends. The variability in settlement throughout tests is little and the settlement is relatively small compared to the total uplift displacement.

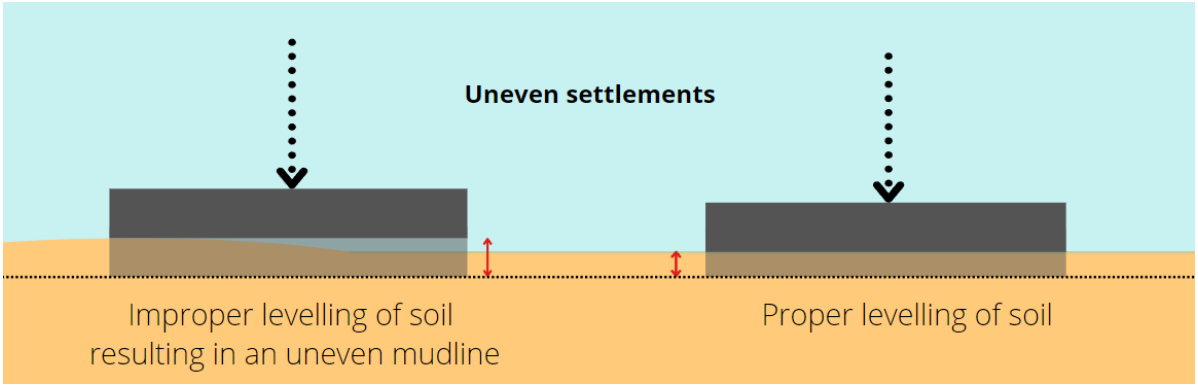


**Figure 9.1:** Uneven settlement caused by improper leveling of the soil can result in illogical settlement trends.

In the experiments, solely data at the mudline is collected. The force is measured in the load cell, which records the forces that act on the foundation, not on the soil. It is not possible to obtain conclusions about the pore pressure changes due to suction generation and relief over depth. The current test set-up only allows for drawing conclusions on the pressure differences that occur near the foundation invert.

After the execution of all tests, it can be concluded that the difference between the applied load rate and the average load rate is within acceptable limits. Next to the average load rate not exactly coinciding

with the input value in the load cell, the practical attainability of the load rates should be discussed. A load rate of $400N/s$ indicates that with a preload of $100N$ the weight of the foundation (in that case $\approx 100 + 40 = 140N$) is lifted in $0.35s$, which is unrealistic. Appendix A.4 displays the weights of the foundations. However, if a preload of $600N$ is applied and the lightest mud-mat ($\approx 600 + 20 = 620N$) is retrieved with a load rate of $40N/s$, only $\approx 6$% of the foundation is carried within a second, which is more realistic. In one centrifuge study, lifting rates of $30$ and $100mm/s$ were applied (Lehane et al., 2008) at $250g$. This seems unrealistic for small-scale tests, as it is ultimately $15mm/s$ in this research. In short, the load rates that are applied in this thesis could be applied in reality and are within the limits of rates applied by other researchers.

The underpressure that can be generated in the small gap between the foundation and an underlying medium is observed during uplift. The foundation was displaced a few millimeters upwards to study this mechanism however, it was not guaranteed whether a gap was formed. It cannot be assumed that the clay is fully detached from the foundation invert. The soil surface after detachment cannot be assumed to be flat, as no visual observations could be made. This uneven surface influences the flow in the gap. It might be that the load rate influences the shape of the mudline immediately after detachment, adding additional friction and resistance to the flow that fills the gap.

### 9.1.2 Pore pressure measurements

The clock that was connected to the microcontroller turned out to occasionally result in unreliable time measurements[1]. The pore pressure data thus needed to be shifted manually to match with the force data over time. This was only possible if changes in pressure due to both compression and uplift were clearly captured by the sensor. Next to that, a porous stone was added to the pore pressure transducer to improve the reliability of the results halfway through the execution of the experiments. The measurements for the same test scenario with and without porous stone were compared and do not show significant differences. The tests with porous stones do have reliable time measurements, as these were verified in real-time.

The pore pressure measurements do not allow for averaging of three tests as there is significant scatter throughout the test runs. This was not a problem for the data of the test bench. This can be explained by the fact that the pore pressure transducer only records the pressures locally, whereas the forces are distributed over the foundation invert.

## 9.2 Scalability of the mechanisms

The main goal of this thesis is to distinguish the different mechanisms that contribute to underpressure generation. It should however be discussed whether the conclusions on the mechanisms based on the experimental results are valid for underpressure generation under mud-mats of pre-piling templates. Spatial scale effects come into play. The diameter of the foundation in the tests is up to $80$ times smaller than a mud-mat would be in reality. The water carrying the uplift pressure will occur for larger diameter foundations as well, the time it takes for water to flow towards to center and relieve the suction will however increase. The adhesion of cohesive soils to the foundation will largely increase when considering larger diameter mud-mats. The adhesion at the foundation invert of mud-mats of diameters of $8$ to $12m$ will substantially contribute to the peak force. One of the largest uncertainties is how the adhesion will be lost and how the gap between the soil and foundation forms needs to be filled. The ”non-dimensionality” of the water carries the uplift pressure applies to the underpressure in water as well. The final mechanism, underpressure in water, in the sequence will occur for larger foundations as well. The sequence of mechanisms in clay and sand is expected to remain unchanged. However, how the underpressure is relieved will change. The amount of water that will get sucked out of the porous medium changes, altering the ratio of water originating from the soil or the surrounding water body. It thus can be assumed that the *generation* of underpressures in small-scale experiments is comparable to offshore practice, as the mechanisms can be interpreted as non-dimensional. However, the relative magnitude and quantitative effectiveness of the mitigation measures cannot be extrapolated in space.

[1]The instant the pore pressure sensor was connected to a power source, the data recording starts. The data is written to a CSV file. The timestamp of the start of the data record is printed to the first line of the file. The timestamp contains the current date, hour, minute, and second.

Next to considering the scaling of the mechanisms in space, the scaling of the results in time is discussed. During decommissioning, the same mechanisms that occur during the retrieval of temporary mud-mats are expected to occur under permanent foundations. The sequence of mechanisms will not alter. The main difference is the effect of the settling time. The soil will likely be in a denser state and consolidation is assumed to be complete. Adhesive bonding is expected to increase. The pore pressures and void ratio at the start of uplift remain uncertain. The Whole Life Design approach in geotechnical engineering of Gourvenec (2022) allows for estimations of soil parameters throughout the lifetime of offshore structures. This approach takes into account events such as storm or snag loads on the structure and episodes that alter the operative soil strength. This could give an indication of the state of the soil at the start of the lifting procedure.

## 9.3 Comparison to other research

The influence of a variety of parameters on the uplift force was obtained from the test results. Comparing the conclusions regarding peak forces or stresses and trends from the experimental results with conclusions drawn from centrifuge, field, laboratory and numerical tests from literature aids in validating the accuracy of the set-up and allows for a better discussion of the test results.

### 9.3.1 Centrifuge tests

Craig and Chua (1990) performed centrifuge tests with spudcans to study extraction forces and conclude that results can be extrapolated to full-scale offshore structures. This claim is made by the comparison of stress levels below major gravity structures to their measurements. Next to that, they state that increased compression loads lead to increased suction due to *good* underbase adherence of the clay. It can be concluded from the experimental results of this research that the increasing preload increases the adhesion and the peak force. These results are thus in line with previous works, although spudcan removal differs from shallow foundation uplift.

Purwana et al. (2005) study spudcans in the centrifuge as well. A distinction between the top and bottom suction is made in their tests. It is shown that during spudcan removal negative pore pressures develop at the base. The negative pore pressures during uplift increase for increased settling time, as it did in the tests in clay in this research.

Lehane et al. (2008) install square anchors with areas of $9$ and $20.25cm^2$ in clay overlying a sand backfill in a centrifuge study. It is found that increased uplift rates lead to increasing anchor capacity, which indicates that the underpressures increase. Partial drainage during load application was observed for an uplift velocity of $0.03mm/s$, as the anchor capacity was relatively low. Faster uplift rates were considered to be fully undrained. Whether this distinction between drained and fully undrained in $mm/s$ can be extended to this study is questioned, because of the fact that the researchers in the paper perform tests in a geotechnical centrifuge. Next to that, the drainage conditions depend heavily on the soils' hydraulic conductivity. Chen et al. (2012) investigated rectangular mud-mats sitting on clay subjected to varying uplift velocities, with and without skirts. They also suggest that the peak force increases with increasing uplift velocities in clay. Contradictory, this was not found in this research.

### 9.3.2 Field tests

In-situ breakout events are studied in the research of Bouwmeester et al. (2009) where a square mud-mat is installed in five different offshore locations across the world. A template was lowered onto a very soft soil, collected soil data by performing a CPT, and was retrieved afterward. The loads in the lifting cable and the depth of the template were recorded. A load rate of over $6kN/s$ was applied, achieving rapid breakout. A clear correlation between the breakout force and load rate is found. The load rates that are applied to the foundation in this research are not unfeasible as in Bouwmeesters' study around $15\%$ of the submerged weight of the template is carried within the first second. The notion that laboratory experiments may be extrapolated to offshore situations is relevant and reinforces the idea that the non-dimensionless of the mechanisms in this research is correct. The comparison to the quantitative results from Bouwmeester et al. is however not possible as the foundation geometry differs.

### 9.3.3 Laboratory tests

Ninomiya et al. (1972) study *three* different phenomena that they presume contribute to suction. Different test set-ups are designed to isolate and distinguish the phenomena: First, a model penetrated a clayey silt sample with $55cm$ and was retrieved after a predefined amount of time. The goal is to study solely side friction, however, that is not possible as the base of the model is in contact with the soil as well. Second, a similar test was performed to investigate the viscous force. The model was allowed to penetrate no further than $30$% of the diameter. Again, this does not solely study one of the phenomena. Lastly, adhesion was tested by allowing the model to settle after which the surrounding soil is removed. Next, the peak force during uplift was measured. It is questioned whether this test set-up isolates the adhesion and whether or not the removal of the surrounding soil alters the confinement and stress state of the soil under the model. It was found however that increased settling times resulted in increased peak forces. Roderick and Lubbad (1975) have similar findings in soft cohesive sediments. Das (1991) reports the same. Das also concluded that the depth of the water above the top of the clay has no effect on the breakout resistance.

Sawicki and Mierczyński (2003) performed experimental investigations to verify their theoretical solutions. A circular foundation ($32cm\varnothing$) was placed on a layer of sand. The settling time was set to $1\ hour$. During uplift, peak forces of $5$ and $20N$ were recorded, which is comparable to the peak force in sand in this study. The duration of the breakout varied from $1.5$ to $6s$ which is comparable to the findings in this study as well.

### 9.3.4 Numerical studies

The input that enters any numerical program impacts the output. The distinction of *four* mechanisms as presented in this research is never acknowledged before, thus present numerical studies only provide an approximation of the uplift resistance. Zhou et al. (2008) do make a distinction between *three* phases of underpressure development. Initially, the foundation is in contact with the soil. The subsoil is a porous, elastic, saturated seabed overlying a rigid seabed. Next, a partial gap develops after which the underpressure in the gap is created in the final, with-gap stage. The equipped equations are derived from studies on fluid mechanics and do not correctly incorporate the sequence of mechanisms that occur during uplift.

Al-Shamrani (1997) models embedded objects. The object pullout is assumed to occur with no soil volume changes, which indicates that the underpressures are not accurately modeled. In the work of Thorn (2004) thin anchor strips are subjected to uplift loading. Large-strain analyses are undertaken, which would not be suitable for numerical modeling shallow foundations as the mechanisms that occur during foundation retrieval result in small strains, near the foundation interface. Two coupled hydro-mechanical interfaces are proposed to model uplift of shallow foundations in the work of Tian et al. (2022). Both the flow in the gap between the foundation and soil and the water originating from the pore spaces is modeled. The effect of varying load rates is incorporated into their method, making a distinction between a drained and undrained response. They however assume that the foundation is porous as well.

### 9.3.5 Mitigation measures

A perforated mud-mat equipped with a geotextile solution was presented in the work of Lieng and Bjorgen (1995). The foundation was designed with discontinuous skirts to allow water to flow through. The mud-mats served as the foundation of a positioning pile guide frame that is constructed and used in practice to install anchors. This frame was able to handle $1.2MN$ in tension, with mats of $9.5m$ in diameter. The thickness of the geotextile is $22mm$. Lab tests were executed in fine silt to verify their novel mud-mat solution. The mat of 400 mm diameter was lifted $45\ minutes$ after installation with an uplift velocity of $6.667mm/s$. This resulted in a reduction of the pullout force of $50$% compared to an unperforated steel mud-mat. This is less than the reduction in the tests in this thesis; % in clay and % in sand. This difference can be explained by the perforated area ($3.1$% of area reduction in the paper, $5.2$% in this research), the soil type, the thickness of the geotextile, and the presence of skirts. Other research did indicate that the perforated area is of large importance in the effectiveness of the mitigation measure (Arts, 2017).

White et al. (2005) performed tests with square mud-mats in soft clay in a large-scale test tank. Some of the mud-mats were perforated with various perforation numbers and sizes. The unperforated foundation area was $0.015625m^2$ and the settling time was $1\ hour$. The researchers recommend finding the optimal perforation ratio to reduce the peak uplift resistance while ensuring the bearing capacity. Comparing the numerical values of the tests to the tests in this thesis is not possible as they work with $s_u$ and solely report $N_c$. Similar to this research, no trend between soil resistance and area is found. The main conclusion however is similar to the conclusions in this research: perforations reduce the peak uplift resistance, which is governed by the separation (loss of adhesion) of the soil from the underside of the foundation.

In the research of Li et al. (2014) rectangular mud-mats are installed in overconsolidated clay. The effect of perforations on underpressure generation both for unskirted and skirted foundations is studied. The researchers use the bearing capacity factor to determine the uplift resistance of the mats. Mud-mats with small and large perforations are tested for which the perforated area is identical. A linear trend between the peak stress and peak negative pore pressures is observed, irrespective of perforation presence or size. A reduction in the peak force of $35.8\%$ and $55.6\%$ is observed for the small and big perforations respectively. The reduction is larger compared to the decrease in this research which is $56.1\%$, this is explained by the perforated area ($19\%$ of area reduction in the paper, $5.2\%$ in this research). They observe a decrease in uplift displacement due to the perforations, which was observed as well in the tests in this study.

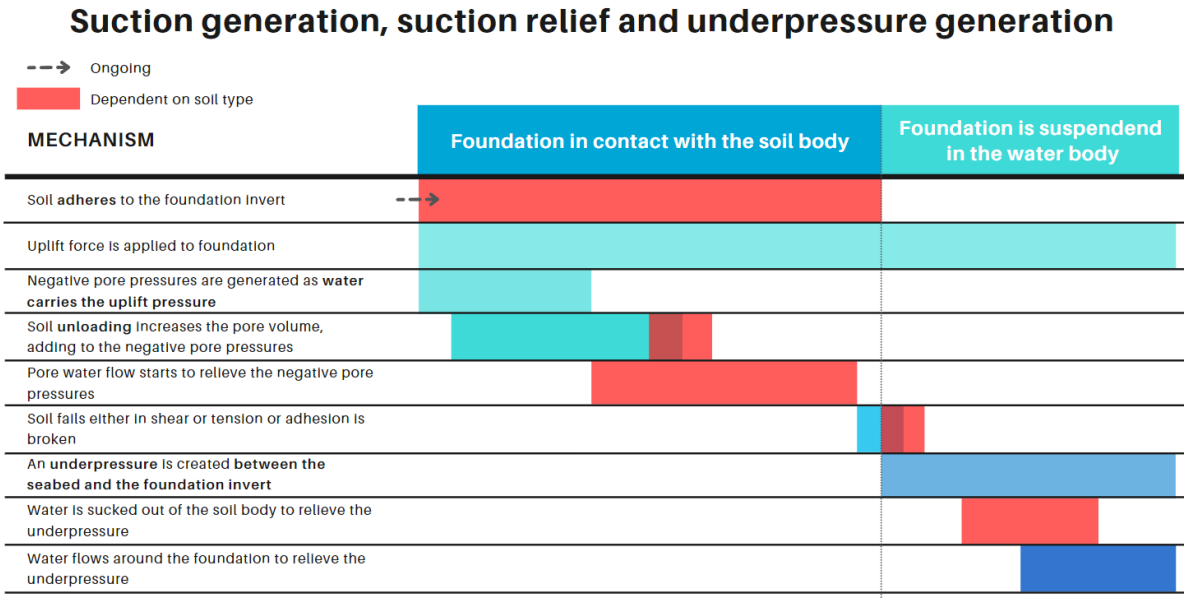


**Figure 9.2:** Expected sequence of mechanisms that contribute to a resisting force or lead to foundation breakout.

## 9.4 Discussion on observations

Figure 9.2 provides the general sequence of the mechanisms. This sequence presents the proposed order of mechanisms without dimensions, solely for increasing time and linearly increasing load. The correctness of this chart is not verified in this research. Not all observations from the results lead to conclusive findings. The listed conclusions are deduced from the experimental results, however, cannot be assumed to be proven or attributed to one of the mechanisms with great certainty.

- It was observed that higher load rates lead to increased pore pressures in clay. There was no recorded trend between the peak force and load rate in clay. It thus cannot be said with certainty that the underpressure in clay depends on the load rate. It is expected that the underpressure development would show a similar trend for the force over time, this was observed neither in clay nor in sand. Further tests are needed, see Recommendation 1.
- The adhesion is assumed to increase over time. Tests with increased settling times in clay resulted in increased peak forces, both with or without geotextile. This cannot be explained by significant

pore pressure dissipation during settling as the permeability of the clay is low and the time span limited. The settlement trend for longer settling times did not provide any additional insights. Van der Waals forces might influence the adhesion, and if present, introduce a dependency of the force on intermolecular distance. It cannot be excluded that adhesion is not dependent on the mineralogy and is purely an effect of the low porosity of clays (Gavin, 2022). If adhesion is found to be time-dependent, see Recommendation 2, the increased bonding of soils and the foundation would also occur in full-scale foundations.

- The fact that adhesion is predominant if the mud-mat is perforated or geotextile is installed, is concluded by deductive reasoning. Excess pore pressures in the soil, both positive and negative are relieved more easily by the shortened drainage paths or paths of lesser resistance. Significant uplift displacements in excess of the settlements are recorded, indicating that despite the mitigation measures the soil is dragged upwards with the foundation invert due to adhesion. See Recommendation 2 for further recommended tests.
- The effect of the unloading behavior on the pore volume and the contribution to the resisting force during uplift cannot be adequately studied with the current set-up. It was found that the displacement due to the unloading behavior of clay is impossible to distinguish from either adhesion or the tiny gap. The interface layer did not prove to be adequate in reducing adhesion and the detachment of the soil from the foundation cannot be observed. Through deduction, it can be reasoned that the unloading does affect suction generation in clay and sand. Recommendation 3 suggests further research to study unloading behavior.

  - Smaller pore volumes at the start of the uplift in clay due to increased preloads or longer settling times are expected to lead to larger pore volume changes upon unloading. This *can* result in a larger underpressure in your soil body.
  - The underpressure in the sand body is quickly relieved by water flow, as there is a load rate dependency of the peak force. The soil skeleton behavior of the sand is supposed to be reversible, the elastic displacement due to the settlements allow for pore volume changes that influence the generation of underpressure.

- The underpressure in water is presumed to be predominant in contributing to the resisting force in sand. This assumption is based on the fact that the uplift displacement is considerably larger than the settlement. As there is no adhesion, this displacement is explained by the tiny gap that is formed and filled with water. This assumption can be proved by further research, see Recommendation 4.

# 10 Conclusion

This study proves that for the uplift of shallow foundations a resisting force is generated by more than just the generation of negative excess pore pressures. A distinction is proposed of four different mechanisms that occur during the uplift of shallow foundations which lead to a resisting force, see Figure 10.1. Next to the negative pore pressures that complicate foundation retrieval, it was found that an additional resisting force is generated by an underpressure in the gap that develops between the detached foundation and the soil which *can* suck pore water out of the upper soil layer. This, among other things, disproves the notion that the ground behavior due to foundation compression is comparable to foundation uplift.

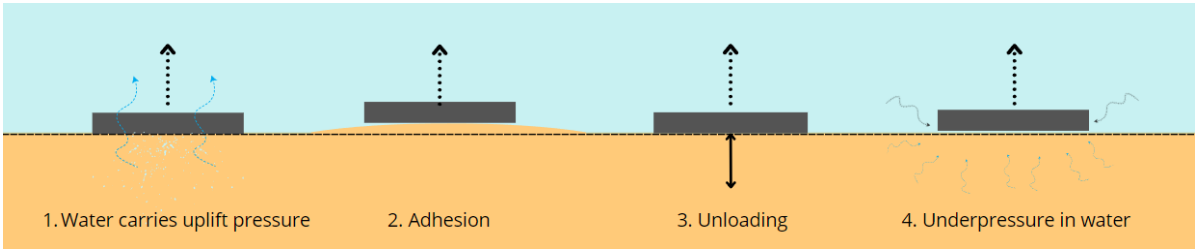


**Figure 10.1:** Four mechanisms that contribute to a resisting force during the uplift of shallow foundations.

1. Negative pore pressures are generated as the upward load is initially carried by the pore water.
2. Adhesive bonding occurs between the soil and the foundation, depending on the soil cohesion.
3. The pore volume increases due to unloading by a combination of shear and tension, this induces additional negative pore pressures.
4. A void between the foundation and soil must be filled with water causing a viscous drag along the foundation invert, which leads to an underpressure in the water body.

The findings in this research are based on the results from the experimental study and the comparison to previous research. The mechanisms are studied in an elaborate series of small-scale tests in clay and sand. Conclusions on the sequence and observability of the mechanisms are discussed in Chapter 9. Section 10.1 draws conclusions on the effects of different conditions such as soil type, load rate, or mitigation measure on underpressure generation and the recognition of the mechanisms.

## 10.1 Underpressure generation

- It can be concluded that the uplift of shallow foundations results in multiple mechanisms that contribute to a resisting force. The mechanisms contribute to underpressure generation both at the mud-mat/soil interface and the space between the mud-mat and soil after detachment.
- It is observed from the experimental results that the pore pressures change the instant that the uplift procedure has commenced, both in clay and sand. This indicates that the water carries the uplift pressure. The extent to which the negative pore pressures develop depends on the load rate and preload. This mechanism is likely to occur in practice in a similar manner, the instant the crane starts the uplift.

- In sands, the pore water will flow through the soil body to relieve the underpressures. This is shown by the load-rate dependency of the peak force.
- An underpressure in a water-filled gap between a foundation and an underlying medium contributes to a resisting force. The underlying medium can be porous or non-porous. Full-scale offshore foundation removal is expected to result in an underpressure in the gap as well.
- The resisting force that is caused by the underpressure due to the delayed filling of the void between the foundation invert and the underlying medium depends on the width of the gap between the foundation and the underlying medium.
- The aforementioned underpressure in the space between the foundation and underlying soil leads to water getting sucked out of sand. This reduces the resisting force. The division of the amount of water originating from the sand or the surrounding water body is not studied.
- The (combined) application of geotextile and perforations reduces the resisting force both in clay and sand and is thus an effective mitigation measure. This is found in the small-scale experiments for varying settling times, including times that are common for temporary foundations in practice.

## 10.2 Modelling underpressures

After understanding the mechanisms that contribute to underpressure generation, a design method could be drafted. Although calculation methods exist, a comprehensive method is not yet offered in literature. It is not within the scope of this study to present a comprehensive design method, however, the suitability of selected parameters is assessed with the conclusions from the experimental study.

Brinch-Hansen and the DNV propose to include the shear strength ($s_u$) and bearing capacity factor ($N_c$), among other parameters, into a calculation method. The shear strength is important for the unloading response and gives an indication of the bearing capacity and thus the settlement of the soil. Next to that, it models the cohesion and thus allows for the estimation of the adhesive stress. The bearing capacity factor does not add value to an equation to model underpressures as there is no distinction between mechanisms. Following Ninomiya et al., the effect of the area ($A$) should be incorporated in a design method. This conclusion however is based on the literature study and is not based on the experiments in this research. The load rate $v$ determines the peak force in sand and peak underpressure in clay and thus should be included as well. Lui proposes to include the settling time $T_{in-situ}$, which determines the pore pressures and pore volume at the start of the uplift. As this impacts the total underpressure that develops and might impact adhesion, the settling time is a parameter of influence on the uplift behavior.

The consolidation theory of Biot is equipped if drained conditions are assumed. The consolidation coefficient ($c_v$) will be calculated with the hydraulic conductivity of the soil and should be included in a design method. The stiffness of the soil ($E$) is of importance as well, as this determines the settlement. However, it should be assessed whether a value for Young's modulus of the soil skeleton that follows from laboratory tests is derived for loading or unloading the sample. The porosity at the start of uplift ($n_0$), as proposed by Sawicki, is of large importance for the underpressure that develops. The initial porosity is however hard to estimate for foundations. The compressibility of the pore fluid $\kappa_D$ is of importance as well, as this influences the water pressure changes.

### 10.2.1 Parameters

Further parameters that should be included in a design method to quantify suction at the mud-mat/soil interface of pre-piling templates are presented in Table 10.1.

**Table 10.1:** Recommended parameters for a design method to quantify pressure differences around a mud-mat/soil interface.

| Recommended parameters | Explanation |
|---|---|
| $A_{eff}$ | The effective area will be reduced if perforations are applied. The effective area might not equal the total area minus the area of the perforations *or* the total area if geotextile is applied. |

| | |
|---|---|
| $e_{max}$ | As the soil is displacing upwards along with the foundation invert, the void ratio increases. Particles stick together due to the suction forces acting on the grains and interparticle binding forces. The maximum void ratio aids in getting an indication of the tensile capacity of the sediment. |
| $U$ | The degree of consolidation is a function of time and is influenced by the installation method of the pin-piles, if considering mud-mats under pre-piling templates. The pile installation impacts both the pore pressure dissipation and regeneration. In studying the retrieval of temporary foundations, it is recommended to take into account the pile installation method to incorporate the effects on pore pressures. |

### 10.2.2 Estimation resisting force

By means of the tests executed, the notion that one will have to overcome a resistance that is at least equal to the submerged weight of the structure (DNV, 2021b) is challenged. It is found that the pressure differences do not lead to a retrieval force of twice the submerged weight of the structure if the foundation is placed on sand or if appropriate mitigation measures are applied. The diameter or geometry of the mud-mats is not incorporated in this DNV recommendation, leading to conservatism. Making a more detailed assessment of the soil characteristics and incorporating the foundation geometry, including mitigation measures, allows for overcoming this conservatism.

# 11 Recommendations

The final Chapter of this research contains recommendations for further research. A distinction is made between recommendations to improve the understanding of underpressure generation in different soil types and recommendations to work towards a *novel* foundation type. Lastly, further recommendations to better model underpressures are presented.

## 11.1 Further research on underpressure generation

Although the experiments performed in this research allow for making conclusions on the mechanisms that contribute to underpressure generation, further studies are recommended. Further research to study the mechanisms with suggested improvements to the test set-up and procedure is presented.

### 11.1.1 Mechanisms

1. It is recommended to install multiple pore pressure transducers in the foundation at different radii to observe the pore pressure distribution along the foundation area over time. The average pore pressure can be calculated to avoid the influence of local heterogeneities if multiple pore pressure transducers are installed at the same radius. Accurately determining the instant when the foundation detaches from the soil aids in drawing conclusions on the transition from one mechanism to another. Observing the initial simultaneous development of pore pressures at different radii from the center indicates that the full foundation area carries the uplift pressure. The suction relief will start at the periphery, reducing the negative excess pore pressures at the transducers further from the center first.
2. The influence of different mineral compositions on the adhesive strength of clay to varying foundation materials is previously studied, see Sass and Burbaum (2009; 2017) and Spagnoli et al. (2019). Still, further tests to understand adhesion as a contributor to a resisting force to the uplift of foundations of different materials are recommended. The test set-up in this research consisted of a stainless steel mud-mat, this would however not be installed in offshore conditions. Often, a coating will be applied to prevent corrosion. The adhesion between a woven synthetic material and clay should be studied, ideally with a pore pressure sensor near the adhesion interface in the soil. The loads on the mud-mat in this study are quasi-static. It is recommended to study the effect of cyclic loads on underpressure development as mud-mats of pre-piling templates are subjected to dynamic loading during pile installation. Cyclic pore pressure accumulation can alter adhesion development and ease subsequent foundation detachment. Taking microscope pictures can provide insights into the molecular bonding forces, and how they change over time.
3. Kong et al. (2021) study the interaction of tension and shear in saturated clays, however, do not include the soil-structure interaction. The unloading behavior of granular soils, the interaction of tension and shear, has not been previously studied. Research on the unloading stiffness of a soil, the maximum void ratio, and changes in pore volume due to dilatancy aid in understanding how unloading impacts suction development. The effects of dilatancy should be examined, as either the *tendency* of the soil to obtain a looser state results in more negative pore pressures or the increased porosity eases water flow towards the area of largest suction. Pore volume changes can be studied using direct shear tests with a steel foundation plate or simple shear tests. Drained

or undrained triaxial extension tests could be executed to study the formation of a shear band under controlled drainage conditions. See Verruijt (2001) for further explanations of experimental methods in geotechnical engineering. Particle Image Velocimetry can provide insights in grain movements and changes in pore space (Li et al., 2014). Do note that the unloading effect will always be coupled to the water carrying the uplift pressure.

4. It is apparent that water is sucked out of the soil, if the permeability is sufficiently low, due to the underpressure in the gap between the foundation and the soil. Adding coloring fluid to the soil medium at varying depths helps in verifying that the water in the gap originates from the soil body. The underpressure can be further studied by comparing pressure values from a water pressure transducer installed at the foundation invert and a pore pressure sensor in the soil body. Next to that, the division of water originating from the soil body or from the surrounding water body can be derived for several foundation shapes and diameters.

### 11.1.2 Test set-up

An improved test set-up is proposed to advance the study of uplift behavior of foundations. Performing laboratory tests on the clay and sand sample to obtain soil parameters allows for better comparisons to previous research. Deriving the shear strength, liquid limit, unit weight, and mineral composition of the clay is suggested. It is recommended to obtain a particle size distribution of the sand as well as the unit weight. After deriving the permeability of the soil, the flow through the soil can be better estimated. Tests in silt will provide additional insights into the effect of permeability on the uplift response, as the hydraulic conductivity is lower than sand, however, no minerals that lead to cohesion are present. Further experiments on underpressures below different foundation geometries are recommended. Although the underpressure *generation* is assumed not to be altered by the foundation geometry, the underpressure *relief* is. This is based on Jardine et al. (2004) who state that the difference in bearing capacity between circular and square foundations is about $2$ or $3\%$. However, the differences in suction between a circular and strip foundation are more than $10\%$ in the experiments of Li et al. (2015), depending on the uplift velocity.

The impact of settlement can be better studied if the levelness of the mudline is guaranteed. Next to that, it is recommended to further study area effects by comparing foundations that differ more in diameter than the foundations in this study. Centrifuge studies must be executed to investigate whether the quantitative results can be extrapolated to offshore practice. Tests with a perforated mud-mat with geotextile should also be tested on full-scale, to study the effectiveness of the mitigation measure in practice.

## 11.2 Further research on flexible foundations

The application of perforations and geotextile leads to significant reductions of underpressures in clay and entirely prevents underpressure generation in sand. Increasing the perforation size leads to steel weight reductions, decreasing the weight of the pre-piling template. Next to that, the geotextile can be pre-tensioned between a grid of steel, decreasing the steel necessitated for the construction of the mud-mat. This *flexible foundation* needs further validation before employment in reality. It needs to be verified that the bearing capacity of such a flexible foundation is sufficient for its application. The vertical bearing capacity of a shallow foundation changes due to perforations (White et al., 2005). Tapper et al. (2015) also observe a reduction in capacity for reduced foundation area due to larger perforations. The reduction depended on the depth profile of the undrained strength. The application of geotextile at the foundation invert will alter the failure mechanism as well. The geotextile will function as a membrane, adding to the vertical bearing capacity, see Figure 8.11. Both the vertical bearing capacity and sliding resistance of a geotextile foundation should be further researched.

The sliding capacity depends on the friction between the subsoil and the geotextile. The friction angle between for example sand and geotextile is derived experimentally and is $30.5^\circ$ (TenCate Geosynthesics BV, 2002), which is lower than the average angle between steel and sand which is around $32^\circ$ (Han et al., 2018). Reduced friction angles result in a differential response if placed on a sloping surface. If the flexible foundation will be equipped as a permanent foundation, interaction diagrams should be derived, as is common for offshore foundations. The geotextile is durable for $100$ years if

covered within one month after installation in soils with a pH between $4$ and $9$ (TenCate Geosynthetics BV, 2020) and thus is suitable to equip in permanent foundations.

Clogging of the geotextile over repeated installation cycles might alter the friction angle. Excessive amounts of clay in the geotextile openings could create a sliding surface parallel to the foundation invert. The chance that clogging poses a problem is low as the large perforations allow the unclogging of the textile as the mud-mat is dragged through the water for pre-piling template retrieval.

Changing foundation shapes, see for example Figure 11.1 for different configurations of a steel grid and pre-tensioned geotextile, lead to differential stress distributions in the geotextile. The sturdiest method of attachment of the geotextile to the steel grid should be sought, such that the detachment of the textile during the pre-piling template lifetime is prevented. The integrity of the geotextile should be further studied to guarantee the stability of the mud-mat. The geotextile might tear due to placement on sharp objects such as boulders or coral. Placement on an uneven seabed or cyclic loading due to mud-mat installation and uplift can lead to plastic deformations of the synthetic threads. Regardless of the further work that needs to be executed, this foundation type is very promising in being suitable for equipment under pre-piling templates.

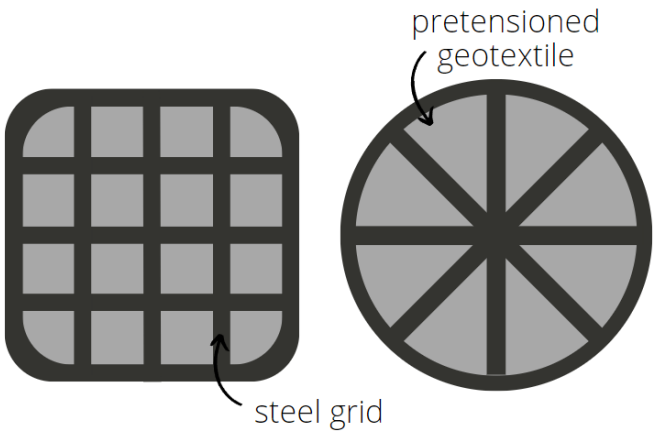


**Figure 11.1:** Examples of flexible foundation geometries

## 11.3 Modelling underpressures

Further work on a design method is necessary. Parameters that should be included in a design method are presented in Chapter 10. A trade-off should be made in a design method: The theoretically accurate quantification of pressure differences due to the different mechanisms is desired. However, the estimation of the resisting force with parameters that can be obtained with site investigation in offshore conditions is simple and fast. The trade-off will lead to the most accurate, upper-bound solution.

Further recommendations for practice include laboratory tests on the adhesion of cohesive sediments to the selected mud-mat coating. Pull-out tests should also be performed to study the adhesion between the geotextile and an in-situ soil sample. Borehole data from the soil could also be utilized for obtaining an estimation of the shear strength at the mud line. A proper design method with these soil parameters will lead to an accurate, upper-bound solution for the pressure differences that will develop under foundations. Optimal foundation design can be achieved by finding the most adequate mitigation measure with the quantification of underpressure reduction.

# References


Al-Shamrani, M. A. (1997). Finite Element Analysis of Breakout Force of Objects Embedded in Sea Bottom. *Civil Engineering Research Magazine*.

API. (2021). API Recommended Partice Part 4 -Geotechnical and foundation design considerations.

Arts, M. M. (2017). *Numerical modelling of the effect of perforations on the uplift force of skirted mudmats* (tech. rep.).

Biot, M. A. (1941). General Theory of Three-Dimensional Consolidation. *Journal of Applied Physics*, *12*, 155. https://doi.org/10.1063/1.1712886

Blume, H.-P., Brümmer, G. W., Fleige, H., Horn, R., Kandeler, E., Kögel-Knabner, I., Kretzschmar, R., Stahr, K., & Wilke, B.-M. (2016). *Soil Science*.

Bouwmeester, D., Peuchen, J., Van Der Wal, T., Sarata, B., Willemse, C. A., Van Baars, S., & Peelen, R. (2009). Prediction of Breakout Forces for Deepwater Seafloor Objects. *Offshore Technology Conference*, 4–7. http://onepetro.org/OTCONF/proceedings-pdf/09OTC/All-09OTC/OTC-19925-MS/1759530/otc-19925-ms.pdf/1

Burbaum, U., & Sass, I. (2017). Physics of adhesion of soils to solid surfaces. *Bulletin of Engineering Geology and the Environment*, *76*(3), 1097–1105. https://doi.org/10.1007/s10064-016-0875-5

Byrne, P., & Finn, W. (1978). Breakout of submerged structures buried to a shallow depth. *Canadian Geotechnical Journal*, *15*, 146–154.

Chang, Y., Huang, L. H., & Yang, F. P. Y. (2015). Two-dimensional lift-up problem for a rigid porous bed. *Phys. Fluids*, *27*, 53101. https://doi.org/10.1063/1.4919434

Chen, R., Gaudin, C., & Cassidy, M. J. (2012). Investigation of the vertical uplift capacity of deep water mudmats in clay. *Canadian Geotechnical Journal*, *49*(7), 853–865. https://doi.org/10.1139/T2012-037

Craig, W. H., & Chua, K. (1990). Extraction Forces For Offshore Foundations Under Undrained Loading. *Journal of Geotechnical Engineering*.

Das, B. M. (1991). Bottom breakout of objects resting on soft clay sediments. *Internation journal of offshore and polar engineering*, *1*(3), 195–199.

Davis, E. H., & Poulos, H. G. (1972). Rate of settlement under two- and three dimensional conditions. *Geotechnique*, *22*(1), 95–114. https://doi.org/10.1680/geot.1972.22.1.95

Dean, E. T. R. (2010). *Offshore Geotechnical Engineering: Principles and practice*.

Den Hertog, C. (2017). *Passive Suction under Mud Mats* (tech. rep.). TU Delft.

Deshpande, S. S. (2016). *Tensile Strength of Soil* (tech. rep.). https://doi.org/10.13140/RG.2.1.1263.9123

DNV. (2019a). OFFSHORE STANDARDS C101 Design of offshore steel structures, general-LRFD method. http://www.dnvgl.com

DNV. (2019b). RECOMMENDED PRACTICE N102 Marine operations during removal of offshore installations.

DNV. (2021a). RECOMMENDED PRACTICE C212 Offshore soil mechanics and geotechnical engineering.

DNV. (2021b). RECOMMENDED PRACTICE N103 Modelling and analysis of marine operations.

DNV. (2021c). STANDARD N001 Marine operations and marine warranty.

Ersdal, G. (2005). *Assessment of existing offshore structures for life extension* (Doctoral dissertation). https://www.researchgate.net/publication/242462159

Finn, W. D. L., & Byrne, P. M. (1972). The Evaluation of the Break-Out Force For a Submerged Ocean Platform. *Offshore Technology Conference*, 863–868. https://doi.org/10.4043/1604-MS

Foda, M. A. (1982). On the extrication of large objects from the ocean bottom (the breakout phenomenon). *Journal of Fluid Mechanics*, *117*, 211–231. https://doi.org/10.1017/S0022112082001591

Gaudin, C., Bienen, B., & Cassidy, M. J. (2011). Investigation of the potential of bottom water jetting to ease spudcan extraction in soft clay. *Geotechnique*, *61*(12), 1043–1054. https://doi.org/10.1680/geot.8.P.152

Gavin, K. (2022). Personal communication with Ken Gavin.

Goncalves, A. (2021). Offshore wind: New horizons demand new approach to operations. https://www.dnv.com/expert-story/maritime-impact/Offshore-wind-New-horizons-demand-new-approach-to-operations.html

Gourvenec, S. (2022). Whole Life Design: Theory and Applications of This New Approach to Offshore Geotechnics. *Indian Geotechnical Journal*, *52*(5), 1129–1154. https://doi.org/10.1007/s40098-022-00627-x

Guha, S. N. (1979). *Breakout of objects from underconsolidated sediments* (tech. rep.).

Han, F., Ganju, E., Salgado, R., & Prezzi, M. (2018). Effects of Interface Roughness, Particle Geometry, and Gradation on the Sand–Steel Interface Friction Angle. *Journal of Geotechnical and Geoenvironmental Engineering*, *144*(12). https://doi.org/10.1061/(asce)gt.1943-5606.0001990

Igoe, D., Doherty, P., & Gavin, K. (2010). The development and testing of an instrumented open-ended model pile. *Geotechnical Testing Journal*, *33*(1). https://doi.org/10.1520/GTJ102708

Jardine, R. J., Rotts, D. M., Higgings, K. G., Randolph, M. F., Jamiolkowski, M. B., & Zdravkovic, L. (2004). Load carrying capacity of foundations. *Proceedings of the Skempton Memorial Conference*, 207–240.

Jo, C.-H., Rho, Y.-H., & Kim, D.-Y. (2013). Investigation Of Jetting Piping System In The Spudcan Of Wind Turbine Installation Jack-Up Vessel. *International Conference on Asian and Pacific Coasts*.

Jones, C. J. (2007). Multifunctional uses of geosynthetics in civil engineering. *Geosynthetics in Civil Engineering*, 97–126. https://doi.org/10.1533/9781845692490.2.97

Kong, X., Cheng, Y., Zhao, B., Liu, Y., & Yang, Z. (2021). Study on Tensile-Shear and Compressive-Shear Coupling Strength of Saturated Clay. *Internation Conference On Environmental Science And Civil Engineering*. https://iopscience.iop.org/article/10.1088/1755-1315/719/4/042053/pdf

Landbo, T., Wiley, N. M., Gorejord, A., & Sveen, D. (2010). Wind Technology Moves into Deeper Water | SNAME Offshore Symposium | OnePetro. https://onepetro.org/SNAMETOS/proceedings-abstract/TOS10/1-TOS10/D013S001R002/3788

Lee, H. J. (1972). *Unaided breakout of partially embedded objects from cohesive seafloor soils* (tech. rep.). Naval Civil Engineering Laboratory. Port Hueneme. https://archive.org/details/unaidedbreakouto00leeh/mode/2up

Lehane, B. M., Gaudin, C., Richards, D. J., & Rattley, M. J. (2008). Rate effects on the vertical uplift capacity of footings founded in clay. *Geotechnique*, *58*(1), 13–21. https://doi.org/10.1680/geot.2008.58.1.13

Li. (2015). *The Uplift of Offshore Shallow Foundations* (Doctoral dissertation). The University of Western Australia.

Li, Gaudin, C., Tian, Y., & Cassidy, M. J. (2014). Effect of perforations on uplift capacity of skirted foundations on clay. *Canadian Geotechnical Journal*, *51*(4), 322–331. https://doi.org/10.1139/cgj-2013-0110

Li, Tang, C. S., Cheng, Q., Li, S. J., Gong, X. P., & Shi, B. (2019). Tensile strength of clayey soil and the strain analysis based on image processing techniques. *Engineering Geology*, *253*, 137–148. https://doi.org/10.1016/J.ENGGEO.2019.03.017

Lieng, J., & Bjorgen, H. (1995). OTC 7671 New Flow-through Mudmat Design for Heidrun Subsea Structure. *Offshore Technology Conference*, 1–4.

Liu, L. (1969). *Ocean Sediment Holding Strength Against Breakout of Embedded Objects* (tech. rep.). U.S. Naval Civil Engineering Laboratory. Port Hueneme.

Liu, R., Zhang, H., Chen, G., & Liu, M. (2020). Study on vertical bearing capacity of solid and perforated mudmats in clay. *Ocean Engineering*, *198*. https://doi.org/10.1016/j.oceaneng.2020.106973

Long, Y., Zhang, Q., Ye, G., & Zhu, W. (2022). Numerical study on the suction force of jack-up mat foundation on marine clay seabed. *Applied Ocean Research*, *121*. https://doi.org/10.1016/j.apor.2022.103084

Mana, D. S., Gourvenec, S., & Randolph, M. F. (2013). Experimental investigation of reverse end bearing of offshore shallow foundations. *Canadian Geotechnical Journal*, *50*(10), 1022–1033. https://doi.org/10.1139/cgj-2012-0428

Mei, C. C., Yeung, R. W., & Liu, K. F. (1985). Lifting of a large object from a porous seabed. *Journal of Fluid Mechanics*, *152*, 203–215. https://doi.org/10.1017/S0022112085000659

Muga, B. (1968). *Ocean bottom breakout forces* (tech. rep.). Naval Civil Engineering Laboratory. Port Hueneme.

Ninomiya, K., Tagaya, K., & Murase, Y. (1972). A Study on Suction and Scouring of Sit-On-Bottom Type Offshore Structure. *Offshore Technology Conference*. http://onepetro.org/OTCONF/proceedings-pdf/72OTC/All-72OTC/OTC-1605-MS/2066814/otc-1605-ms.pdf/1

Purwana, O. A., Leung, C. F., Chow, Y. K., & Foo, K. S. (2005). Influence of base suction on extraction of jack-up spudcans. *Geotechnique*, *55*(10), 741–753. https://www.researchgate.net/publication/245411496_Influence_of_base_suction_on_extraction_of_jack-up_spudcans

Randolph, M., & Gourvenec, S. (2011). *Offshore geotechnical engineering*. Taylor & Francis Group.

Ravindran, S., & Gratchev, I. (2022). Effect of Water Content on Apparent Cohesion of Soils from Landslide Sites. *Geotechnics*, *2*(2), 385–394. https://doi.org/10.3390/geotechnics2020017

Roderick, G. L. (1975). Electroosmotic reduction of ocean bottom breakout forces and times. *Canadian Geotechnical Journal*, *12*, 289–295. https://doi.org/10.1139/t75-034

Roderick, G. L., & Lubbad, A. (1975). Effect of Object In-situ Time on Bottom Breakout. *Offshore Technology Conference*. http://onepetro.org/OTCONF/proceedings-pdf/75OTC/All-75OTC/OTC-2184-MS/2068426/otc-2184-ms.pdf/1

Rosingh, P. (2018). *Hydrodynamic behaviour of perforated mudmat foundations Added mass and added damping close to the seabed* (tech. rep.). http://repository.tudelft.nl/.

Sass, I., & Burbaum, U. (2009). A method for assessing adhesion of clays to tunneling machines. *Bulletin of Engineering Geology and the Environment*, *68*(1), 27–34. https://doi.org/10.1007/S10064-008-0178-6/FIGURES/10

Sawicki, A., & Mierczyński, J. (2003). Mechanics of the breakout phenomenon. *Computers and Geotechnics*, *30*(3), 231–243. https://doi.org/10.1016/S0266-352X(02)00063-0

Sawicki, A. (1995). Soil suction forces and the breakout phenomenon. *Studia Geotechnica et Mechanica*.

Selvadurai, A. P. (2021). Irreversibility of soil skeletal deformations: The Pedagogical Limitations of Terzaghi's celebrated model for soil consolidation. *Computers and Geotechnics*, *135*, 104137. https://doi.org/10.1016/J.COMPGEO.2021.104137

Spagnoli, G., Feinendegen, M., & Seidl, W. (2019). The impact of mineralogy and chemical conditioning on the mechanical and adhesive properties of clays. *17th European Conference on Soil Mechanics and Geotechnical Engineering, ECSMGE 2019 - Proceedings*, *2019-September*. https://doi.org/10.32075/17ECSMGE-2019-0166

Spagnoli, G., Klitzsch, N., Fernández-Steeger, T., Feinendegen, M., Rey, A. R., Stanjek, H., & Azzam, R. (2011). Application of electro-osmosis to reduce the adhesion of clay during mechanical tunnel driving. *Environmental and Engineering Geoscience*, *17*(4), 417–426. https://doi.org/10.2113/gseegeosci.17.4.417

Tamrakar S, Mitachi, T., & Kung, G. T. C. (2013). Tensile strength and suction of naturally available saturated clays with modified tensile testing apparatus and their relationships with unconfined compressive strength. *Disaster Advances*. https://www.researchgate.net/publication/287535934

Tapper, L., Martin, C. M., Byrne, B. W., & Lehane, B. M. (2015). Undrained vertical bearing capacity of perforated shallow foundations. *Frontiers in Offshore Geotechnics III - 3rd International Symposium on Frontiers in Offshore Geotechnics*, 813–818. https://doi.org/10.1201/b18442-114

TenCate Geosynthesics BV. (2002). *Geolon PP 100 Friction EN ISO* (tech. rep.). Hengelo.

TenCate Geosynthetics BV. (2020). *TenCate Geotube GT1000M-MB* (tech. rep.). Hengelo.

Thorne, C. P., Wang, C. X., & Carter, J. P. (2004). Uplift capacity of rapidly loaded strip anchors in uniform strength clay. *54*(8), 507–517. https://www.researchgate.net/publication/239410990_Uplift_capacity_of_rapidly_loaded_strip_anchors_in_uniform_strength_clay

Tian, Y., Ren, J., Zhou, T., Peng, M., & Cassidy, M. J. (2022). Coupled hydro-mechanical interfaces to enable uplift modelling in offshore engineering. *Ocean Engineering*, *245*. https://doi.org/10.1016/j.oceaneng.2022.110570

TWD. (2018). BOKA pre-piling template.

TWD. (2019a). *Piling Template Design Guide* (tech. rep.).

TWD. (2019b). Van Oord Wind Drilling Template St. Brieuc.

Verruijt, A. (1982). *Theory of Groundwater Flow*. Macmillan Education UK. https://doi.org/10.1007/978-1-349-16769-2

Verruijt, A. (2001). *SOIL MECHANICS*. http://geo.verruijt.net/.

Verruijt, A., & Merwehoofd, A. V. (1994). *OFFSHORE SOIL MECHANICS*. http://geo.verruijt.net

Vesic, A. S. (1969). *Breakout Resistance of Objects Embedded in Ocean Bottom* (tech. rep.). U.S. Naval Civil Engineering Laboratory. Durham.

White, D. J., Maconochie, A. J., Cheuk, C. Y., Bolton, M. D., Joray, D., & Springman, S. M. (2005). An investigation into the vertical bearing capacity of perforated mudmats. *Frontiers in Offshore Geotechnics, ISFOG 2005 - Proceedings of the 1st International Symposium on Frontiers in Offshore Geotechnics*, 459–465. https://www.researchgate.net/publication/290288995_An_investigation_into_the_vertical_bearing_capacity_of_perforated_mudmats

Yan, S. W., Zhang, J. J., Tian, Y. H., & Sun, L. Q. (2016). Pore pressure characteristics in isotropic consolidated saturated clay under unloading conditions. *Journal of Marine Science and Technology (Taiwan)*, *24*(1), 19–25. https://www.researchgate.net/publication/301717651_Pore_pressure_characteristics_in_isotropic_consolidated_saturated_clay_under_unloading_conditions

Zhou, X. X., Chow, Y. K., & Leung, C. F. (2008). Numerical modeling of breakout process of objects lying on the seabed surface. *Computers and Geotechnics*, *35*(5), 686–702. https://doi.org/10.1016/j.compgeo.2007.11.004

# A Additional information experiments

## A.1 Pore pressure sensor

| Property | Value |
|---|---|
| Medium | liquid/gas without corrosion |
| Wiring | Gravity-3Pin (Signal-VCC-GND) |
| Pressure Measurement Range | 0 1 Mpa |
| Input Voltage | +5 VDC |
| Output Voltage | 0.5 4.5 V |
| Measurement Accuracy | 0.5% 55°C) |
| Threadably | G1/4 |
| Adapter | G1/2 to G1/4 |
| Waterproof Level | IP68 |
| Operating Temperature | -20 85°C |
| Response Time | <2.0 ms |
| Quiescent Current | 2.8 mA |
| Normal Operating Pressure | ≤2.0 Mpa |
| Damaged Pressure | ≥3.0 Mpa |
| Service Life | ≥10’000’000 times (10 million) |

**Table A.1:** Specifications of Water Pressure Sensor SKU SEN0257

## A.2 Arduino microcontroller

| Property | Value |
|---|---|
| Selected data recording frequency | 500 Hz |
| Microcontroller | ATmega328 |
| Operating Voltage | 5V |
| Input Voltage (recommended) | 7-12V |
| Input Voltage (limits) | 6-20V |
| Digital I/O Pins | 14 (of which 6 provide PWM output) |
| Analog Input Pins | 6 |
| DC Current per I/O Pin | 40 mA |
| DC Current for 3.3V Pin | 50 mA |
| Flash Memory | 32 KB (ATmega328) |
| SRAM | 2 KB (ATmega328) |
| EEPROM | 1 KB (ATmega328) |
| Clock Speed | 16 MHz |
| Length | 68.6 mm |
| Width | 53.4 mm |
| Weight | 25 g |
| Delay | 1 ms |

**Table A.2:** Specifications of Arduino Uno R3

## A.3 Test bench

| **Manual input** | **Maximum value** |
|---|---|
| Installation rate | $100mm/min$ |
| Hold speed | $1mm/min$ |
| Nominal speed | $1mm/min$ |
| Data recording frequency | $250Hz$ |
| **Machine specifications** | **Value** |
| Machine Capacity | $50kN$ |
| Speed Range | $0.00001$ to $1000mm/min$ |
| Crosshead Travel (excluding grips) | $950mm$ |
| Distance Between Columns | $420mm$ |

**Table A.3:** Specifications of Testometric X500-50kN Test Bench

## A.4 Mud-mat

| Property | Value |
|---|---|
| Area unperforated mud-mat (D = 150 mm) | $0.017671m^2$ |
| Area unperforated mud-mat (D = 200 mm) | $0.031416m^2$ |
| Area perforated mud-mat (D = 150 mm) | $0.016747m^2$ |
| Weight unperforated mud-mat (D = 150 mm), with double suspension mechanism | $40.3N$ |
| Weight unperforated mud-mat (D = 200 mm), with single suspension mechanism | $27.1N$ |
| Weight perforated mud-mat (D = 150 mm), with single suspension mechanism | $26.6N$ |
| Material | Stainless steel* |
| Thickness plate | $7mm$ |
| Stiffness plate | Assumed to be $\infty kPa$ |
| Thickness porous stone | $5mm$ |

**Table A.4:** Specifications of mud-mat foundations

*In offshore practice, a coating is applied to most steel foundations, however the coating might degrade or wear during testing. Thus a stainless steel mud-mat is equipped in the test set-up.

## A.5 Geotextile

*Confidential*

## A.6 Test procedure

- Prepare soil sample
  - Mix soil sample to redistribute sediment
  - Compress soil sample to remove air bubbles
  - Level soil sample to ensure full connection between foundation and soil
  - Let soil rest for approximately one minute to settle under its own weight and prevent further water intrusion into soil during test
- Check connection pressure sensor to foundation plate
- Check microcontroller wiring
- Connect microcontroller to power bank to start data recording
- List approximate time start data recording pressure sensor
- Start test method in test bench
- List start time data recording test bench and test number for later reference
- After test, remove microcontroller from power bank
- Retrieve data from SD card, saved in CSV file
- After three successful test runs, export Excel from test bench with correct sample number (e.g. *T12-P2-CL*)

# A.7 Borehole from the location of retrieval of clay sample

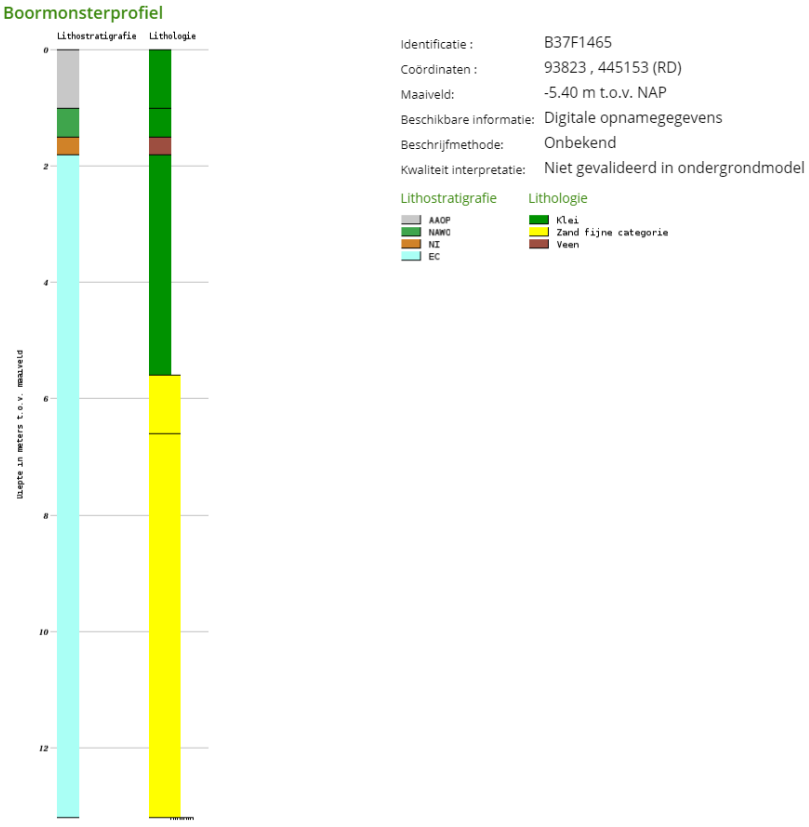


**Figure A.1:** DINOloket Borehole from the location of retrieval of clay sample

# B

# Experimental program

## B.1 Experimental program Clay

| Sample name | ∅ [mm] | Mud-mat type | Uplift velocity [N/s] | Settling time [min] | Preload [N] | Soil type | Uplift load increment |
|---|---|---|---|---|---|---|---|
| T01-P1-CL | 150 | unperforated | 400 | 2 | 100 | clay | linear |
| T02-P1-CL | 150 | unperforated | 40 | 2 | 100 | clay | linear |
| T03-P1-CL | 150 | unperforated | 200 | 2 | 100 | clay | linear |
| T04-P1-CL | 150 | unperforated | 600 | 2 | 100 | clay | linear |
| T05-P1-CL | 200 | unperforated | 600 | 2 | 100 | clay | linear |
| T06-P1-CL | 150 | perforated | 400 | 2 | 100 | clay | linear |
| T07-P1-CL | 200 | unperforated | 400 | 2 | 100 | clay | stepwise |
| T08-P1-CL | 150 | unperforated | 40 | 2 | 100 | clay | stepwise |
| T09-P1-CL | 150 | unperforated | 400 | 2 | 100 | clay | stepwise |
| T11-P1-CL | 150 | unperforated | 800 | 2 | 100 | clay | linear |
| T12-P1-CL | 150 | unperforated | 1 | 2 | 100 | clay | linear |
| T13-P1-CL | 150 | unperforated | 4 | 2 | 100 | clay | linear |

**Table B.1:** Water carries uplift pressure

| Sample name | ∅ [mm] | Mud-mat type | Uplift velocity [N/s] | Settling time [min] | Preload [N] | Soil type | Uplift load increment |
|---|---|---|---|---|---|---|---|
| T01-P1-CL | 150 | unperforated | 400 | 2 | 100 | clay | linear |
| T02-P2-CL | 150 | unperforated | 400 | 2 | 150 | clay | linear |
| T03-P2-CL | 150 | unperforated | 400 | 2 | 200 | clay | linear |
| T04-P2-CL | 200 | unperforated | 400 | 10 | 100 | clay | linear |
| T05-P2-CL | 200 | unperforated | 400 | 2 | 100 | clay | linear |
| T06-P2-CL | 200 | unperforated | 400 | 30 | 100 | clay | linear |
| T07-P2-CL | 200 | unperforated | 40 | 2 | 100 | clay | linear |
| T08-P2-CL | 200 | unperforated | 10 | 2 | 100 | clay | linear |
| T09-P2-CL | 150 | geotextile | 400 | 2 | 100 | clay | linear |
| T10-P2-CL | 150 | geotextile | 40 | 2 | 100 | clay | linear |
| T11-P2-CL | 150 | unperforated | 400 | 2 | 50 | clay | linear |
| T12-P2-CL | 150 | unperforated | 400 | 20 sec | 100 | clay | linear |
| T13-P2-CL | 150 | geotextile | 400 | 30 sec | 100 | clay | linear |
| T14-P2-CL | 150 | perforated+geotextile | 400 | 2 | 100 | clay | linear |
| T15-P2-CL | 150 | perforated+geotextile | 400 | 2 | 50 | clay | linear |
| T16-P2-CL | 150 | perforated+geotextile | 400 | 2 | 100 | clay | stepwise |
| T17-P2-CL | 150 | unperforated | 400 | 2 hours | 100 | clay | linear |
| T18-P2-CL | 150 | unperforated | 400 | 14 hours | 100 | clay | linear |
| T19-P2-CL | 150 | perforated | 80 | 2 | 100 | clay | linear |
| T20-P2-CL | 150 | perforated+geotextile | 800 | 2 | 100 | clay | linear |
| T21-P2-CL | 150 | perforated+geotextile | 400 | 30 sec | 100 | clay | linear |
| T22-P2-CL | 150 | geotextile | 400 | 2 | 100 | clay | stepwise |
| T23-P2-CL | 150 | geotextile | 800 | 2 | 100 | clay | linear |
| T24-P2-CL | 150 | geotextile | 400 | 14 hours | 100 | clay | linear |

**Table B.2:** Adhesion

| Sample name | ∅ [mm] | Mud-mat type | Uplift velocity [N/s] | Settling time [min] | Preload [N] | Soil type | Uplift load increment |
|---|---|---|---|---|---|---|---|
| T01-P3-CL | 150 | unperforated | 400 | 2 | 100 | clay | linear |
| T02-P3-CL | 150 | unperforated | 400 | 2 | 50 | clay | linear |
| T03-P3-CL | 150 | unperforated | 400 | 20 sec | 100 | clay | linear |
| T04-P3-CL | 150 | unperforated | 400 | 2 | 150 | clay | linear |
| T05-P3-CL | 150 | unperforated | 400 | 2 | 100 | clay | stepwise |

**Table B.3:** Unloading

| Sample name | ∅ [mm] | Mud-mat type | Uplift velocity [N/s] | Hanging time [sec] | Gap width [mm] | Soil type | Uplift load increment | Preload [N] |
|---|---|---|---|---|---|---|---|---|
| T01-P4-CL | 200 | unperforated | 400 | 30 | 15 | clay | linear | 100 |
| T02-P4-CL | 150 | perforated | 400 | 30 | 2 | clay | linear | 100 |
| T03-P4-CL | 150 | unperforated | 40 | 30 | 10 | clay | linear | 100 |
| T05-P4-CL | 150 | unperforated | 40 | 10 | 3 | clay | linear | 100 |
| T06-P4-CL | 150 | unperforated | 400 | 10 | 3 | clay | linear | 100 |
| T07-P4-CL | 150 | unperforated | 400 | 10 | 1 | clay | linear | 100 |
| T08-P4-CL | 150 | unperforated | 400 | 10 | 2 | clay | linear | 100 |

**Table B.4:** Underpressure in water

## B.2 Experimental program Sand

| Sample name | ∅ [mm] | Mud-mat type | Uplift velocity [N/s] | Settling time [min] | Preload [N] | Soil type | Uplift load increment |
|---|---|---|---|---|---|---|---|
| T01-P1-FS | 150 | unperforated | 400 | 2 | 600 | fine sand | linear |
| T02-P1-FS | 150 | unperforated | 40 | 2 | 600 | fine sand | linear |
| T03-P1-FS | 150 | unperforated | 200 | 2 | 600 | fine sand | linear |
| T04-P1-FS | 150 | unperforated | 600 | 2 | 600 | fine sand | linear |
| T05-P1-FS | 200 | unperforated | 400 | 2 | 400 | fine sand | linear |
| T06-P1-FS | 200 | unperforated | 400 | 2 | 800 | fine sand | linear |
| T07-P1-FS | 200 | unperforated | 40 | 2 | 400 | fine sand | linear |
| T08-P1-FS | 200 | unperforated | 400 | 20 sec | 600 | fine sand | linear |
| T09-P1-FS | 150 | unperforted | 100 | 2 | 600 | fine sand | linear |
| T13-P1-FS | 150 | perforated | 800 | 2 | 600 | fine sand | linear |
| T14-P1-FS | 150 | unperforated | 400 | 2 | 600 | fine sand | stepwise |
| T15-P1-FS | 150 | unperforated | 40 | 2 | 600 | fine sand | stepwise |
| T16-P1-FS | 150 | geotextile | 400 | 2 | 600 | fine sand | stepwise |

**Table B.5:** Water carries uplift pressure

| Sample name | ∅ [mm] | Mud-mat type | Uplift velocity [N/s] | Settling time [min] | Preload [N] | Soil type | Uplift load increment |
|---|---|---|---|---|---|---|---|
| T01-P1-FS | 150 | unperforated | 400 | 2 | 600 | fine sand | linear |
| T05-P2-FS | 150 | unperforated | 400 | 2 | 200 | fine sand | linear |
| T06-P2-FS | 150 | unperforated | 40 | 2 | 1000 | fine sand | linear |
| T07-P2-FS | 150 | unperforated | 400 | 2 | 1000 | fine sand | linear |
| T08-P2-FS | 150 | unperforated | 400 | 20 sec | 600 | fine sand | linear |
| T12-P2-FS | 150 | unperforated | 400 | 1 hour | 600 | fine sand | linear |
| T14-P2-FS | 150 | perforated | 400 | 2 | 600 | fine sand | linear |
| T15-P2-FS | 150 | perforated | 40 | 2 | 600 | fine sand | linear |
| T16-P2-FS | 150 | perforated | 600 | 2 | 600 | fine sand | linear |
| T17-P2-FS | 150 | perforated+geotextile | 600 | 2 | 600 | fine sand | linear |
| T18-P2-FS | 150 | perforated+geotextile | 800 | 2 | 600 | fine sand | linear |
| T19-P2-FS | 150 | geotextile | 800 | 2 | 600 | fine sand | linear |
| T20-P2-FS | 150 | geotextile | 600 | 2 | 600 | fine sand | linear |

**Table B.6:** Adhesion

| Sample name | ∅ [mm] | Mud-mat type | Uplift velocity [N/s] | Settling time [min] | Preload [N] | Soil type | Uplift load increment |
|---|---|---|---|---|---|---|---|
| T01-P3-FS | 150 | unperforated | 400 | 2 | 600 | fine sand | linear |

**Table B.7:** Unloading

| Sample name | ∅ [mm] | Mud-mat type | Uplift velocity [N/s] | Hanging time [min] | Gap width [mm] | Soil type | Uplift load increment | Preload |
|---|---|---|---|---|---|---|---|---|
| T01-P4-FS | 150 | unperforated | 400 | 0.5 | 0.5 | fine sand | linear | 400 |
| T02-P4-FS | 150 | unperforated | 800 | 0.5 | 0.5 | fine sand | linear | 400 |
| T05-P4-FS | 200 | unperforated | 400 | 0.5 | 0.5 | fine sand | linear | 400 |
| T06-P4-FS | 200 | unperforated | 800 | 0.5 | 0.5 | fine sand | linear | 400 |
| T07-P4-FS | 150 | unperforated | 400 | 0.5 | 1 | fine sand | linear | 400 |
| T09-P4-FS | 150 | unperforated | 400 | 0.5 | 2 | fine sand | linear | 400 |
| T10-P4-FS | 150 | unperforated | 400 | 0.5 | 3 | fine sand | linear | 400 |

**Table B.8:** Underpressure in water

## B.3 Experimental program Steel

| Sample name | ∅ [mm] | Mud-mat type | Uplift velocity [N/s] | Gap width [mm] | Material type | Uplift load increment | Preload [N] |
|---|---|---|---|---|---|---|---|
| T01-NP | 200 | unperforated | 800 | 0.5 | steel | linear | 200 |
| T02-NP | 200 | unperforated | 800 | 1 | steel | linear | 200 |
| T03-NP | 200 | unperforated | 800 | 2 | steel | linear | 200 |
| T04-NP | 200 | unperforated | 800 | 3 | steel | linear | 200 |
| T05-NP | 200 | unperforated | 800 | 0 | steel | linear | 200 |
| T06-NP | 200 | unperforated, wrap | 800 | 0 | steel | linear | 200 |
| T07-NP | 200 | unperforated, wrap | 400 | 0 | steel | linear | 200 |

**Table B.9:** Non-porous medium

# C

# Graphs test clay

The reader is referred to Section 5.4 for an explanation of the post-processing and data representation in this research.

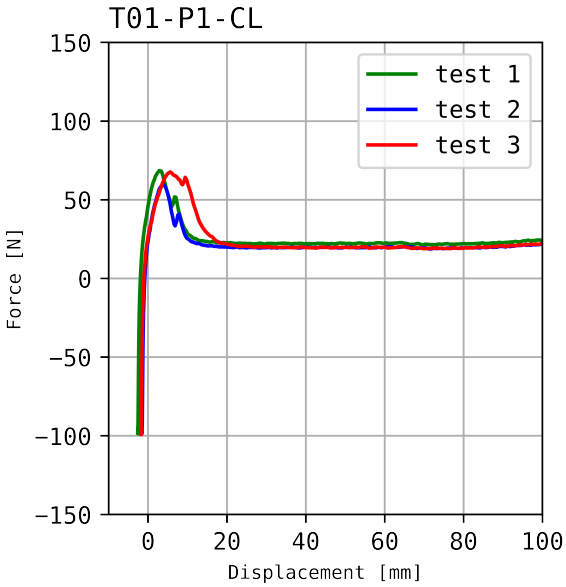


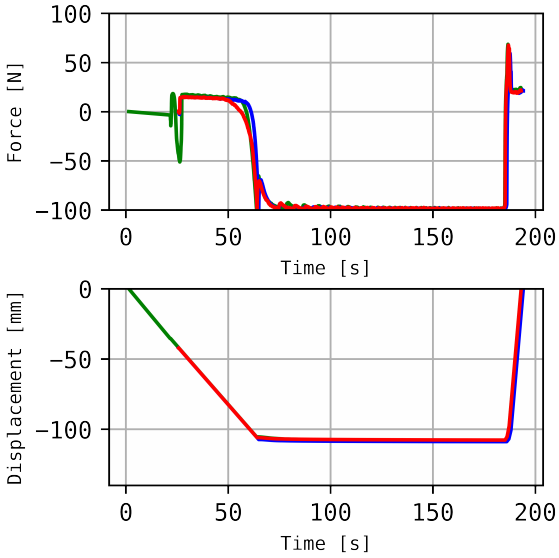

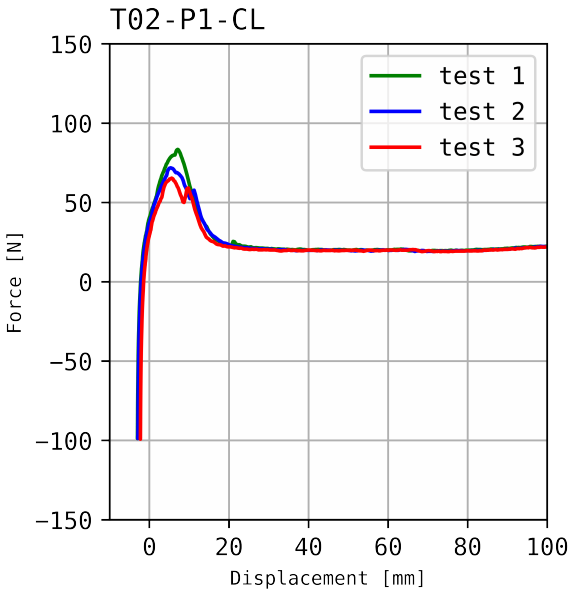
T02-P1-CL
test 1
test 2
test 3
Force [N]
Displacement [mm]

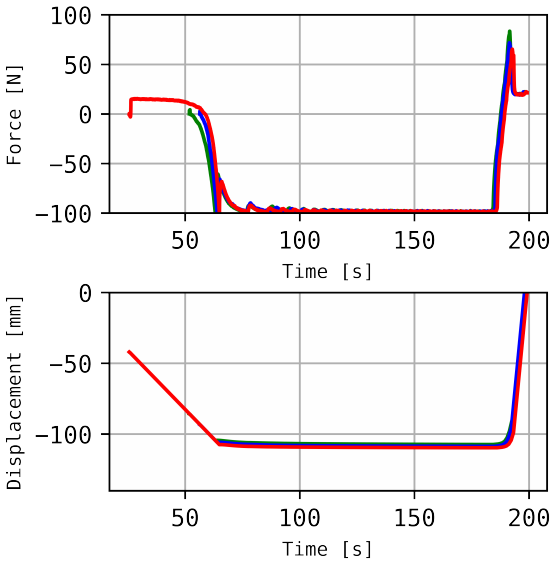
Force [N]
Time [s]
Displacement [mm]
Time [s]

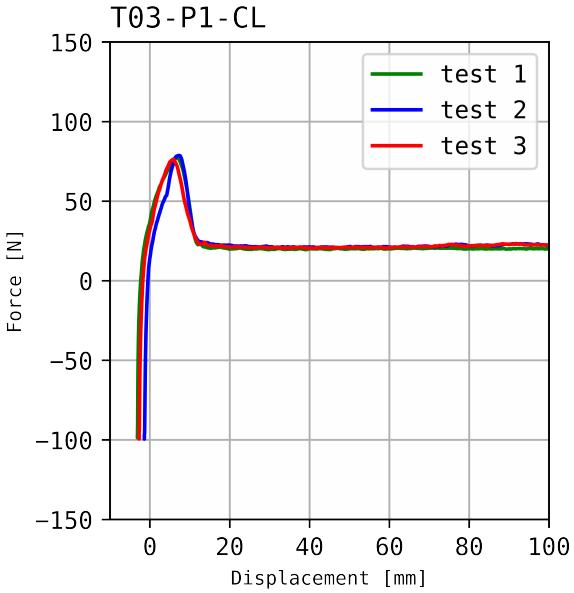
T03-P1-CL
test 1
test 2
test 3
Force [N]
Displacement [mm]

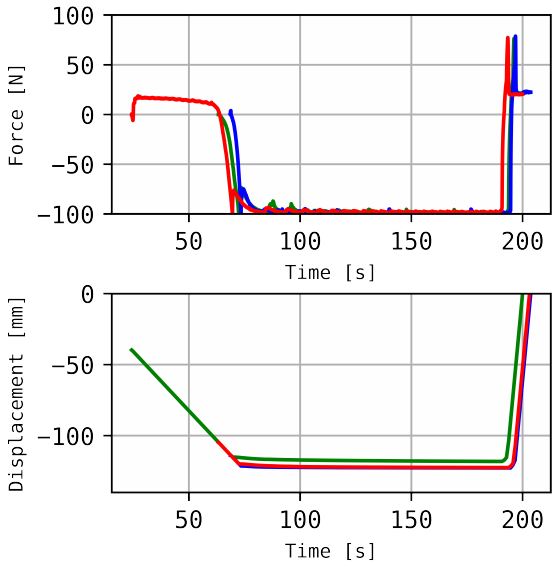
Force [N]
Time [s]
Displacement [mm]
Time [s]

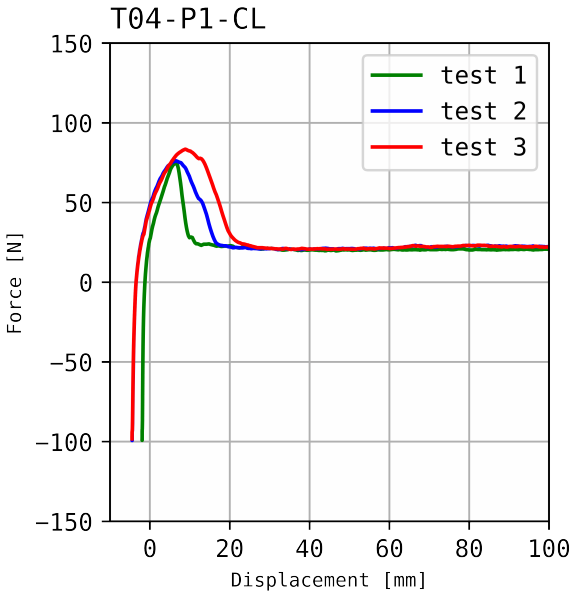
T04-P1-CL
test 1
test 2
test 3
Force [N]
Displacement [mm]

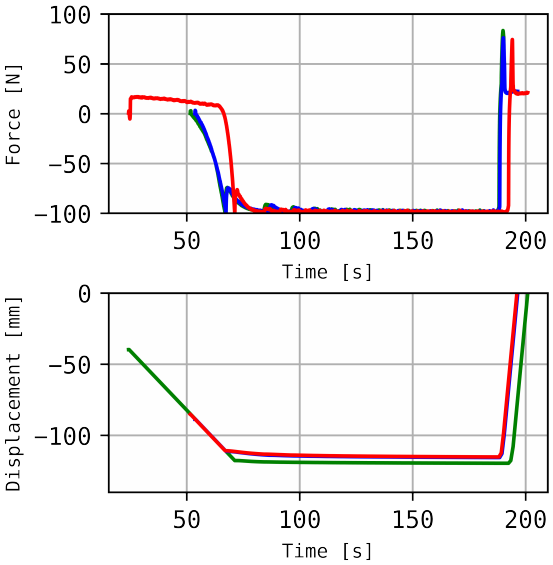
Force [N]
Time [s]
Displacement [mm]
Time [s]

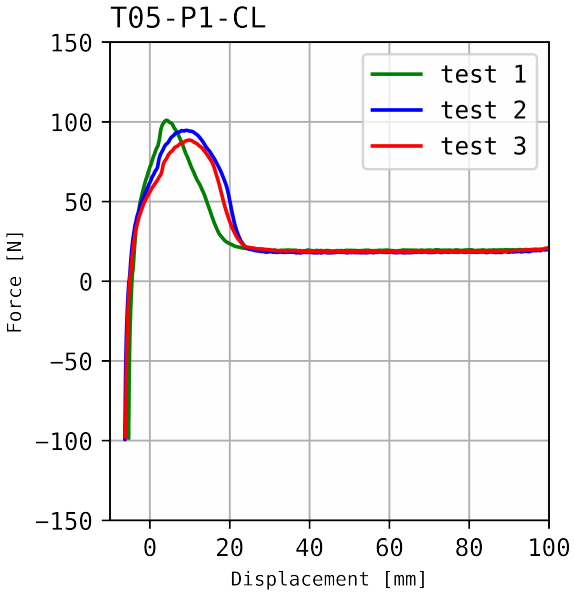
T05-P1-CL
test 1
test 2
test 3
Force [N]
Displacement [mm]

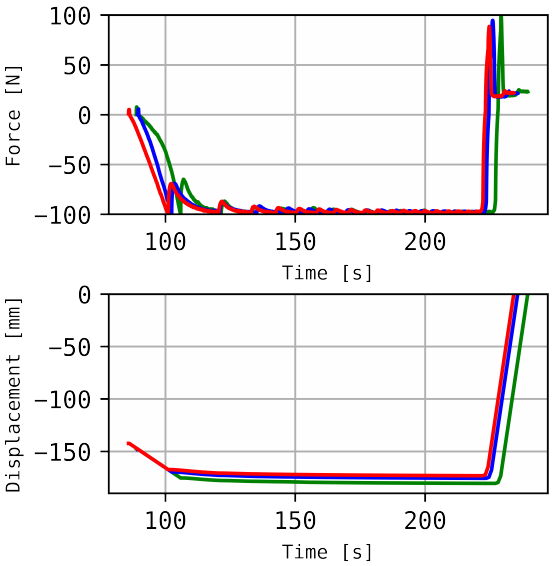
Force [N]
Time [s]
Displacement [mm]
Time [s]

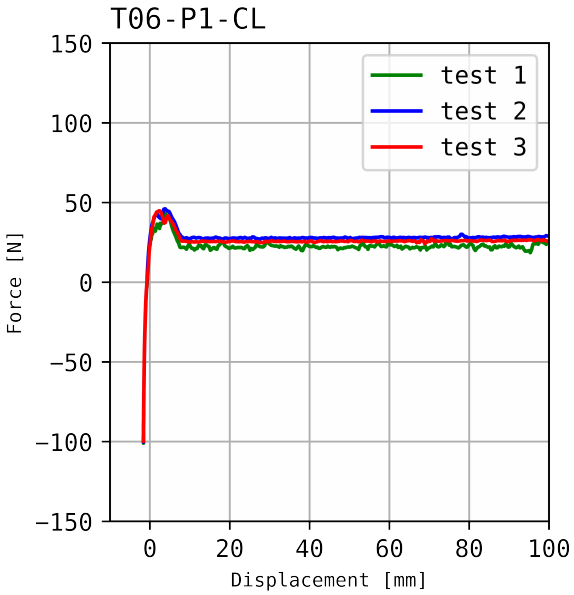
T06-P1-CL
test 1
test 2
test 3
Force [N]
Displacement [mm]

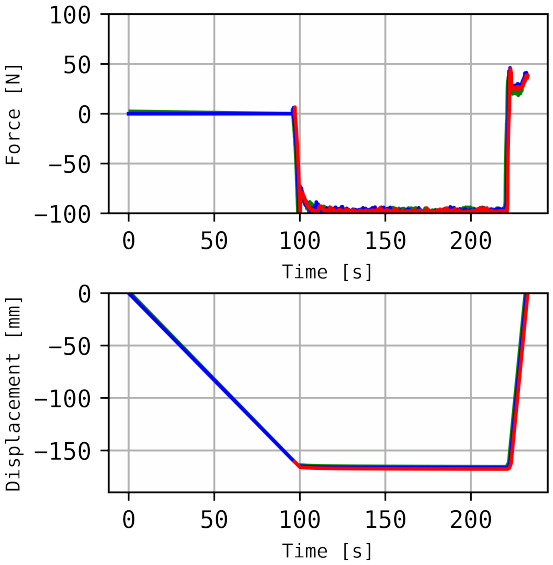
Force [N]
Time [s]
Displacement [mm]
Time [s]

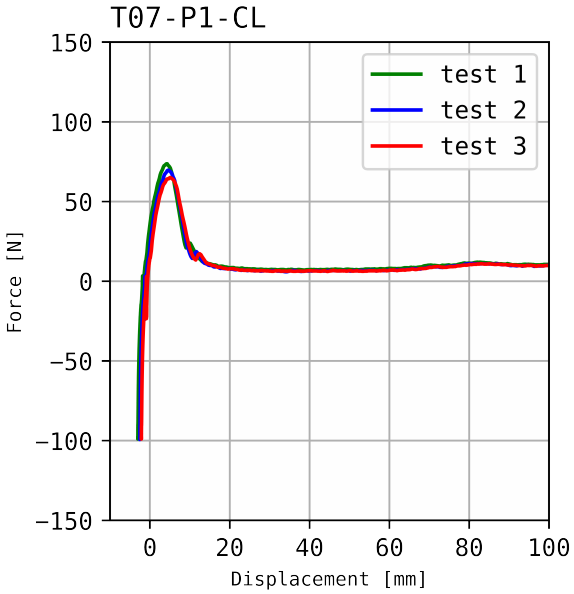
T07-P1-CL
test 1
test 2
test 3
Force [N]
Displacement [mm]

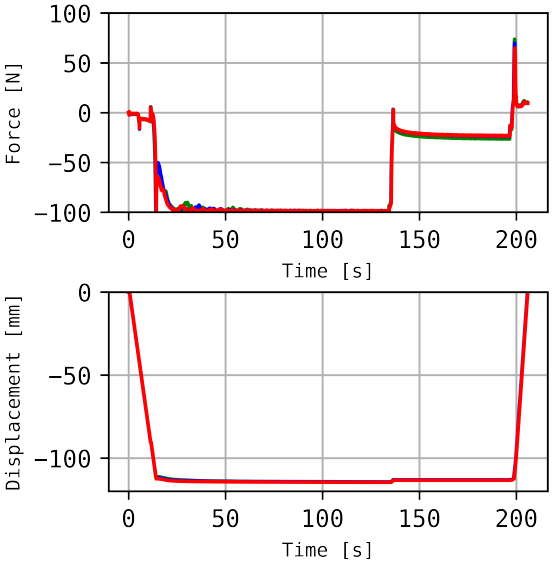
Force [N]
Time [s]
Displacement [mm]
Time [s]

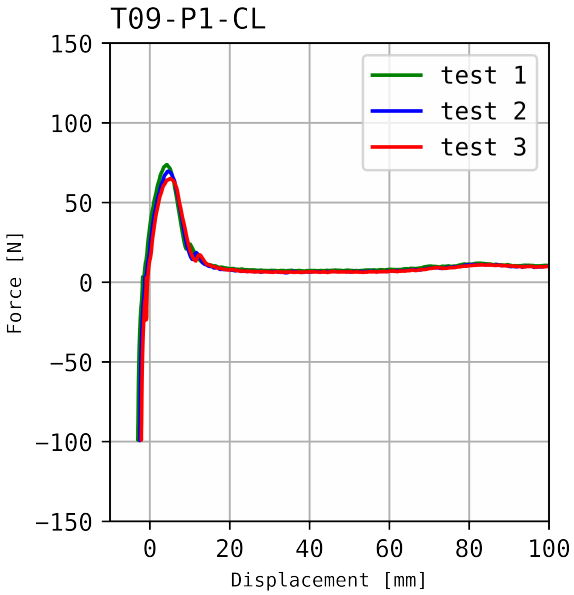
T09-P1-CL
test 1
test 2
test 3
Force [N]
Displacement [mm]

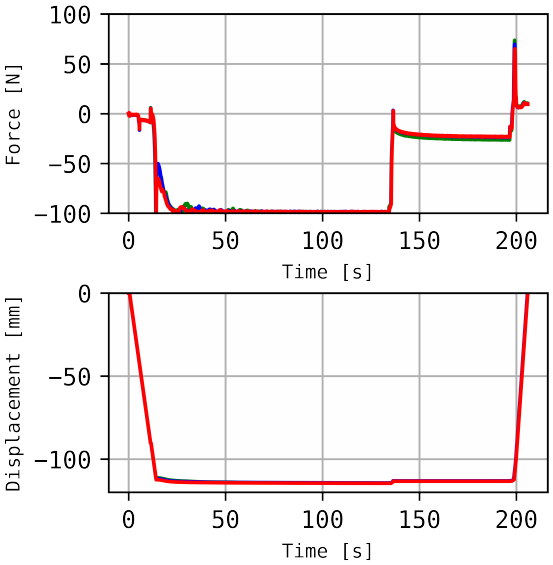
Force [N]
Time [s]
Displacement [mm]
Time [s]

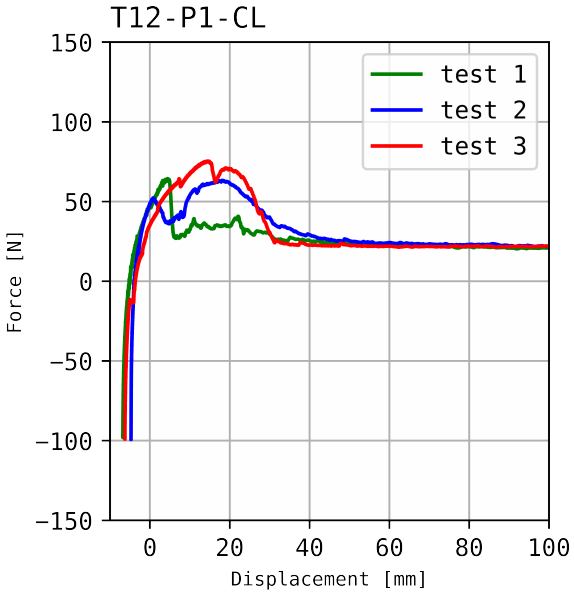
T12-P1-CL
test 1
test 2
test 3
Force [N]
Displacement [mm]

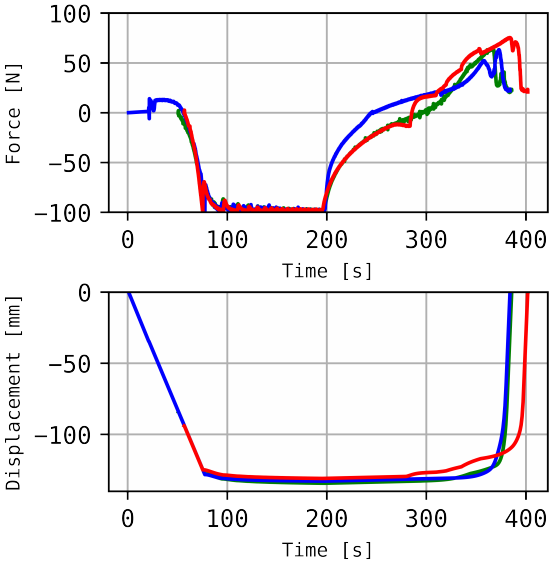
Force [N]
Time [s]
Displacement [mm]
Time [s]

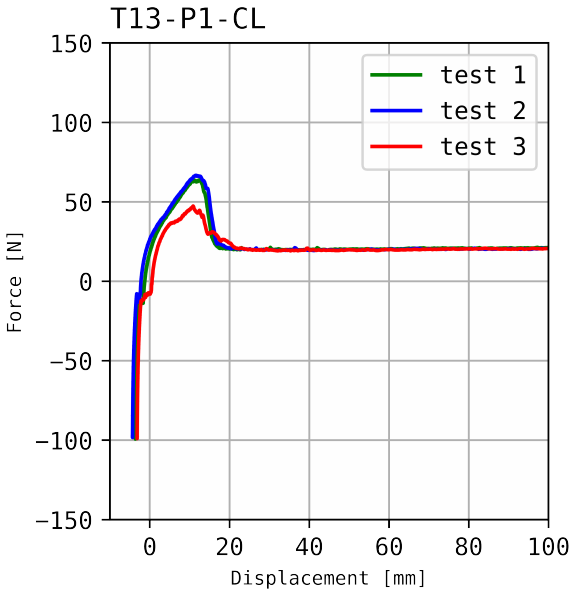
T13-P1-CL
test 1
test 2
test 3
Force [N]
Displacement [mm]

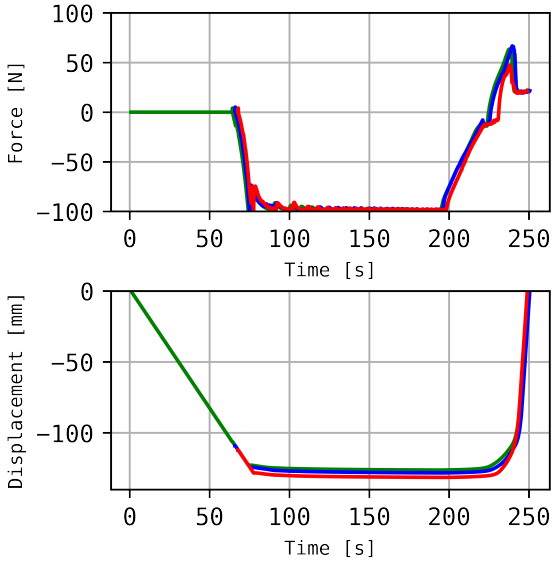
Force [N]
Time [s]
Displacement [mm]
Time [s]

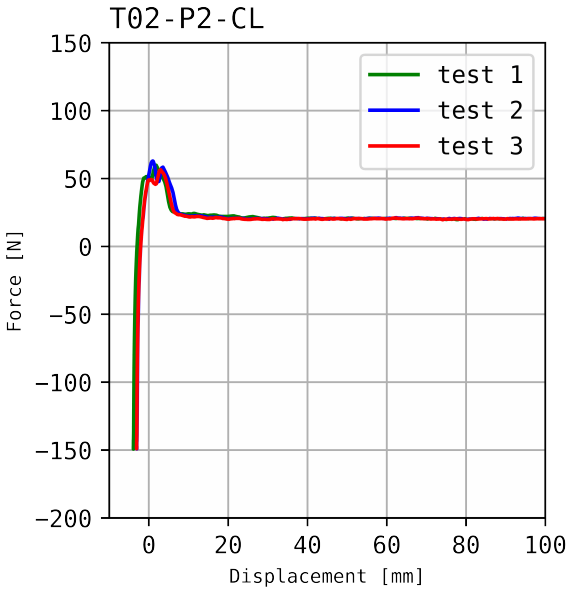
T02-P2-CL
test 1
test 2
test 3
Force [N]
Displacement [mm]

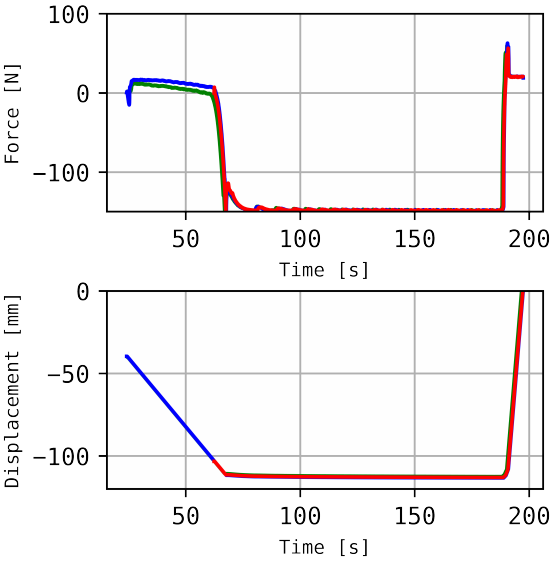
Force [N]
Time [s]
Displacement [mm]
Time [s]

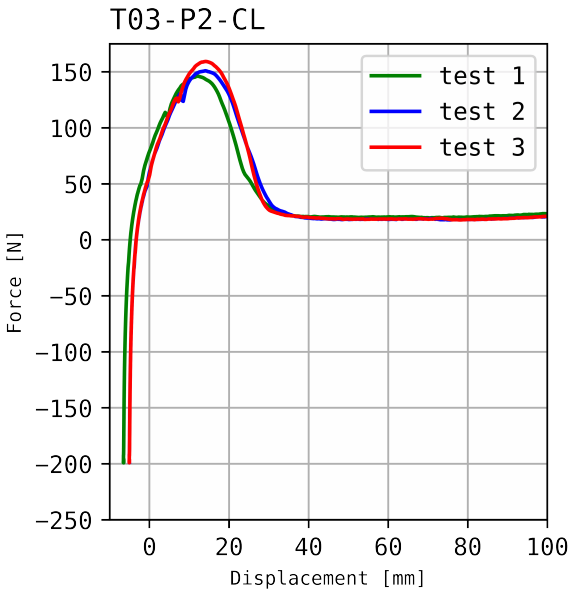
T03-P2-CL
test 1
test 2
test 3
Force [N]
Displacement [mm]

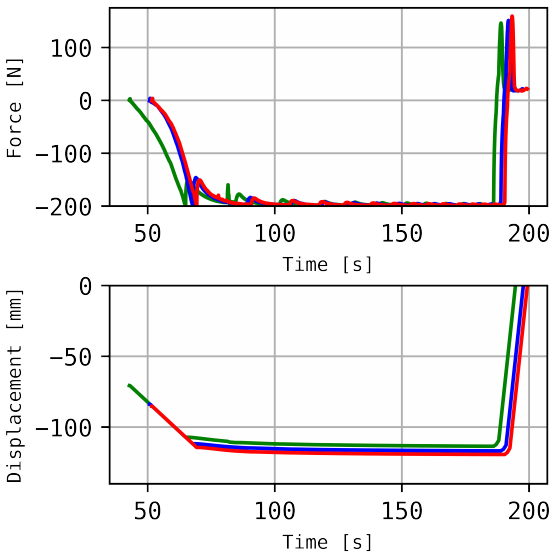
Force [N]
Time [s]
Displacement [mm]
Time [s]

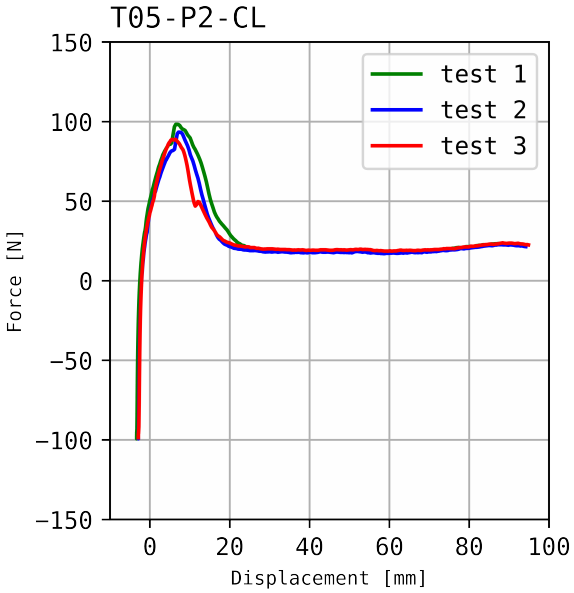
T05-P2-CL
test 1
test 2
test 3
Force [N]
Displacement [mm]

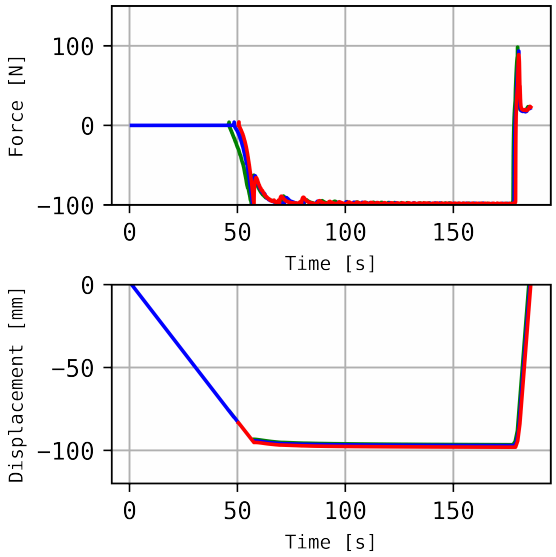
Force [N]
Time [s]
Displacement [mm]
Time [s]

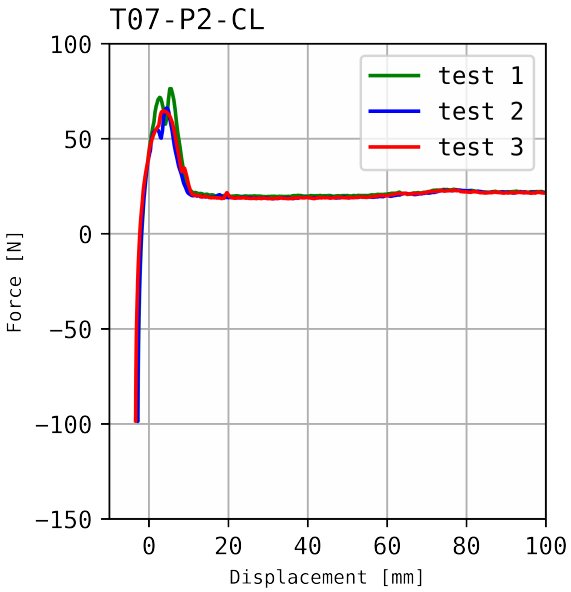
T07-P2-CL
test 1
test 2
test 3
Force [N]
Displacement [mm]

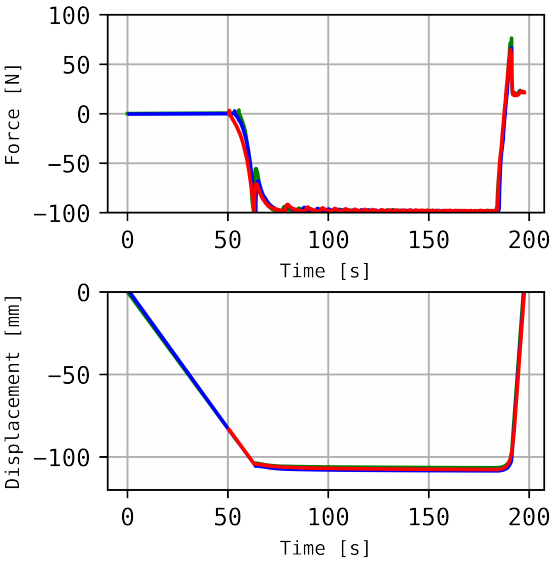
Force [N]
Time [s]
Displacement [mm]
Time [s]

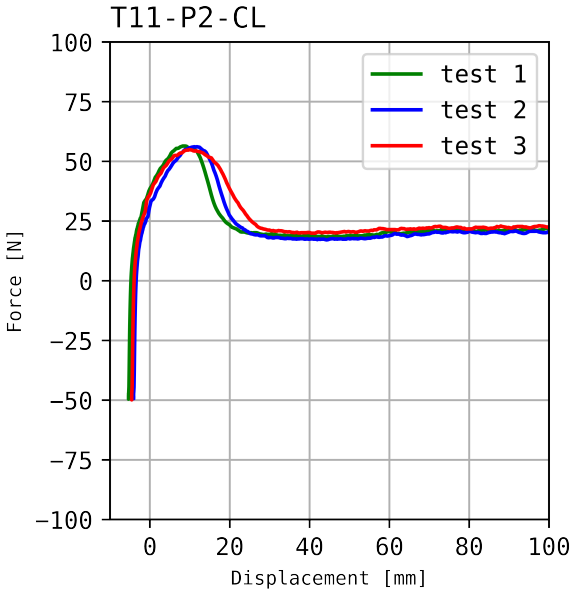
T11-P2-CL
test 1
test 2
test 3
Force [N]
Displacement [mm]

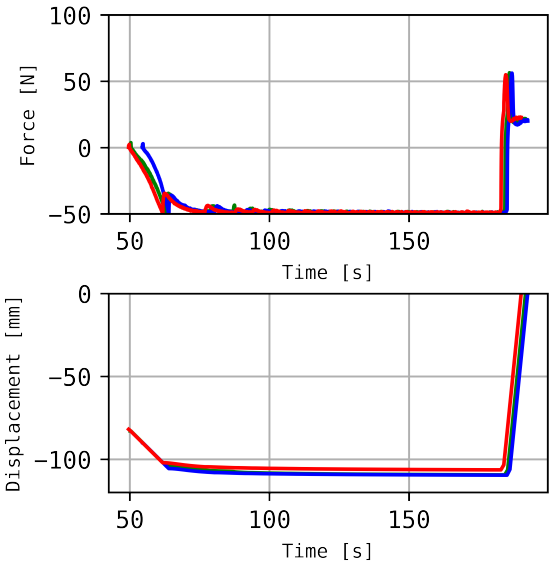
Force [N]
Time [s]
Displacement [mm]
Time [s]

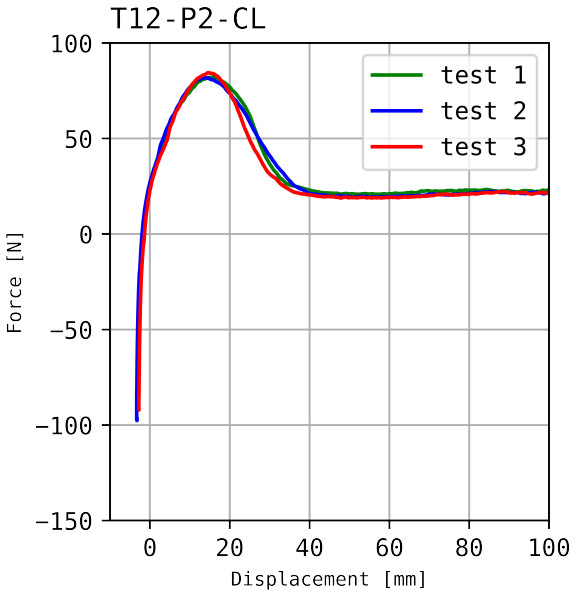
T12-P2-CL
test 1
test 2
test 3
Force [N]
Displacement [mm]

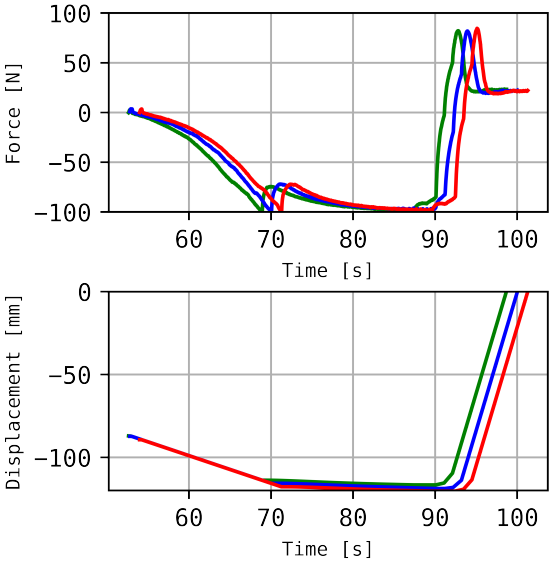
Force [N]
Time [s]
Displacement [mm]
Time [s]

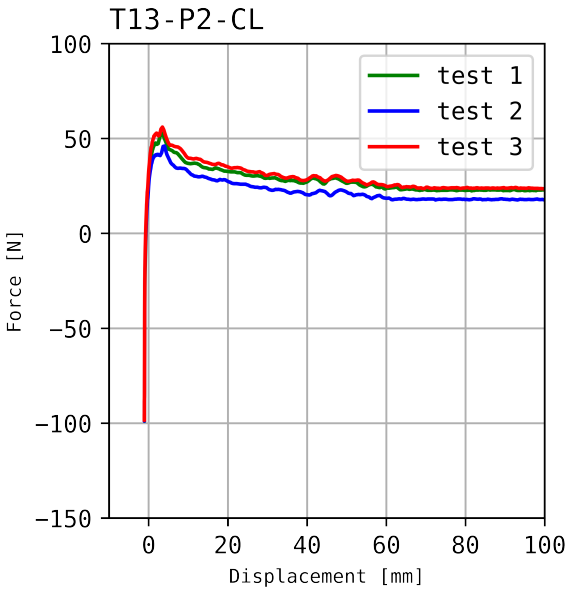
T13-P2-CL
test 1
test 2
test 3
Force [N]
Displacement [mm]

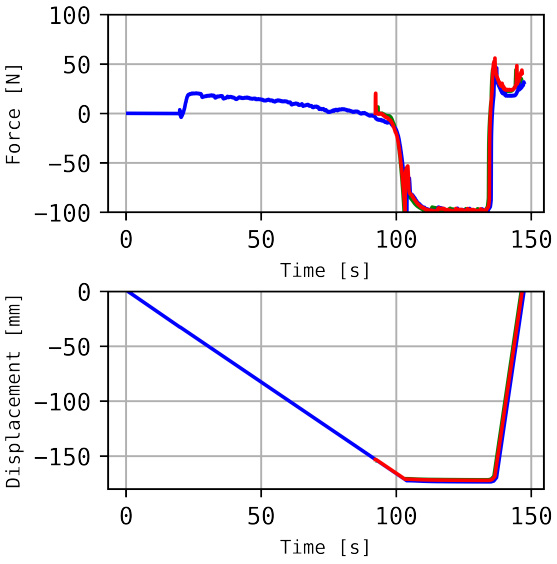
Force [N]
Time [s]
Displacement [mm]
Time [s]

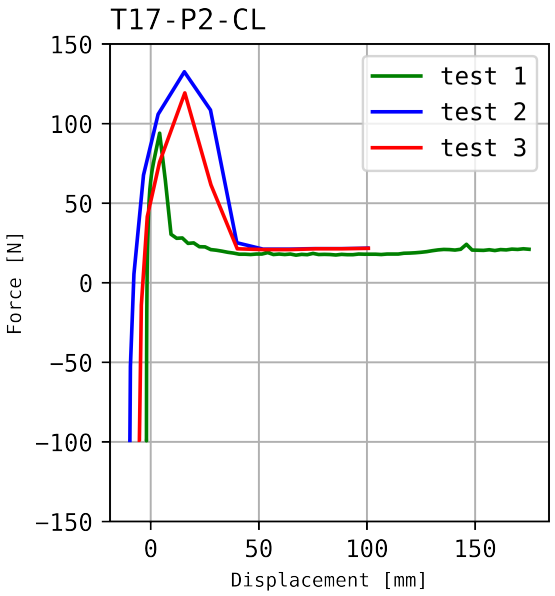
T17-P2-CL
test 1
test 2
test 3
Force [N]
Displacement [mm]

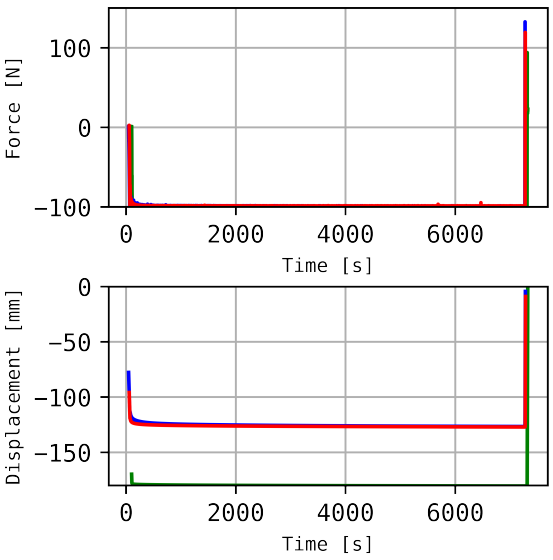
Force [N]
Time [s]
Displacement [mm]
Time [s]

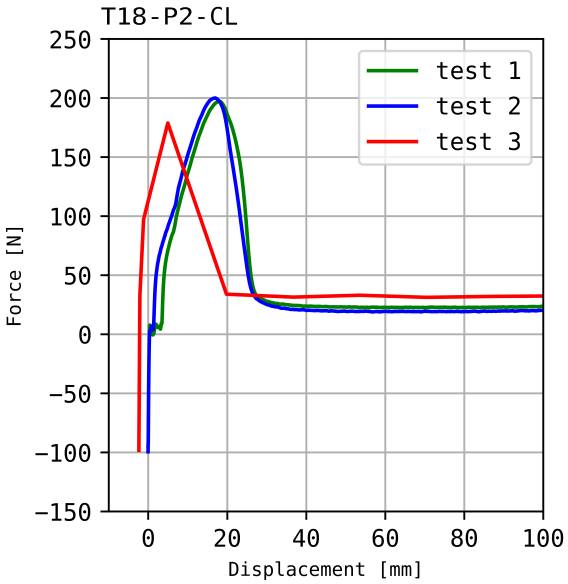
T18-P2-CL
test 1
test 2
test 3
Force [N]
Displacement [mm]

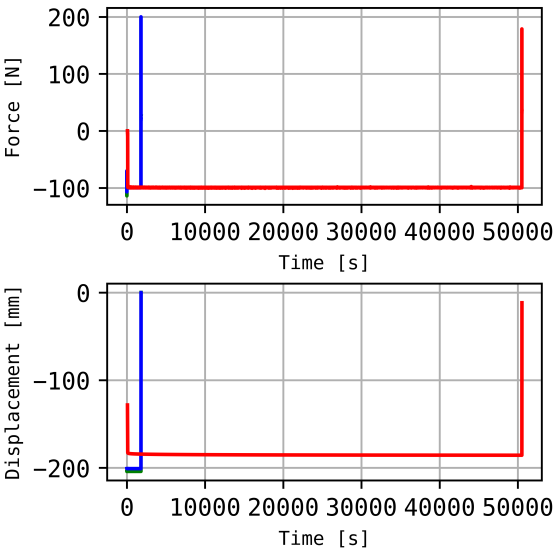
Force [N]
Time [s]
Displacement [mm]
Time [s]

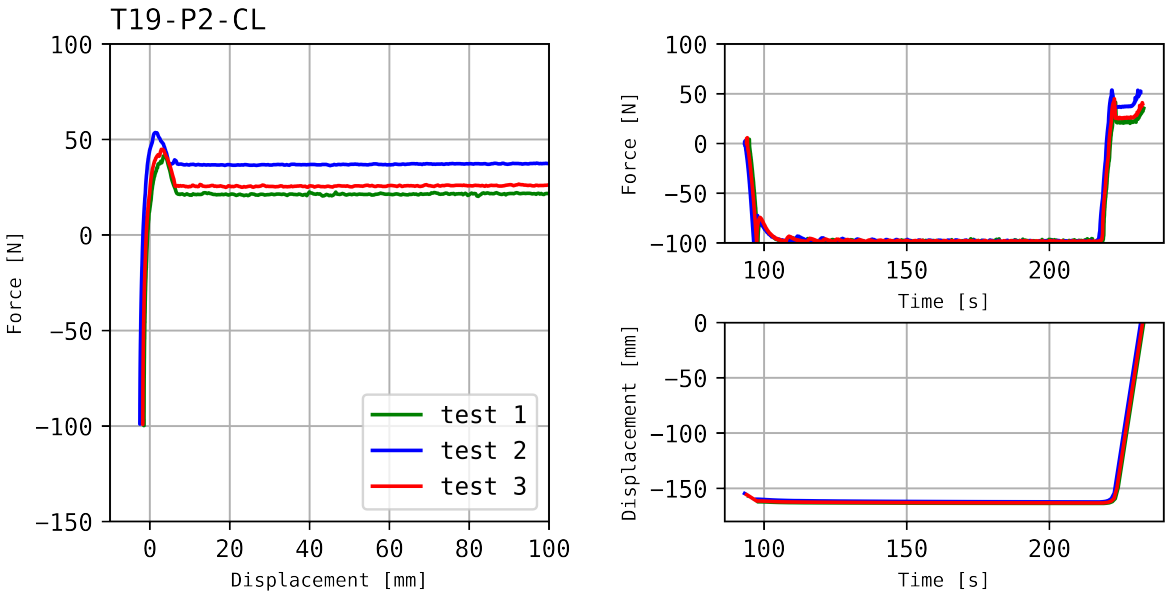
T19-P2-CL
Force [N]
Displacement [mm]
test 1
test 2
test 3
Force [N]
Time [s]
Displacement [mm]
Time [s]

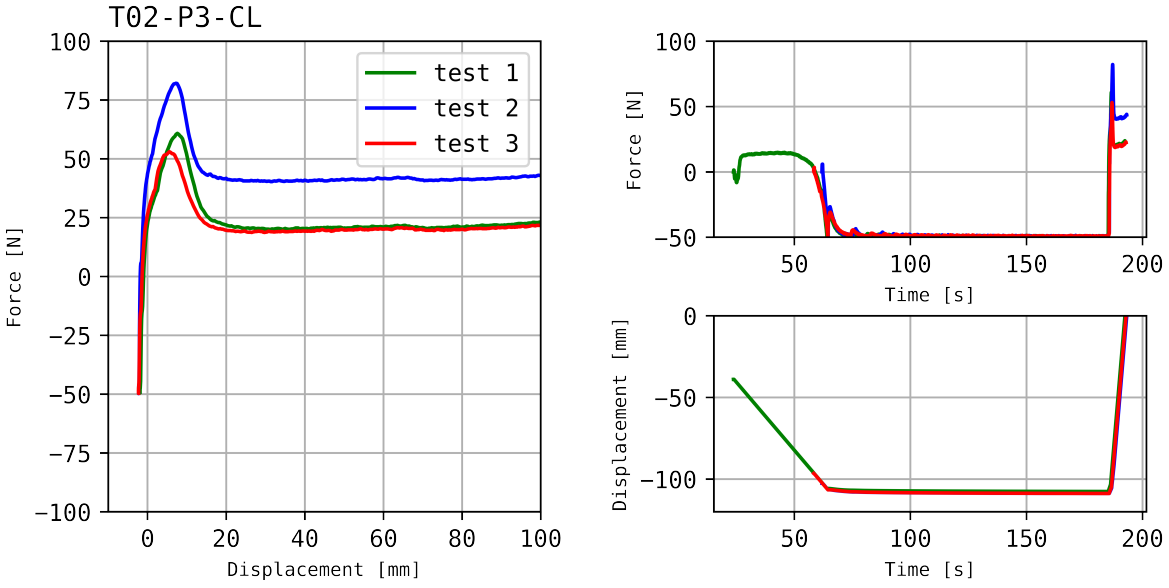
T02-P3-CL
Force [N]
Displacement [mm]
test 1
test 2
test 3
Force [N]
Time [s]
Displacement [mm]
Time [s]

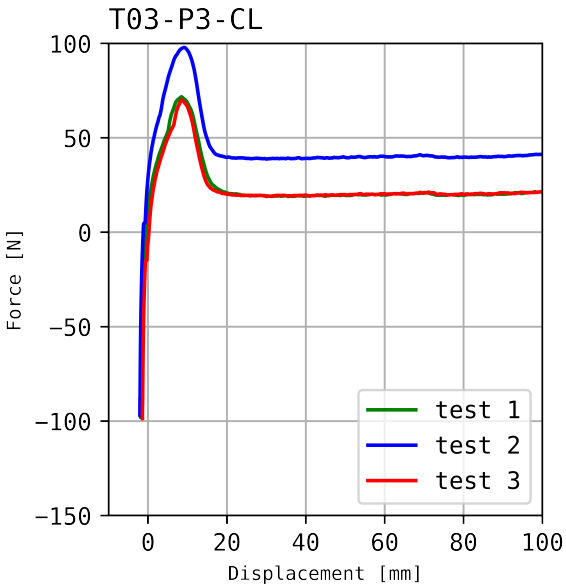
T03-P3-CL
Force [N]
Displacement [mm]
test 1
test 2
test 3

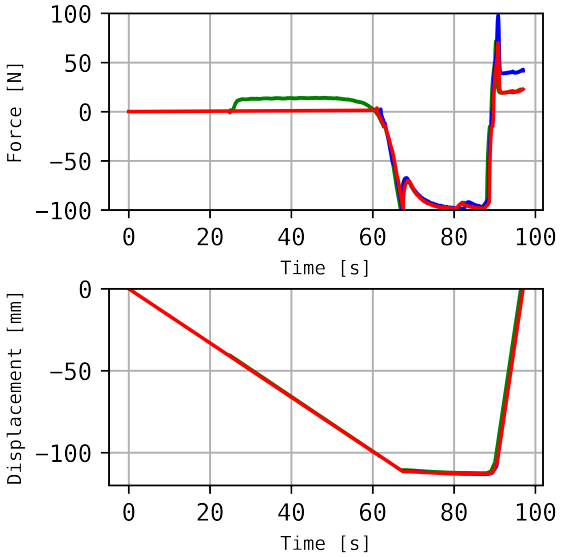
Force [N]
Time [s]
Displacement [mm]
Time [s]

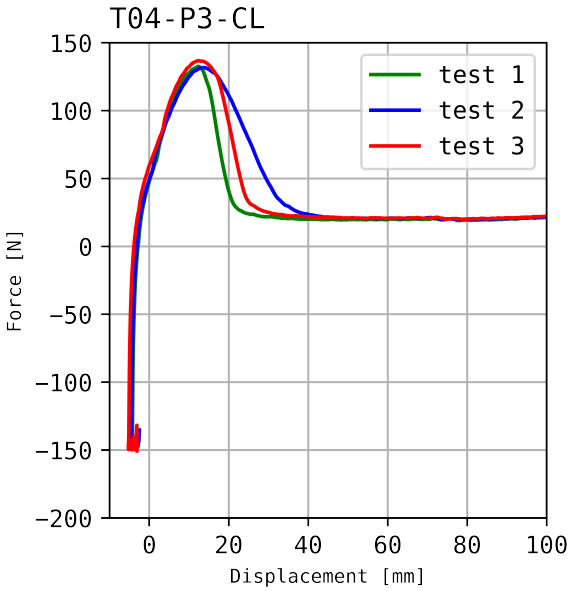
T04-P3-CL
Force [N]
Displacement [mm]
test 1
test 2
test 3

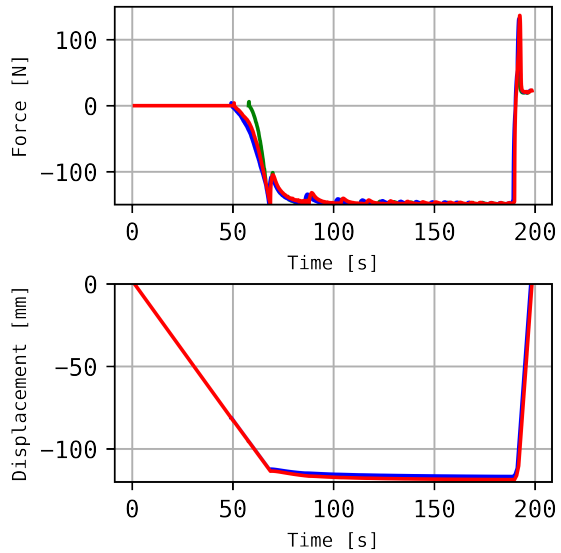
Force [N]
Time [s]
Displacement [mm]
Time [s]

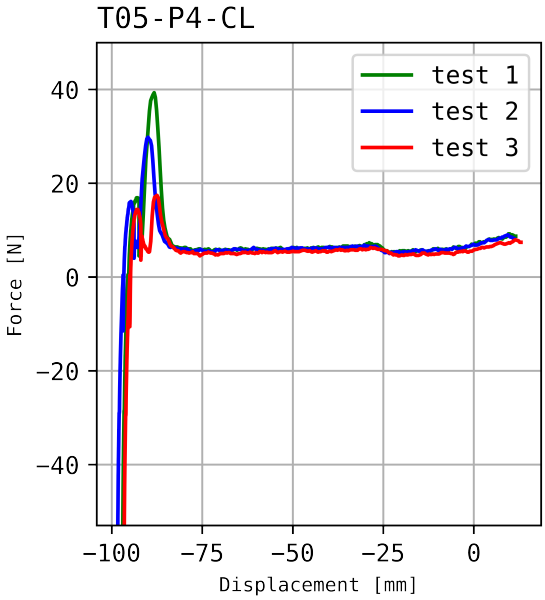
T05-P4-CL
test 1
test 2
test 3
Force [N]
Displacement [mm]

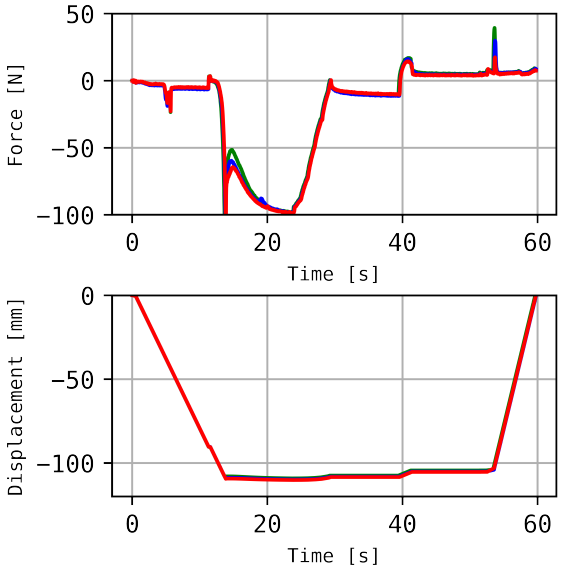
Force [N]
Time [s]
Displacement [mm]
Time [s]

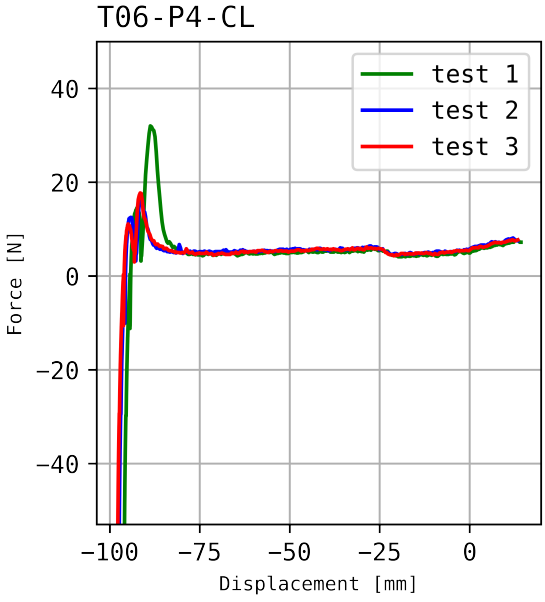
T06-P4-CL
test 1
test 2
test 3
Force [N]
Displacement [mm]

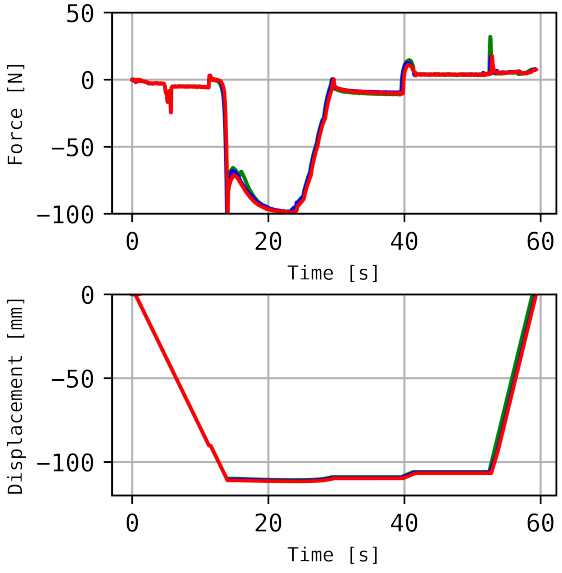
Force [N]
Time [s]
Displacement [mm]
Time [s]

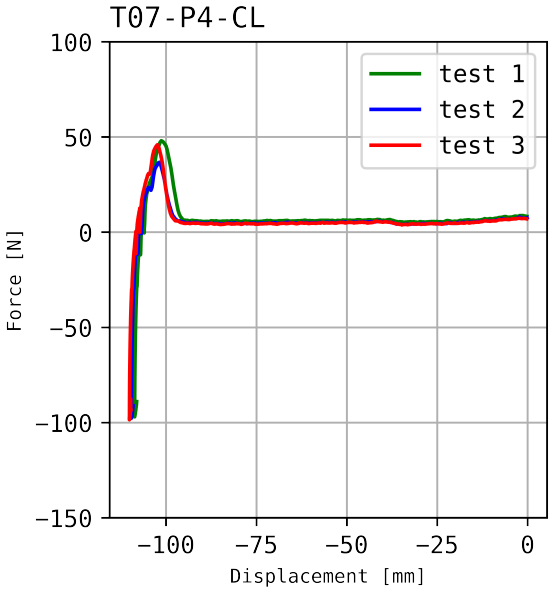
T07-P4-CL
test 1
test 2
test 3
Force [N]
Displacement [mm]

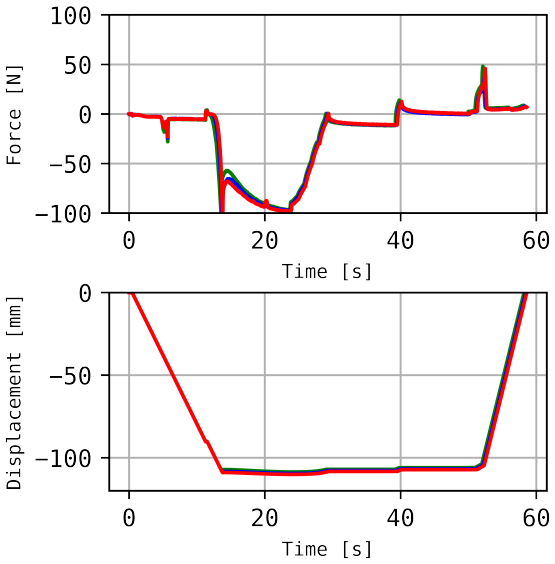
Force [N]
Time [s]
Displacement [mm]
Time [s]

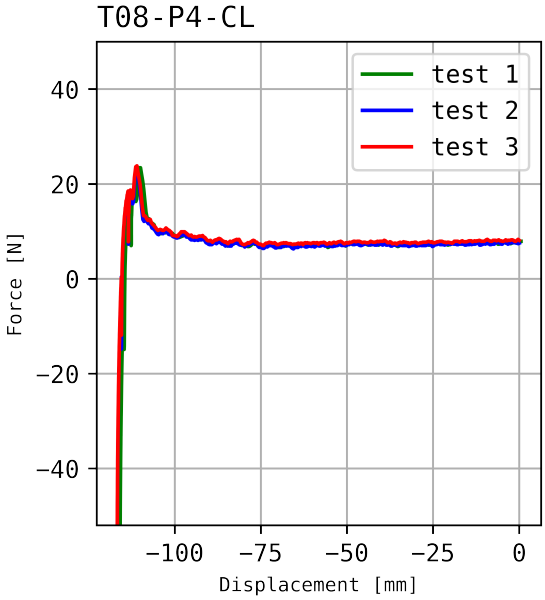
T08-P4-CL
test 1
test 2
test 3
Force [N]
Displacement [mm]

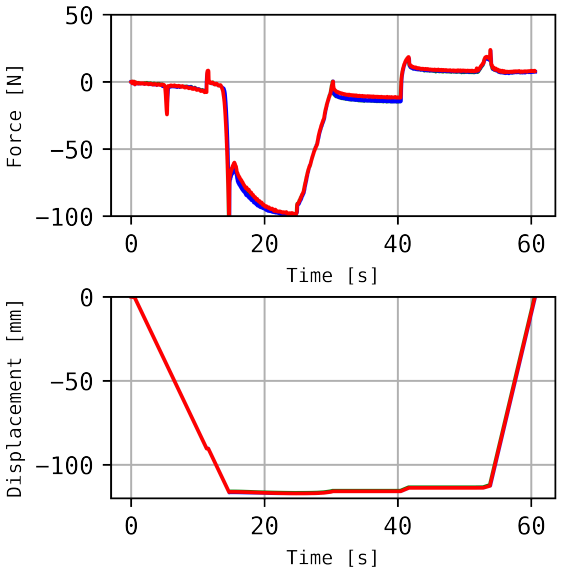
Force [N]
Time [s]
Displacement [mm]
Time [s]

# D

# Graphs test sand

The reader is referred to Section 5.4 for an explanation of the post-processing and data representation in this research.

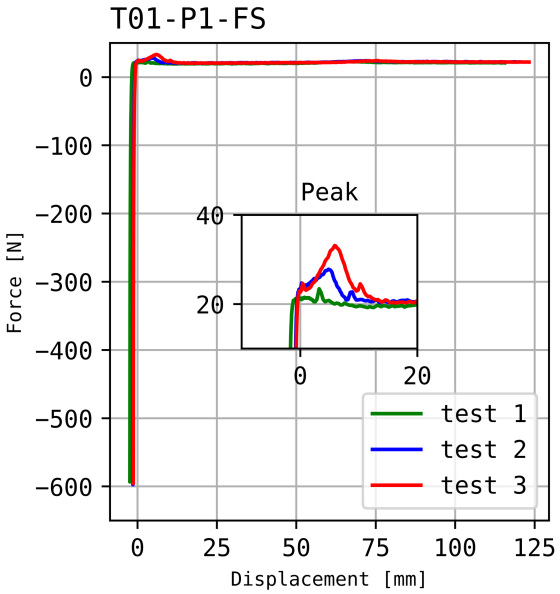


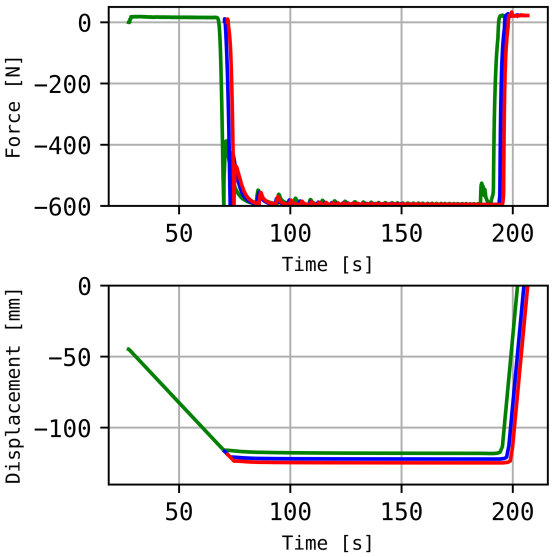

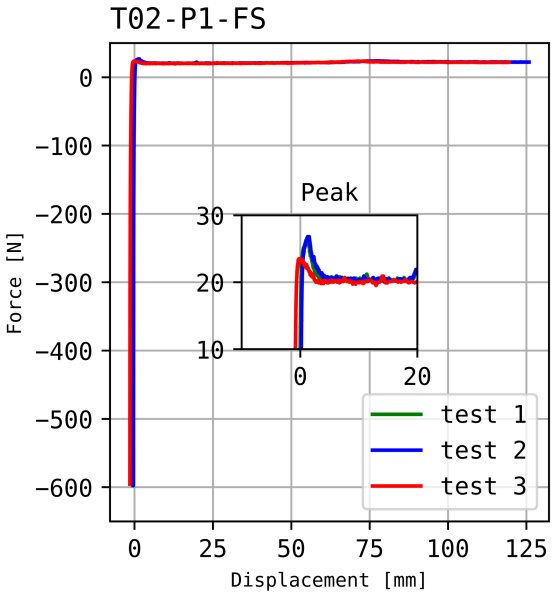
T02-P1-FS
Force [N]
Displacement [mm]
Peak
test 1
test 2
test 3

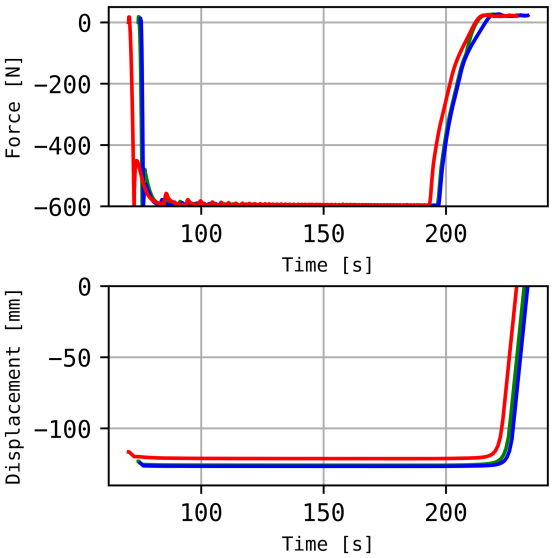
Force [N]
Time [s]
Displacement [mm]
Time [s]

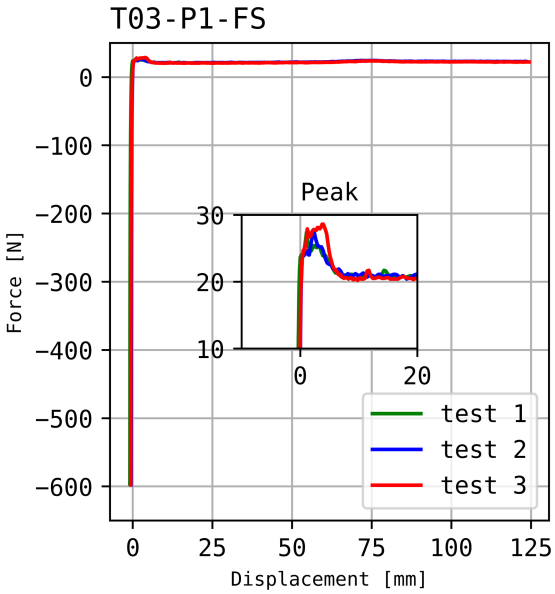
T03-P1-FS
Force [N]
Displacement [mm]
Peak
test 1
test 2
test 3

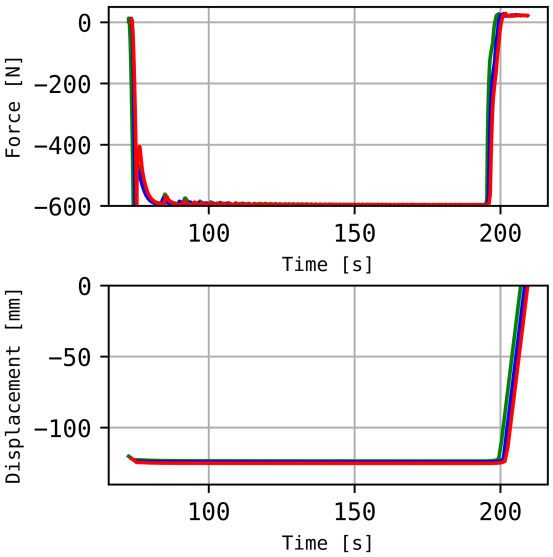
Force [N]
Time [s]
Displacement [mm]
Time [s]

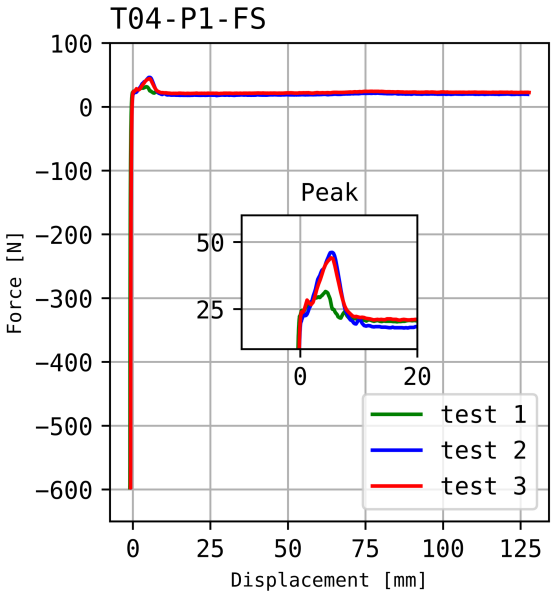
T04-P1-FS
Force [N]
Displacement [mm]
Peak
test 1
test 2
test 3

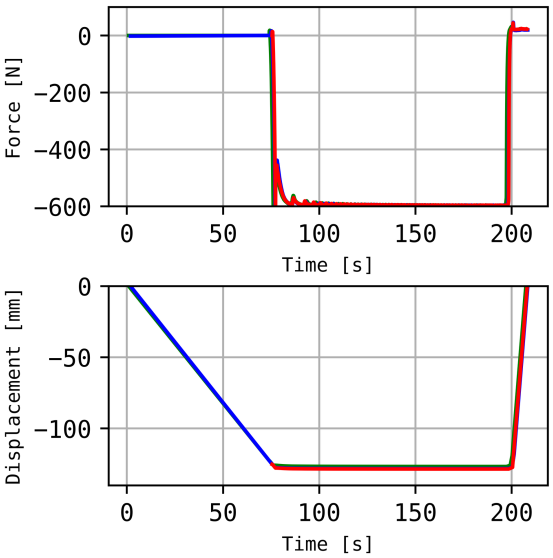
Force [N]
Time [s]
Displacement [mm]
Time [s]

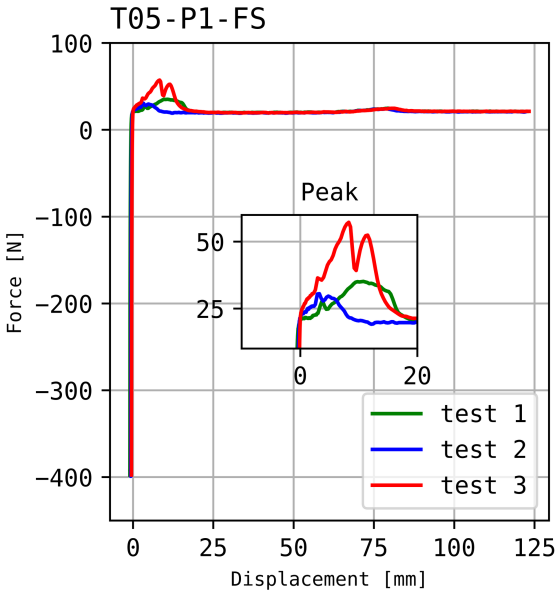
T05-P1-FS
Force [N]
Displacement [mm]
Peak
test 1
test 2
test 3

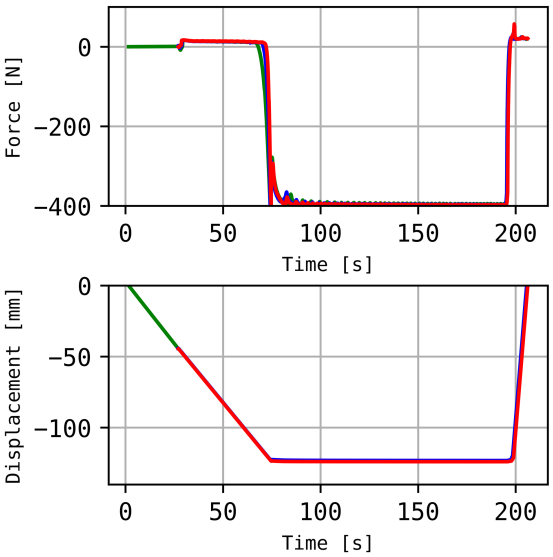
Force [N]
Time [s]
Displacement [mm]
Time [s]

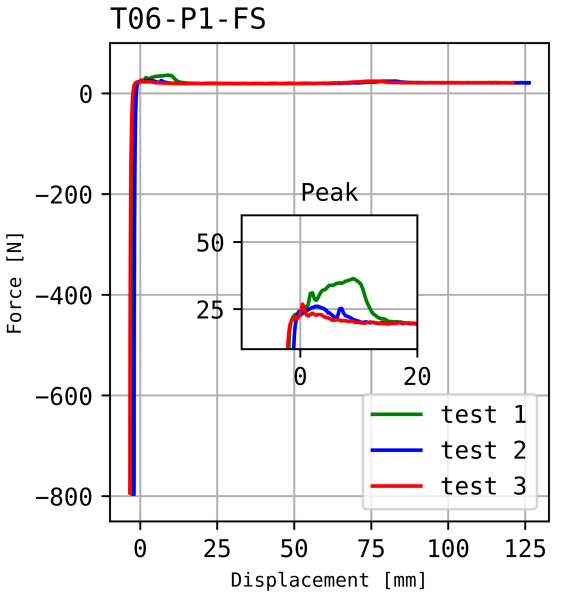
T06-P1-FS
Force [N]
Displacement [mm]
Peak
test 1
test 2
test 3

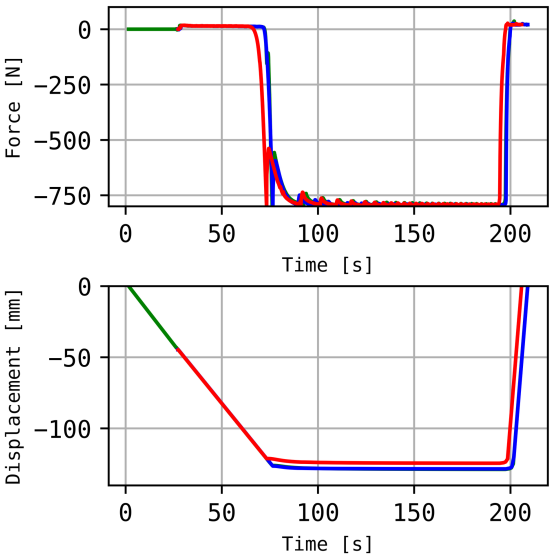
Force [N]
Time [s]
Displacement [mm]
Time [s]

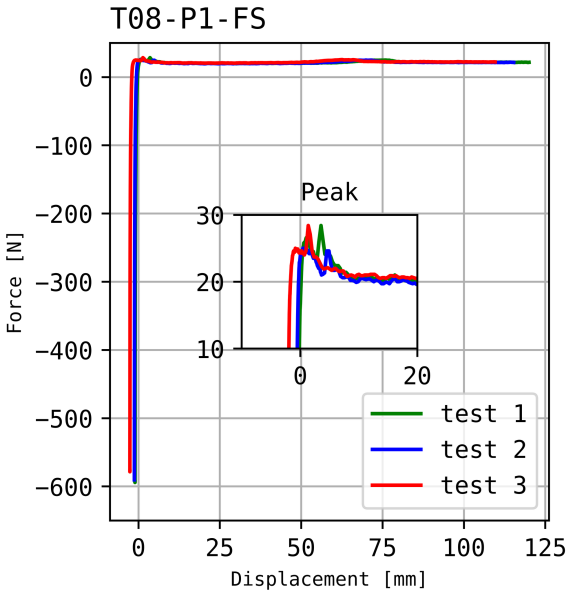
T08-P1-FS
Force [N]
Displacement [mm]
Peak
test 1
test 2
test 3

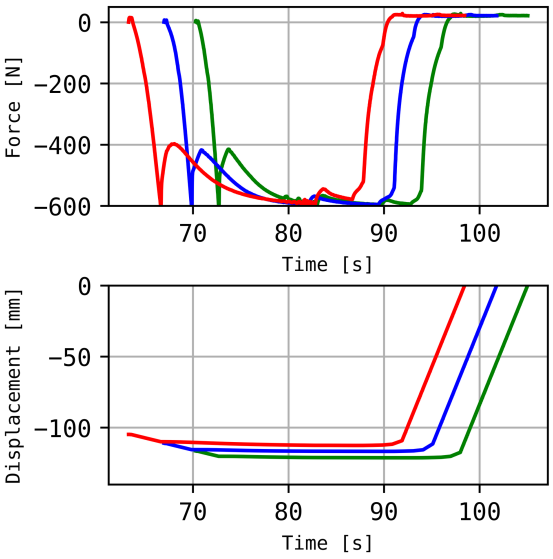
Force [N]
Time [s]
Displacement [mm]
Time [s]

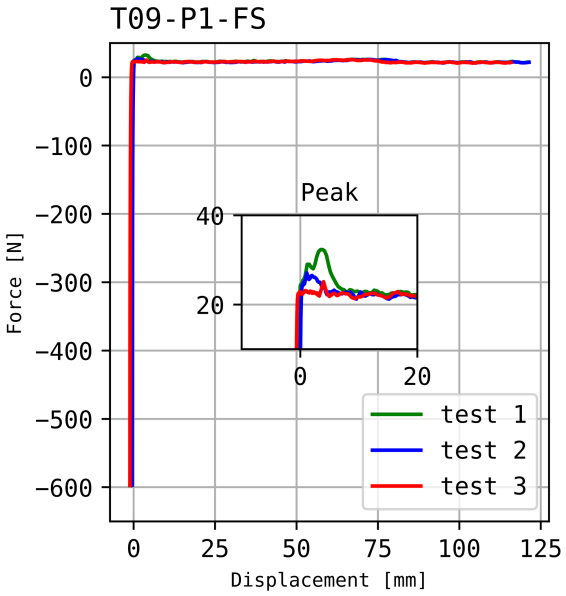
T09-P1-FS
Force [N]
Displacement [mm]
Peak
test 1
test 2
test 3

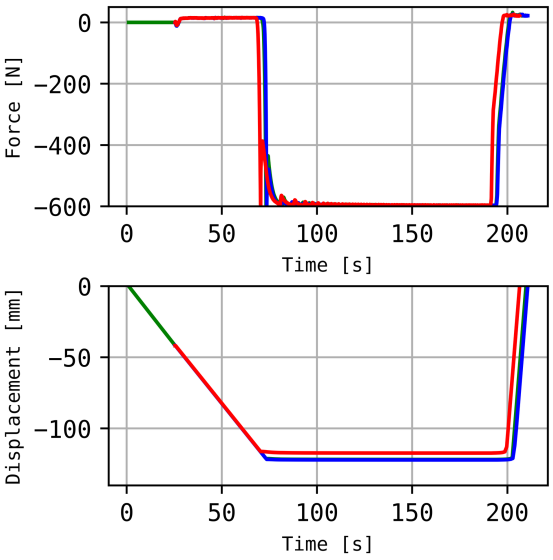
Force [N]
Time [s]
Displacement [mm]
Time [s]

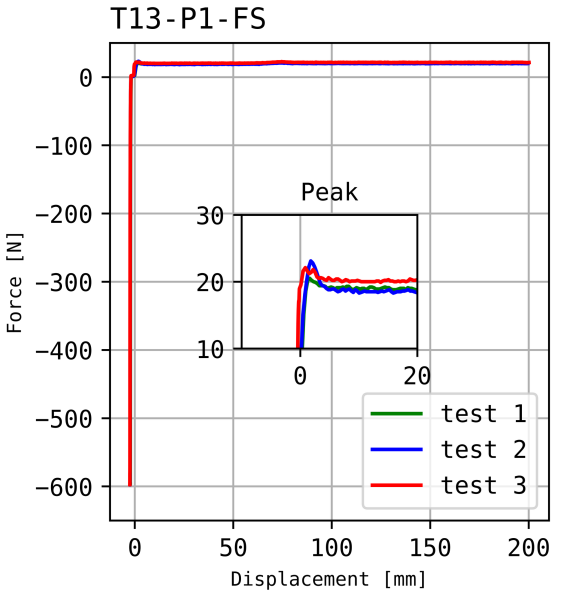
T13-P1-FS
Force [N]
Displacement [mm]
Peak
test 1
test 2
test 3

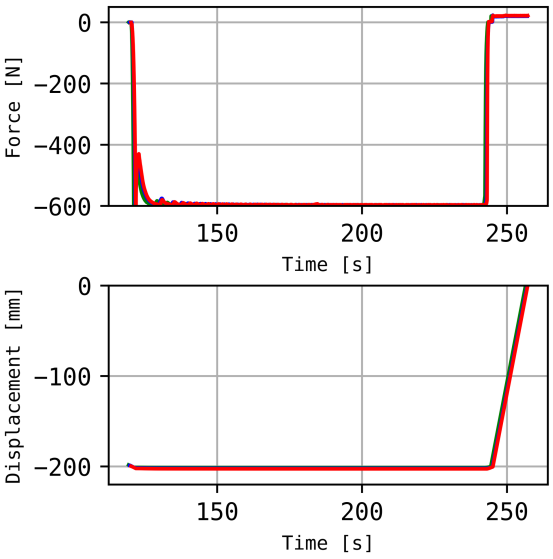
Force [N]
Time [s]
Displacement [mm]
Time [s]

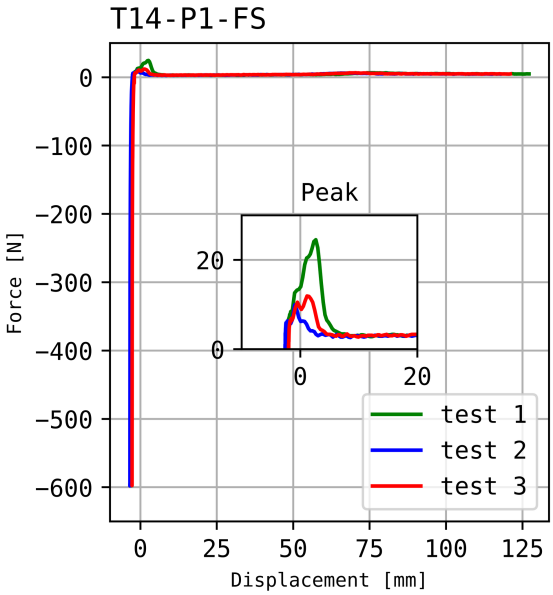
T14-P1-FS
Force [N]
Displacement [mm]
Peak
test 1
test 2
test 3

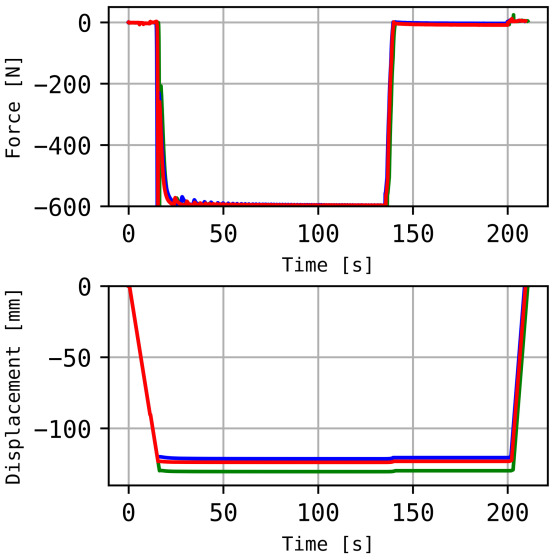
Force [N]
Time [s]
Displacement [mm]
Time [s]

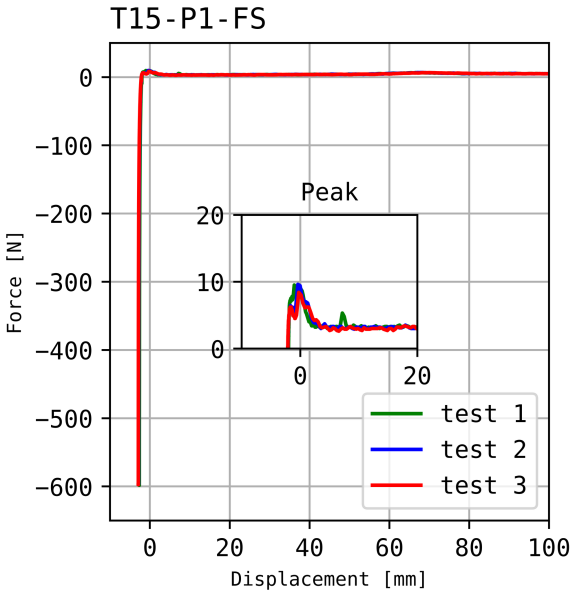
T15-P1-FS
Force [N]
Displacement [mm]
Peak
test 1
test 2
test 3

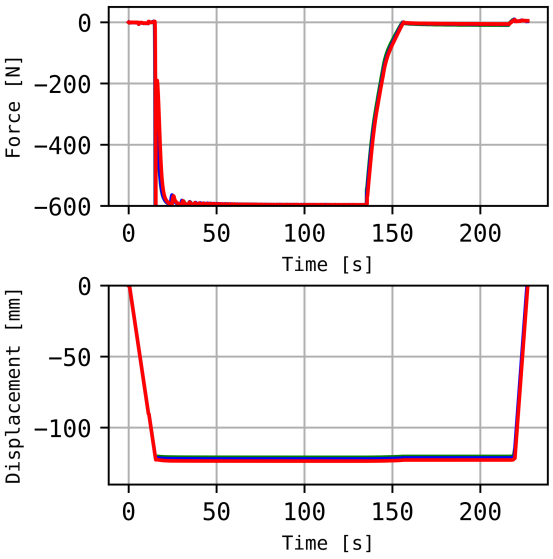
Force [N]
Time [s]
Displacement [mm]
Time [s]

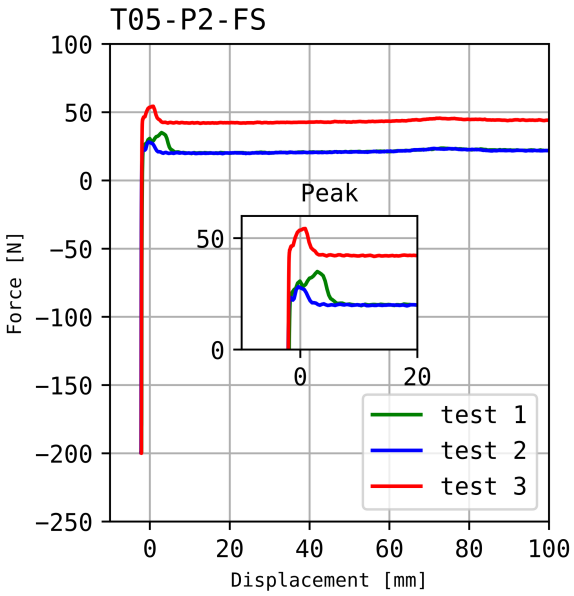
T05-P2-FS
Force [N]
Displacement [mm]
Peak
test 1
test 2
test 3

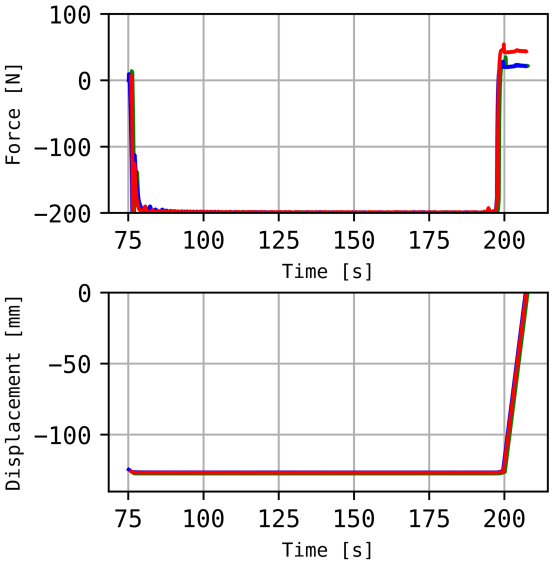
Force [N]
Time [s]
Displacement [mm]
Time [s]

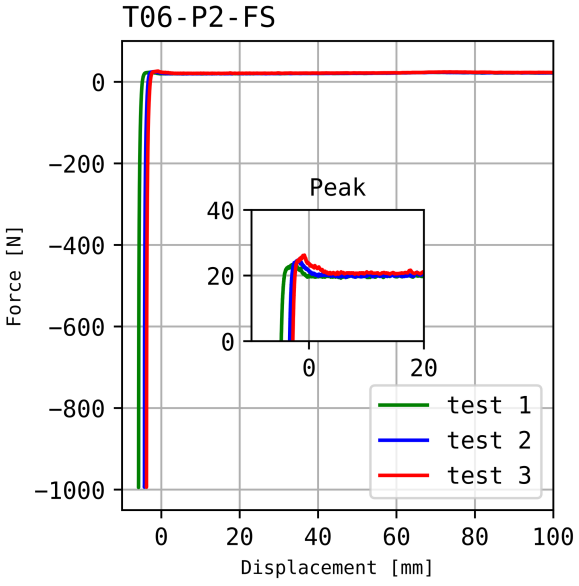
T06-P2-FS
Force [N]
Displacement [mm]
Peak
test 1
test 2
test 3

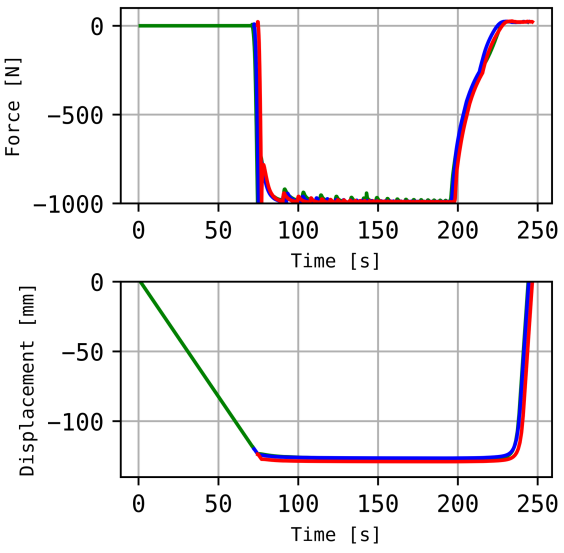
Force [N]
Time [s]
Displacement [mm]
Time [s]

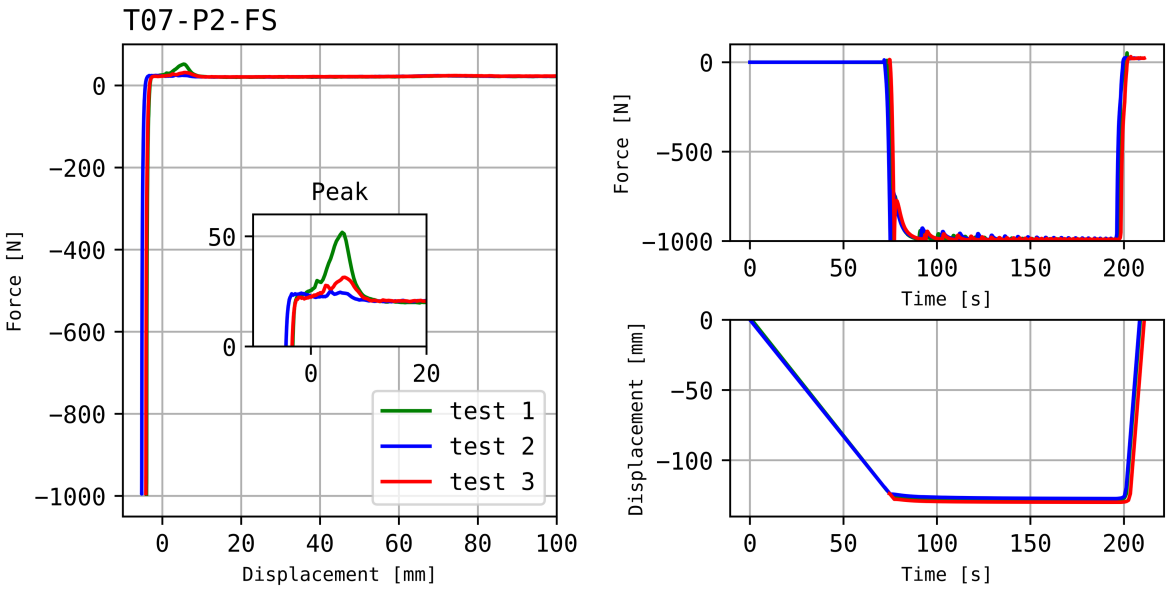
T07-P2-FS
Force [N]
Displacement [mm]
Peak
test 1
test 2
test 3
Force [N]
Time [s]
Displacement [mm]
Time [s]

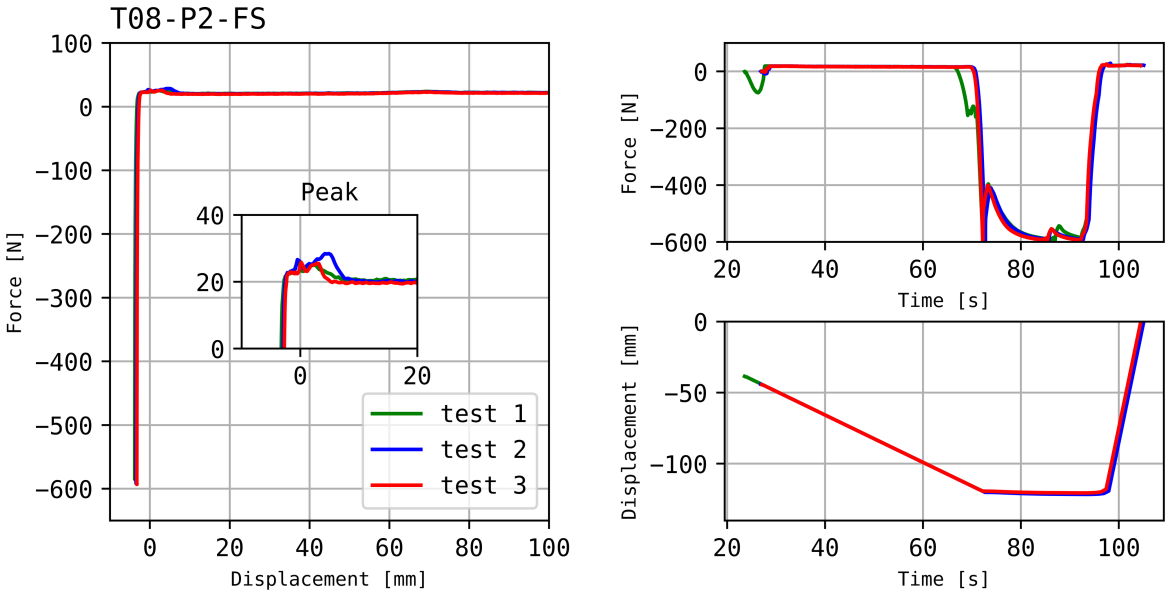
T08-P2-FS
Force [N]
Displacement [mm]
Peak
test 1
test 2
test 3
Force [N]
Time [s]
Displacement [mm]
Time [s]

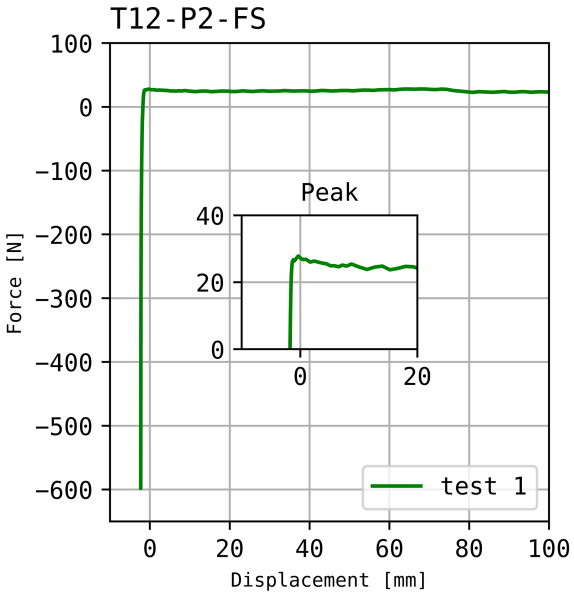
T12-P2-FS
Force [N]
Displacement [mm]
Peak
test 1

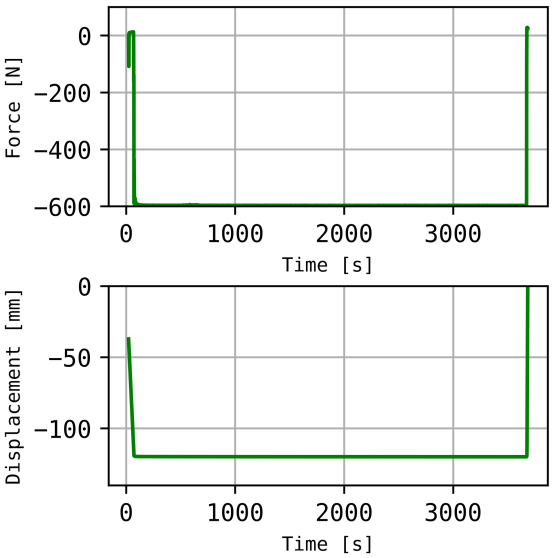
Force [N]
Time [s]
Displacement [mm]
Time [s]

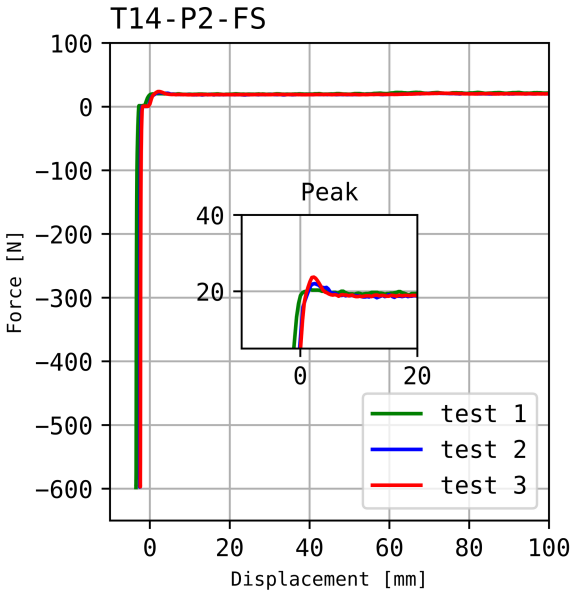
T14-P2-FS
Force [N]
Displacement [mm]
Peak
test 1
test 2
test 3

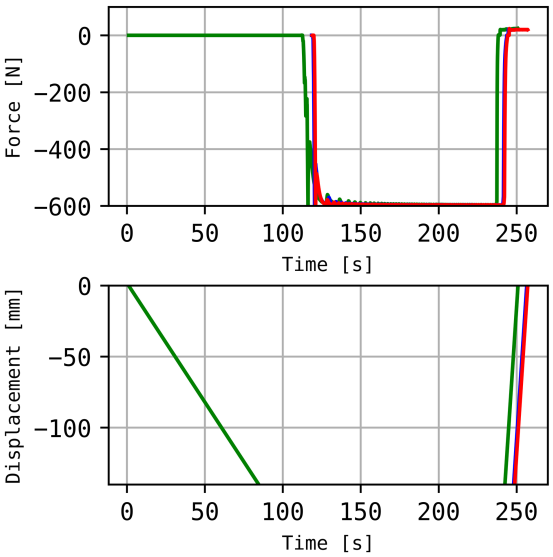
Force [N]
Time [s]
Displacement [mm]
Time [s]

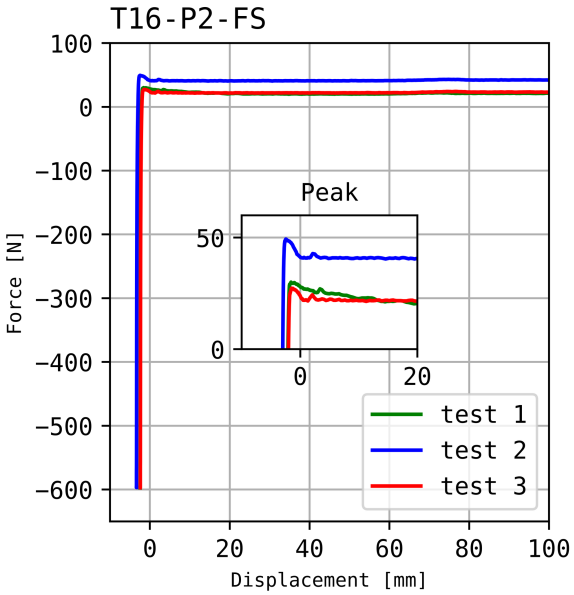
T16-P2-FS
Force [N]
Displacement [mm]
Peak
test 1
test 2
test 3

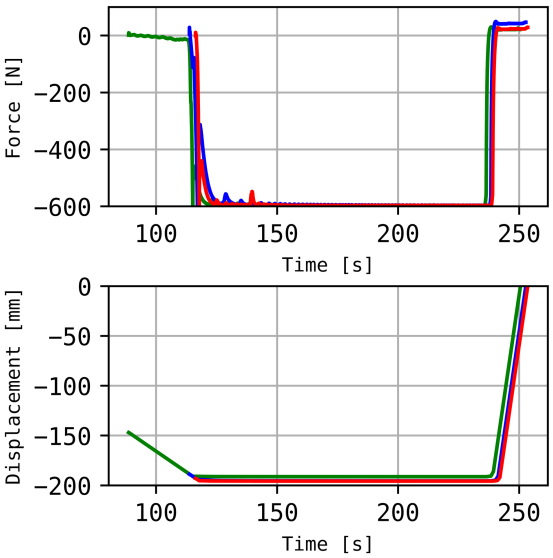
Force [N]
Time [s]
Displacement [mm]
Time [s]

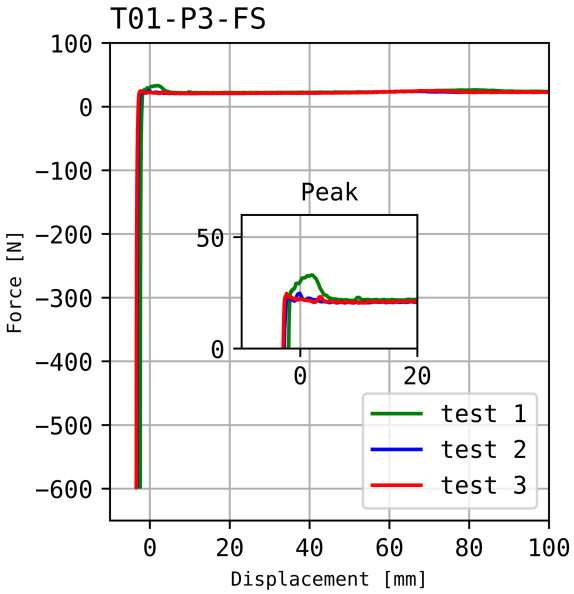
T01-P3-FS
Force [N]
Displacement [mm]
Peak
test 1
test 2
test 3

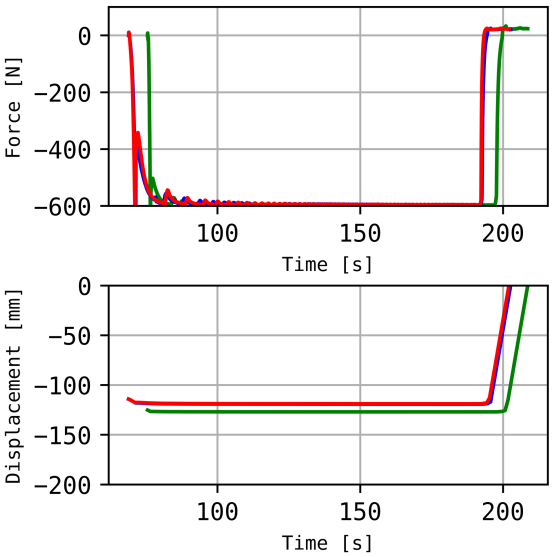
Force [N]
Time [s]
Displacement [mm]
Time [s]

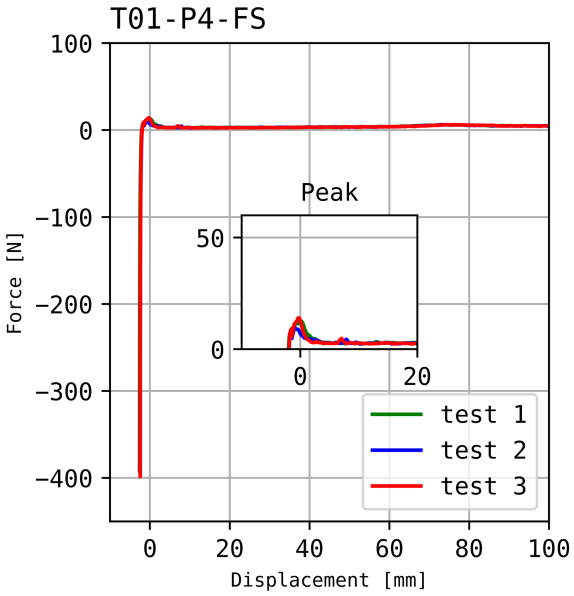
T01-P4-FS
Force [N]
Displacement [mm]
Peak
test 1
test 2
test 3

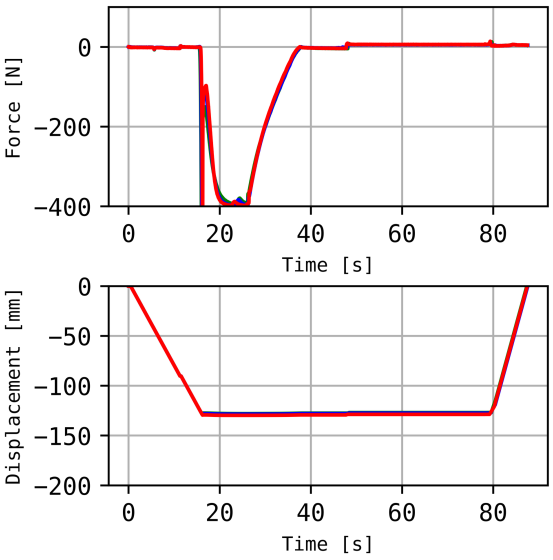
Force [N]
Time [s]
Displacement [mm]
Time [s]

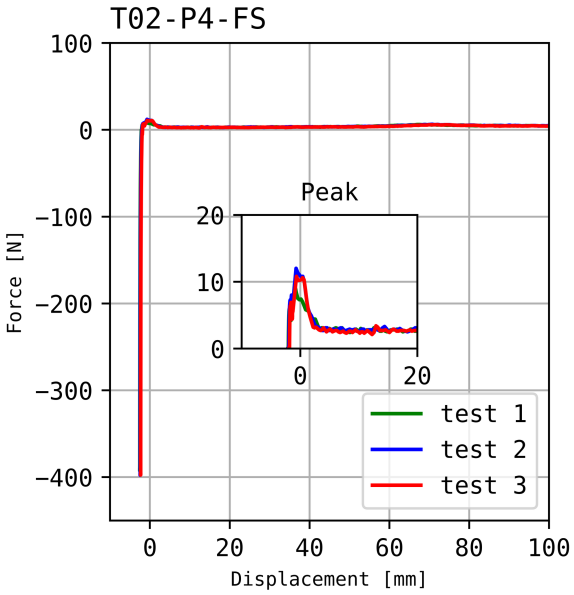
T02-P4-FS
Force [N]
Displacement [mm]
Peak
test 1
test 2
test 3

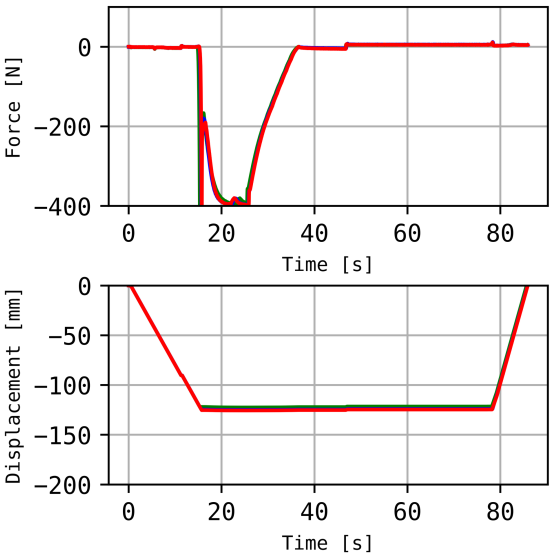
Force [N]
Time [s]
Displacement [mm]
Time [s]

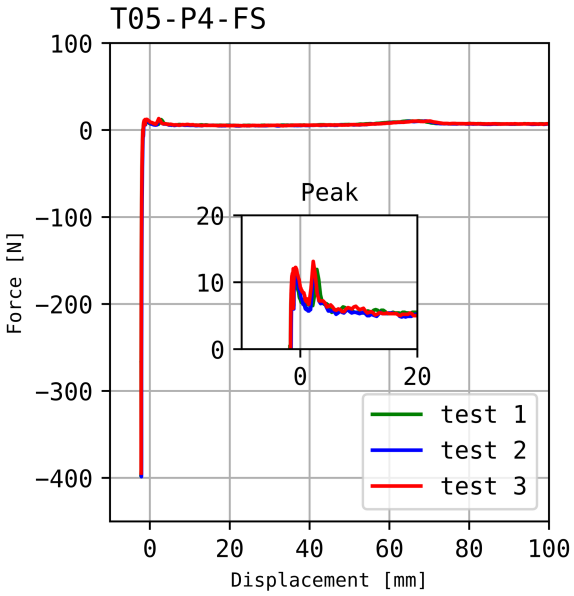
T05-P4-FS
Force [N]
Displacement [mm]
Peak
test 1
test 2
test 3

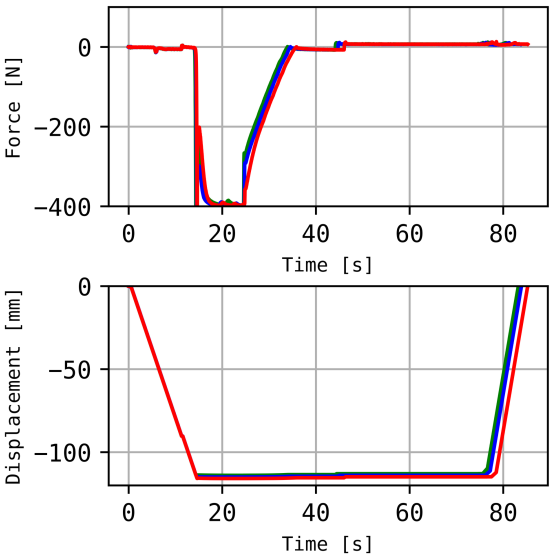
Force [N]
Time [s]
Displacement [mm]
Time [s]

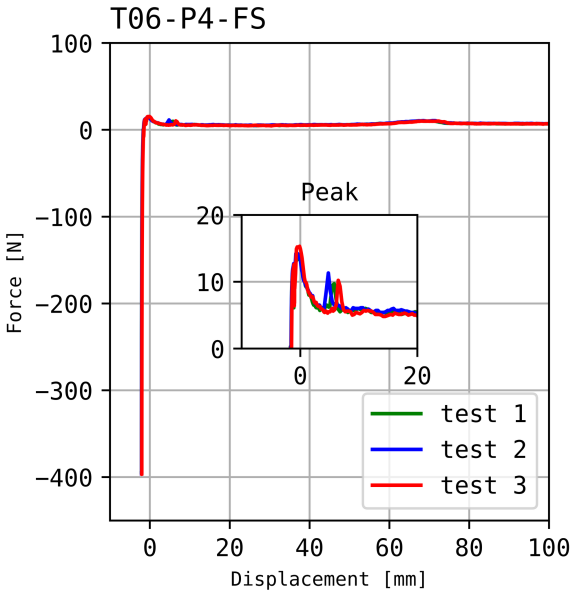
T06-P4-FS
Force [N]
Displacement [mm]
Peak
test 1
test 2
test 3

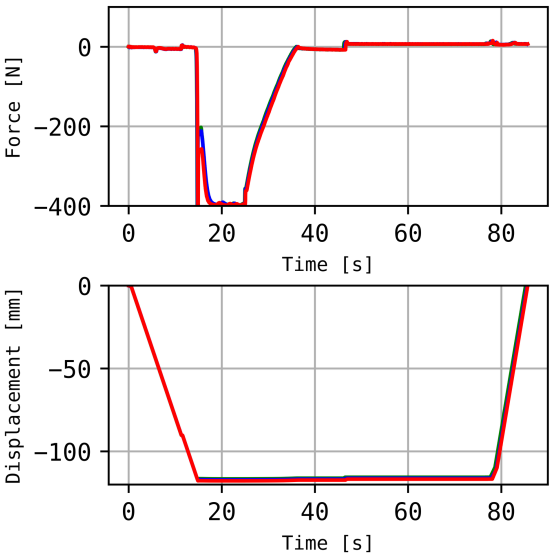
Force [N]
Time [s]
Displacement [mm]
Time [s]

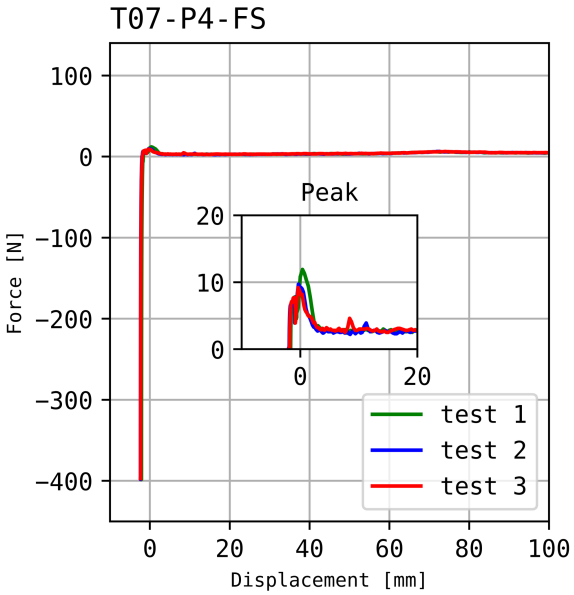
T07-P4-FS
Force [N]
Displacement [mm]
Peak
test 1
test 2
test 3

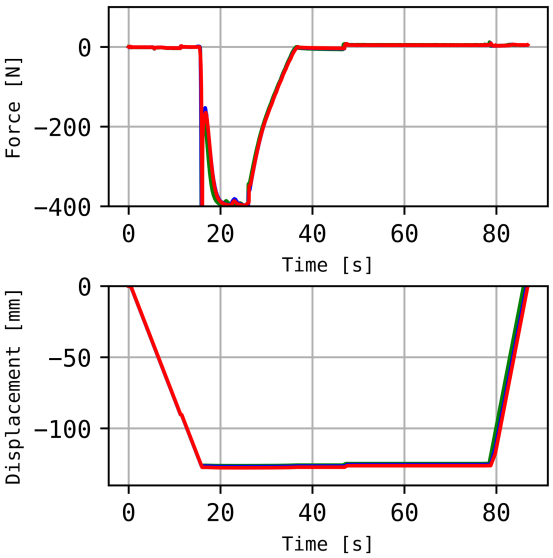
Force [N]
Time [s]
Displacement [mm]
Time [s]

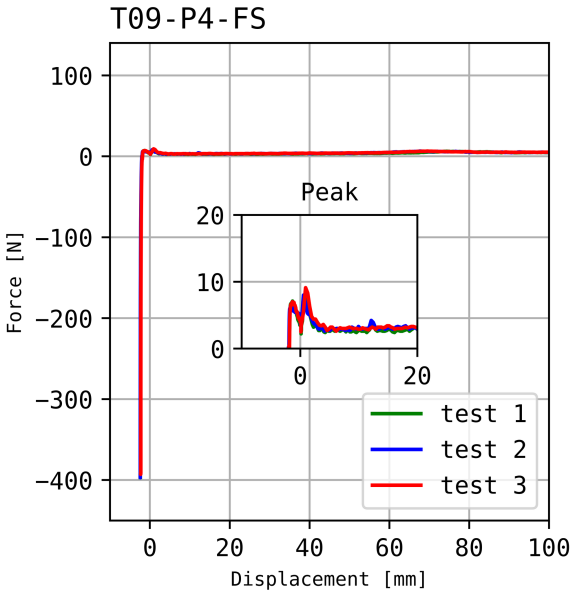
T09-P4-FS
Force [N]
Displacement [mm]
Peak
test 1
test 2
test 3

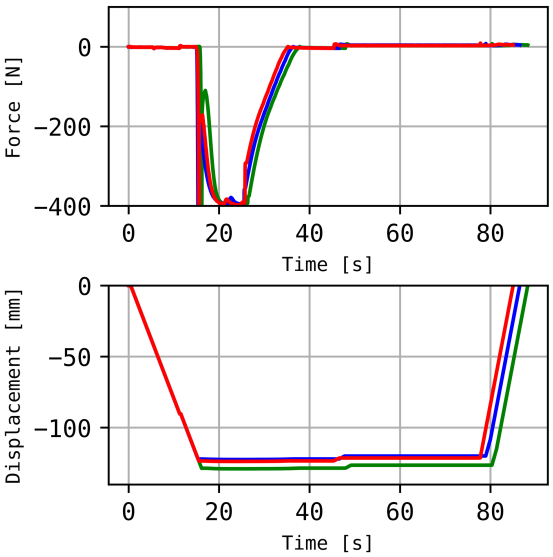
Force [N]
Time [s]
Displacement [mm]
Time [s]

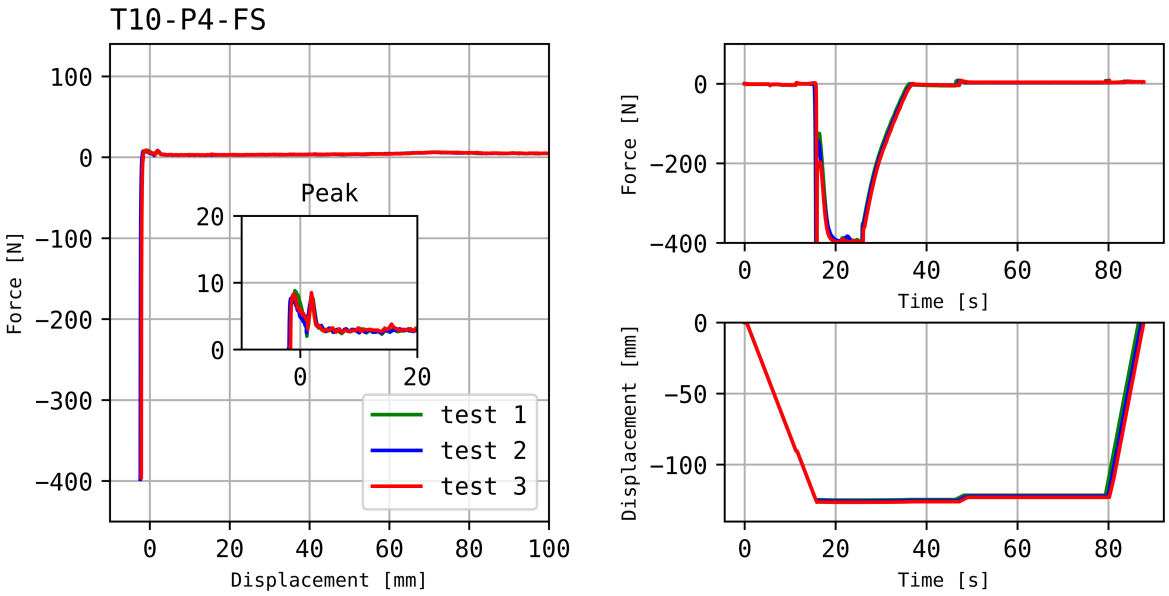
T10-P4-FS
Force [N]
Displacement [mm]
Peak
test 1
test 2
test 3
Force [N]
Time [s]
Displacement [mm]
Time [s]

# E

# Graphs test steel

The reader is referred to Section 5.4 for an explanation of the post-processing and data representation in this research.

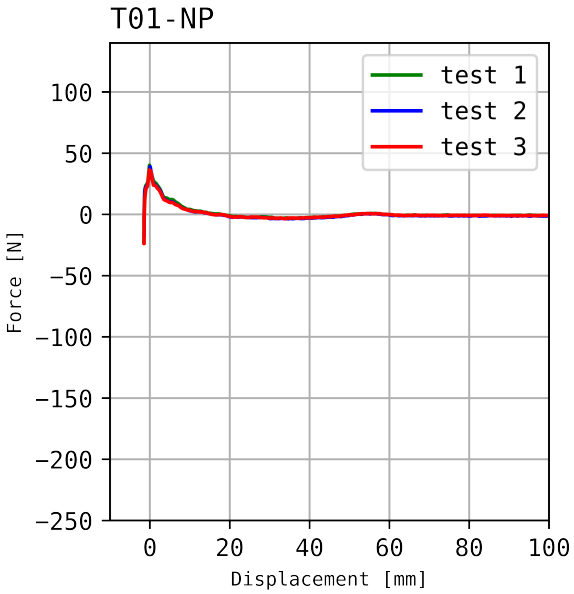


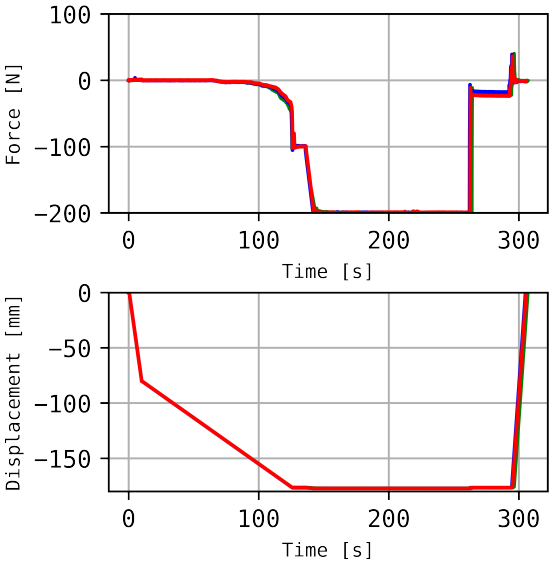

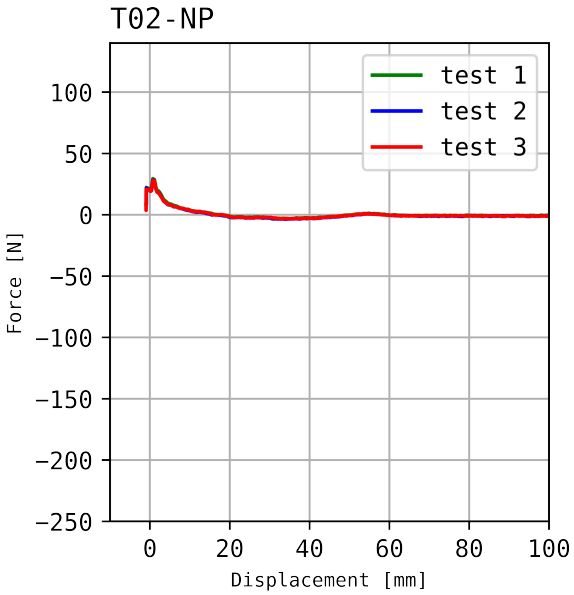
T02-NP
test 1
test 2
test 3
Force [N]
Displacement [mm]

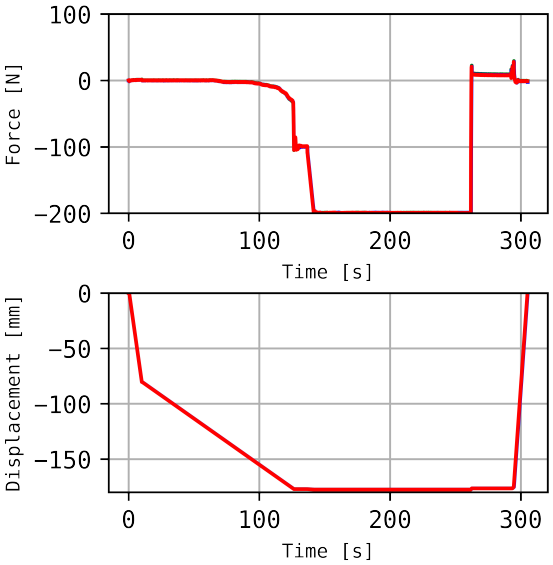
Force [N]
Time [s]
Displacement [mm]
Time [s]

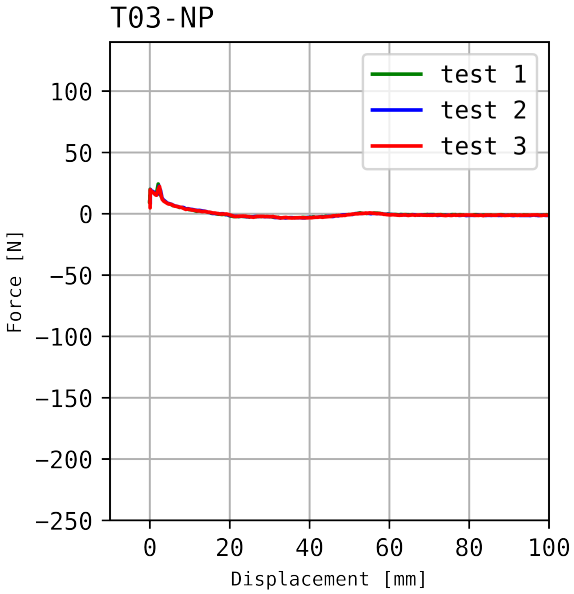
T03-NP
test 1
test 2
test 3
Force [N]
Displacement [mm]

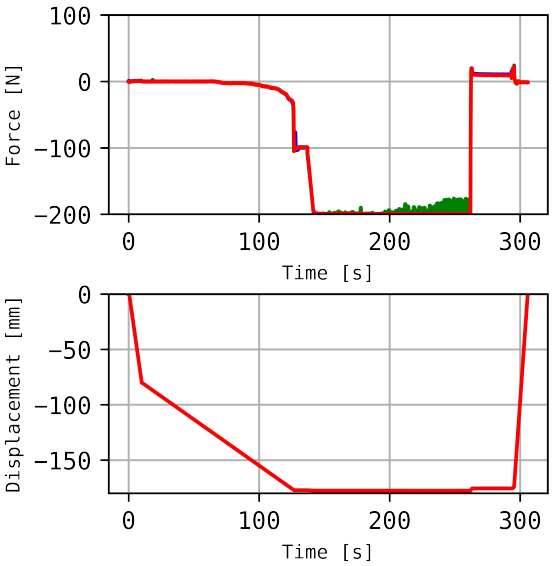
Force [N]
Time [s]
Displacement [mm]
Time [s]

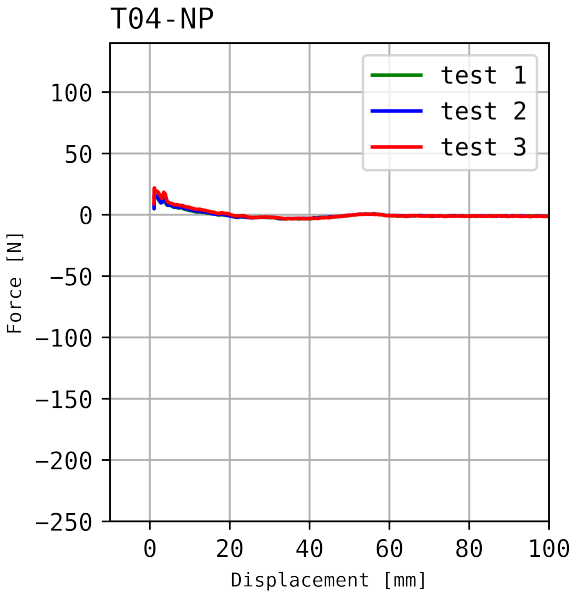
T04-NP
test 1
test 2
test 3
Force [N]
Displacement [mm]

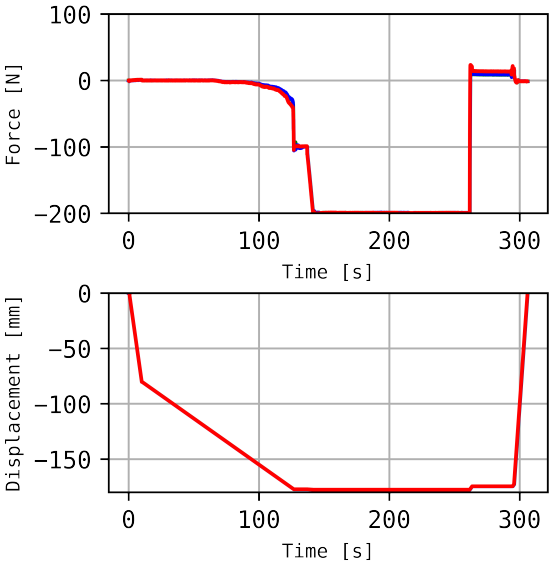
Force [N]
Time [s]
Displacement [mm]
Time [s]

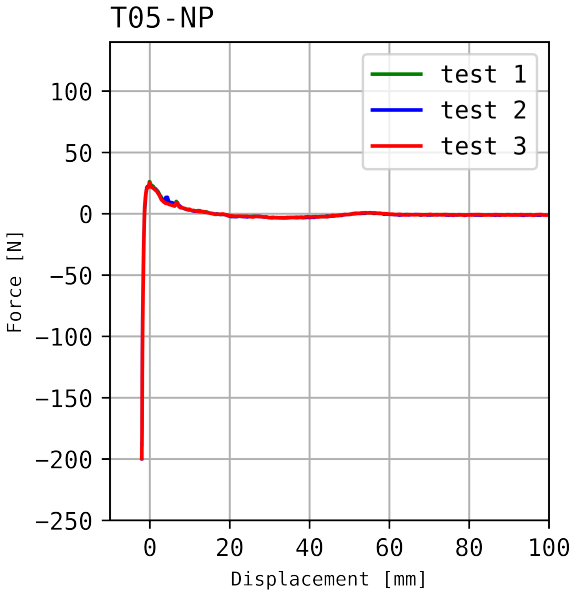
T05-NP
test 1
test 2
test 3
Force [N]
Displacement [mm]

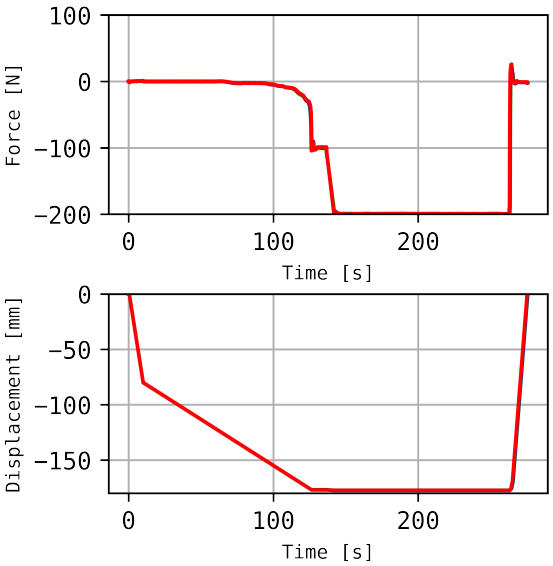
Force [N]
Time [s]
Displacement [mm]
Time [s]

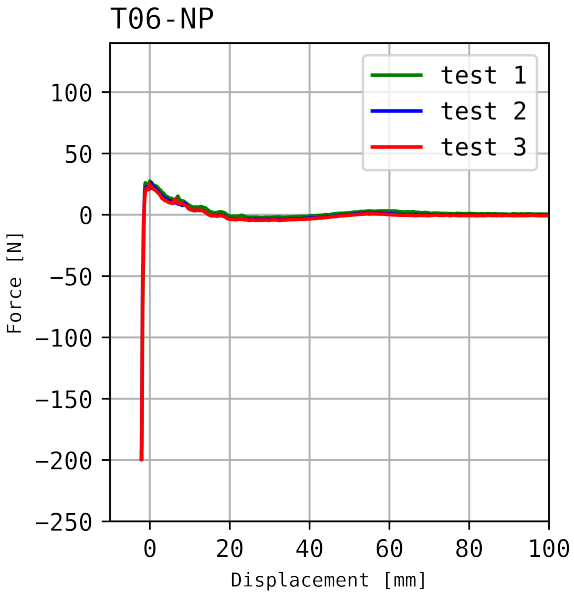
T06-NP
test 1
test 2
test 3
Force [N]
Displacement [mm]

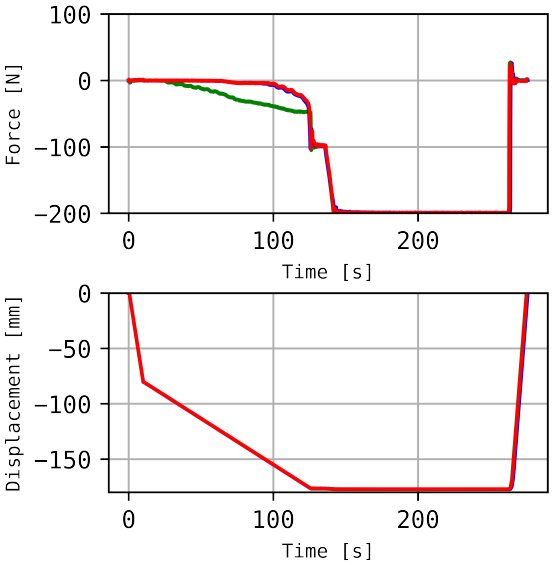
Force [N]
Time [s]
Displacement [mm]
Time [s]

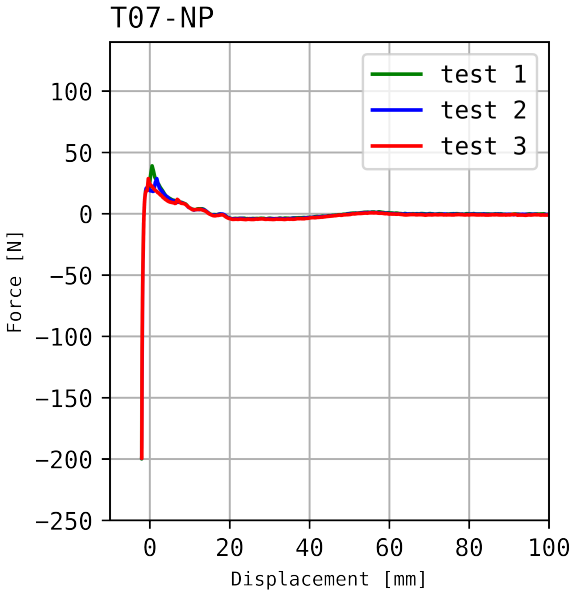
T07-NP
test 1
test 2
test 3
Force [N]
Displacement [mm]

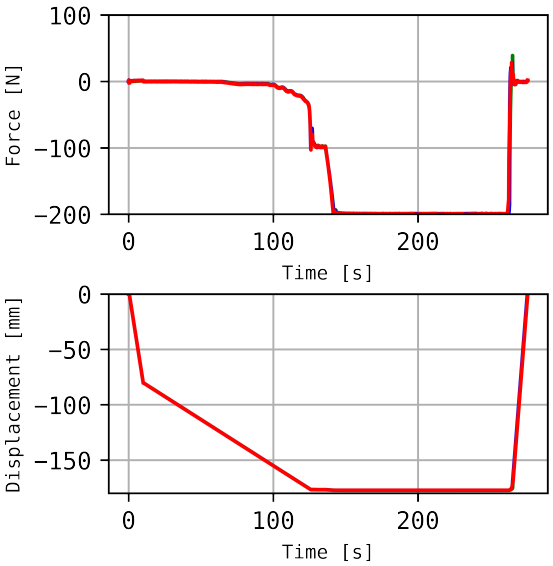
Force [N]
Time [s]
Displacement [mm]
Time [s]

Delft University of Technology